CalVal Envisat

Envisat RA2/MWR ocean data validation and cross-calibration activities. Yearly report 2009.

Contract No 60453/00 - lot2.C

Reference : CLS.DOS/NT/10.018

Nomenclature : SALP-RP-MA-EA-21800-CLS

Issue : 1rev 1

Date : June 30, 2010

CLS - 8-10 Rue Hermès - Parc Technologique du Canal - 31520 Ramonville St-Agne - FRANCE
Téléphone 33 5 61 39 47 00 / Télécopie 33 5 61 75 10 14

Chronology Issues :		
Issue :	Date :	Reason for change :
1.0	22/01/2010	Created
1.1	30/06/2010	Updated

	AUTHORS	COMPANY	DATE	INITIALS
WRITTEN BY	A. Ollivier Y. Faugere	CLS CLS		
APPROVED BY	JP. Dumont	CLS		
QUALITY VISA	DT/AQM	CLS		
APPLICATION AUTHORISED BY				

Index sheet :	
Context	
Keywords	Envisat, Jason-1, Jason-2, Calval, MSL, orbits, reprocessing
hyperlink	

Distribution :		
Company	Means of distribution	Names
CLS/DOS	J. DORANDEU	1 electronic copy
	V. ROSMORDUC	1 electronic copy
	P. ESCUDIER	1 electronic copy
DOC/CLS-DT/AQM	DOCUMENTATION	1 version papier + 1 CD
CNES	T. GUINLE	1 CD
CNES	D. CHERMAIN	1 CD
CNES	E. BRONNER	1 CD
CNES	T. AL ARISS	1 CD
CNES	T. CORREALE	1 CD
CNES	E. BRONNER	via gestion du CNES
CNES	N. PICOT	via gestion du CNES
CNES	J. LAMBIN	via gestion du CNES
CNES	A. LOMBARD	via gestion du CNES

List of tables and figures :

List of Tables

List of Figures

List of items to be defined or to be confirmed :

Applicable documents / reference documents :

Contents

LIST OF ACRONYMS

ECMWF	European Center for Medium range Weather Forecasts
GDR-A	Geophysical Data Record version A (before cycle 41 for Envisat mission)
GDR-B	Geophysical Data Record version B (after cycle 41 for Envisat mission)
MSL	Mean Sea Level
MWR	MicroWave Radiometer
POE	Precise Orbit Estimation
SLA	Sea Level Anomalies
SSB	Sea State Bias
USO	Ultra Stable Oscillator

1. Introduction

This report is an overview of Envisat validation and cross calibration studies carried out at CLS during the year 2009. It is basically concerned with long-term monitoring of the Envisat altimeter system over ocean.

Envisat GDR data are routinely ingested in the Calval 1-Hz altimeter database maintained by the CLS Spatial Oceanography Division in the frame of the CNES Altimetry Ground Segment (SALP) and funded by ESA through F-PAC activities (SALP contract N ° 60453/00 - lot2.C). In this frame, besides continuous analysis in terms of altimeter data quality, Envisat GDR Quality Assessment Reports (e.g. Faugere et al. 2003 [26]) are routinely produced in conjunction with data dissemination.

Data from GDR cycles 9 through 84spanning more than seven years have been used for this analysis. All relevant altimeter parameters deduced from Ocean 1 retracking, radiometer parameters and geophysical corrections are evaluated and tested.

Some of the results described here were presented at the OSTST meeting (Seattle, June 2009) and at the Quality Working Group (QWG) meetings (Toulouse, May 2009 and Barcelona, November 2009).

The work performed in terms of data quality assessment also includes cross-calibration with Jason-1, ERS-2 and Jason-2. This kind of comparisons between coincident altimeter missions provides a large number of estimations and consequently efficient long-term monitoring of instrument measurements. This enables the detection of instrument drifts and inter-mission biases essential to obtain a consistent multi-satellite data set. The complete reprocessing of Jason-1 products in GDR C version has been performed during the year 2009. Concerning Envisat, a full reprocessing in GDR C version is also expected to start in 2010. And yet, a new orbit was delivered on GDR-C standard and has been analysed through some particular studies.

Since July 2008, the new available Jason-2 data were also used for the cross-calibration with Envisat in its GDR type version. The various comparisons performed between both missions show a very good consistency with a standard deviation of cross-over differences of around 3.4 cm. The geographically correlated biases between Envisat and Jason 2 also show a very good agreement of both data sets. These results are encouraging for insuring a good continuity on the long term monitoring already initiated with Jason-1 since 2002.

After a preliminary section describing the data used, the report is split into 5 main sections: first, data coverage and measurement validity issues are presented. Second, a monitoring of the main altimeter and radiometer parameters is performed, describing the major impact in terms of data accuracy. Then, performances are assessed and discussed with respect to the major sources of errors. Then, Envisat Sea Surface height (SSH) bias is analyzed. Finally, an additional part presents the particular investigations that have been performed during this year:
- particular studies about MSL issues,
- an extensive study on the orbits standards using the brand new GDR-C version concerning long term trends, ascending/descending consistency and geographical biases on monomission and cross calibration results.
- a particular study concerning a new SSB version.
- a particular study concerning a new tide model version.

2. Quality overview

Ra-2 instrumental status:
Due to the permanent RA2 S-band power drop which occured on January 17th 2008, 23:23:40 (Cycle 65 pass 289) all the S-band parameters, including the dual ionospheric correction remain unrelevant and MUST NOT be used from then on.
Instead, users are advised to use the ionospheric correction from GIM model, which is available in GDR data products.

No **USO anomaly** were noticed during 2009.
However, it affected intermittently (see Figure 3) Ra-2 data from cycle 46 to cycle 65 pass 451 (2008/01/23). To correct the effect of the USO anomaly, ESA proposed auxiliary files, so that Envisat Ra-2 data remain at the same high level of accuracy.
Users are strongly advised NOT to use the range parameter in Ku and S Band without this correction, even for the non-anomalous periods, in order to correct the range from the long term drift of the USO device. More information is available on http://earth.esa.int/pcs/envisat/ra2/auxdata/

Missing measurements:
The unavailability of data over ocean for year 2009 is very low, about 1.3% in average.
The MWR unavailability is also very stable and very low around 0.4%.

Long term monitoring of RA-2 and MWR parameters:
The ocean-1 altimeter and radiometer parameters are consistent with expected values. They have a very good stability and high performances, comparable to Jason-1. A very good availability on every surface and very low editing ratios over ocean are observed since the beginning of the mission. The high frequency content of Ku-band Ra-2 parameters is very stable.

The MWR performances are very good. Note that since the beginning of the mission, the instrumental parameters at 36.5 GHz were known to be slighly drifting. Moreover from cycle 46 onwards, the comparison to ECMWF model is hardened by the numerous improvements of this operational model inducing (around 1.5mm) jumps in the time series.

Since the loss of the S Band at the beginning of year 2008, the solar activity is still in a low period, therefore thanks to the GIM model correction used instead of the dual-frequency correction in the SSH equation, data were weakly impacted in terms of variance.

Mean Sea Level:
Envisat POD orbit reprocessing was performed from cycle 15 onwards. This enabled to analyse the mission's long term behavior, performances and geographicall patterns. This had a weak impact on the long term global trend, but on the contrary, the worrying discrepancies between ascending and descending passes were shown to be largely reduced. This very good result was further analysed through a comparison with previous ESOC and CNES solution and could be attributed to either the DORIS pre-processing applied on the data and/or to the upgrade of the ITRF version wich changed from 2000 to 2005. This shall be investigated more precisely soon. These analysis show dramaticall improvement of the geographical consistency between both missions and should enable local trend analysis for current 2010. These were previously impossible due to the inhomogeneity of the versions along the mission's life.

Comparisons between Jason-1 and Envisat Mean Sea Level trend estimated at CLS were carried on. Missions still show significant differences before September 2005. They are very similar between September 2005 and tend to diverge again after July 2008. Anyway, differences between both missions can be analysed more and more finelly. Even if wet tropospheric correction still remain a large source of error in the trend computation for all mission due to ECMWF operational jumps due to frequent improvements and due to inhomogeneity of radiometric processing (drift corrections, side lobe effects correction...). The most probable suspicious points are curently being instrumental origins (bad taken into account of instrumental corrections) and should be clarified at the latest after reprocessing.

3. Data used and processing

3.1. Data used

Envisat Geophysical Data Records (GDRs) from cycle 10 to cycle 84have been used to derive the results presented in this report. This corresponds to nearly seven-years spanning from September 30th 2002 to December 6th 2009. The routine production started on September 2003 with cycle 15. In parallel, a backward reprocessing of cycles 14 to 9 was implemented. With only 7 days of available data, cycle 9 has not been used in this report. 11 GDR cycles have been produced this year: cycles 73 to 84as part of the routine processing.

The Envisat GDR data are generated using two softwares: the IPF, from Level0 to Level1B, and the CMA, from Level1B to Level2. As shown in Table 1 several IPF processing chain and CMA Reference Software have been used to produce all the GDR cycles. Tables 2 and 3 describe the main evolutions respectively associated with the IPF and CMA versions.

Cycles	IPF version	CMA version
9 to 10	4.58	6.3
11 to 12	4.57	6.3
13 to 14	4.56	6.3
15 to 21	4.54	6.1
22 to 24	4.56	6.2
25 to 26	4.56	6.3
27 to 28	4.57	6.3
29 to 40	4.58	6.3
38 to 40	5.02	7.1
41 to 47 pass 790	5.02	7.1
47 to 48 pass 849	5.06	9.0
48 to 51 pass 7	5.02	7.1
51 to 58 pass 843	5.03	8.0
58 to 64	5.06	9.0
65 to 67	5.06	9.1
68 to 84	5.06	9.2

Table 1: *I*PF/CMA Processing versions

Note that for cycle 47-48, the instrument sub-system Radio Frequency Module was switched to

B-side during 37 days, from the 15/05/2006 14:21:50 to the 21/06/2006 11:37:32 (cycle 47 pass 794 to cycle 48 pass 847). First of all, an error in the configuration Side-B file made cycles 47 and 48 uncorrect. In 2008, passes 1 to 790 of cycle 47 and passes 1 to 849 of cycle 48 were reprocessed and delivered, RA2 RFSS properly configured to side B redundancy. Those two cycles are now used into the following report.

Version	Changes
IPF 4.56	-Extrapolation of AGC value to the Waveform center (49.5) for both Ku- and S-Band -Correction for an error found in the evaluation of S band AGC
IPF 4.57	No impact on data
IPF 4.58	-Addition of a Pass Number Field in Fast Delivery Level 2 products
IPF 5.02	-MWR Side Lobe correction upgrade -USO clock period units correction -Rain Flag tuning to compensate for the increase of the S band Sigma0 -Monthly IF mask taken into account -DORIS Navigator CFI upgrade (RA-2 and MWR) -S-band anomaly flag
IPF 5.03	-Correction for an error found in the Channel 2 brightness temperature -Correction for an error in the window delay (for the 80 and 20 MHz bandwidths) -S-band anomaly flag upgrade, now properly implemented -Correction of Rx-Fine parameter -MWR second channel corrected (Side Lobes correction)
IPF 5.06	None

Table 2: *I*PF changes impacting the Envisat GDR or Level2 data

The change from IPF 4.58/CMA6.3 to IPF 5.02/CMA7.1 strongly impacted the data. The Sea-State bias table has been recomputed ([41]) accounting for the impact of the new orbit and the new geophysical corrections (MOG2D, GOT00 ocean tide correction with the S2 component corrected once only, new wind speed algorithm from Abdalla, 2006 [1]). The new SSB correction is shifted in average by +2.0 cm in comparison with the previous one. New standards are used for the computation of the Envisat Precise Orbit Estimation. One of the main evolutions is the use

of the GRACE gravity model EIGEN GC03C. This new model implies a strong reduction of the geographically correlated radial orbit errors. In order to take into account the dynamical effects and wind forcing, a new correction is computed from the MOG2D (Carrere and Lyard, 2003 [9]) barotropic model forced by pressure (without S1 and S2 constituents) and wind. The use of such a correction in the SSH strongly improves the performances. All the corresponding evolutions are detailed in [21].

The change from IPF 5.06/CMA9.1 to IPF 5.06/CMA9.2 has a weak impact on the data regarding the short period of time available:
- Change of orbit: New standards are used for the computation of the Envisat Precise Orbit Estimation (POD GDR-C configuration including notably a time varying gravity field, ...). The impact should be weak but studies performed on Jason-1 for the GDR C reprocessing show an unexpected trend on long term monitoring. Updates of the orbit standard solved this problem (by cancelling the linear term of the time variability gravity field) leading to improve the orbit once more.
- Change of DAC correction: A new High Resolution Dynamic Atmospheric Correction MOG2D correction was computed and added to the products. Internal studies show that this new correction improves the variance by a gain of 1 to 2cm^2 for Jason-1 and Envisat with a greater impact near coasts and on open ocean, in the South pacific area (Bellingshausen basin), [12].

Version	Changes
CMA 6.1	-MSS CLS01 -Rain flag -MWR neural algorithm -Sea Ice tuning -Sea State Bias Table file -GOT00.2 Ocean Tide Sol 1 Map file -FES 2002 Ocean Tide Sol 2 Map file -FES 2002 Tidal Loading Coeff Map
CMA 6.2	No impacts on Envisat products
CMA 6.3	-Updated OCOG retracking thresholds Ice1 Conf file -Increased GDR data coverage by the use of both consolidated and non-consolidated data prods in inputs.
CMA 7.1	-Improving the mispointing estimation -Addition of square of the SWH in Ku and S band

.../...

Version	Changes
	-Addition of GOT2000.2 loading tide -FES2004 tide and loading tide -New DEM AUX file (MACESS) merge of ACE land elevation data and Smith and Sandwell ocean bathymetry -New orbit standards -New SSB solution -new wind table -Mog2D upgraded -New S1S2 wave model in dry troposphere -GOT00.2 includes two extra waves, S1 and S2 -GIM model ionospheric correction added in the products
CMA 8	No impacts
CMA 9	Correction of an anomaly in the relative orbit field inside the product header. No scientific impact.
CMA 9.1	Separating the processing of Jason-1 and Envisat No scientific impact.
CMA 9.2	-New POD orbit configuration. -New Dynamic Atmospheric Correction (DAC/MOG2D High Resolution)

Table 3: *C*MA changes impacting the Envisat GDR

3.2. Processing

3.2.1. GDR products and quality assesment method

To perform this quality assessment work, conventional validation tools are used including editing procedures, crossover analysis, collinear differences, and a large number of statistical monitoring and visualization tools. All these tools are integrated and maintained as part of the CNES SALP altimetry ground segment and F-PAC (French Processing and Archiving Centre) tools operated at CLS premises. Each cycle is carefully routinely analyzed before data release to end users. The main data quality features are reported in a cyclic quality assessment report available on http://www.aviso.oceanobs.com/html/donnees/calval/validation_report/en/welcome_uk.html. The purpose of this document is to report the major features of the data quality from the Envisat mission.

As for all other existing altimeters, the Envisat GDR data are ingested in the Calval 1-Hz altimeter database maintained by the CLS Spatial Oceanography Division. This allows us to cross-calibrate and cross-compare Envisat data to other missions. In this study data from Jason-1 (GDRs cycles 27 to 252), ERS-2 (OPRs Cycle 78 to 108) are used. Jason-1 is the most suitable for Envisat cross calibration as it is available throughout the whole Envisat mission and has been extensively calibrated to T/P (Dorandeu et al., 2004b [18]). In 2007, a full reprocessing of Jason-1 data GDR-B version had been completed in order to have an homogeneous data set [4]. Since May 2008 however, the new GDR-C version came out. The complete reprocessing of Jason-1 products in GDR C version began mid-2008 and is has been completed in early 2010. Concerning Envisat, a full reprocessing will also begin in 2010. Therefore, a new homogeneous Envisat/Jason-1 data set will be available. The cross-calibration between Envisat and Jason-1 takes into account Jason-1 reprocessing. The periods concerned by each version is summed up on Figure 2.

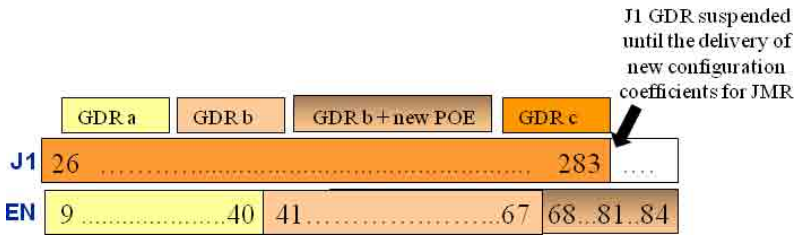

Figure 1: *Status on the GDR reprocessing for Jason-1 and Envisat.*

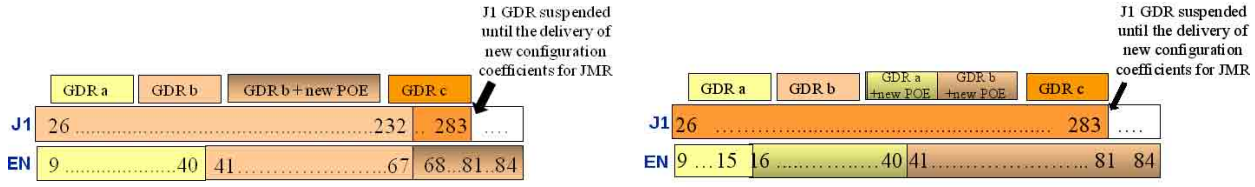

Figure 2: *GDR used in this report for Jason-1 and Envisat. Different data sets are used for systematic calval and particuliar studies. A left: reprocessed J1 data were available during current 2009. B right: Since few month Envisat reprocessed GDRc POE are also available and are used in some studies.*

Comparisons between Jason-1 and Envisat altimeter and radiometer parameters have been carried out using 10-day dual crossovers for SSH comparison and 3-hour dual crossovers for altimeter and radiometer comparisons. The geographical distribution of the dual crossovers with short time lags strongly changes from one Envisat cycle to another. Indeed, contrary to Envisat which is sun-synchronous, Jason-1 observes the same place at the same local time every 12 cycles (120-day). Following the method detailed in Stum et al. (1998) [72], estimates of the differences are computed using a 120 day running window to keep a constant geographical coverage. ERS-2, flying on same ground track as Envisat only 30 minutes apart, has had a coverage limited to the North Atlantic since the failure of the on-board register in June 2003 (EOHelp message of 4 July 2003). To improve the significance of the Envisat/ERS-2 comparison, long term monitoring of altimeter parameters difference is performed on this restricted area all over the Envisat period using a repeat-track method.

3.2.2. Particular updates added to the GDR products

Most of this work has been carried out using parameters available in the GDR products. However, a few updates have been necessary to complete the analysis (those are listed in the product disclaimer document available at http://earth.esa.int/dataproducts/availability/ [62]):

- **S-Band anomaly**: A method has been developed to detect data corrupted by S-Band anomaly. It has been applied until cycle 53. From cycle 54 onwards the product flag, available since cycle 51, has been used (see 4.3.1.). Since cycle 60, the cause of the anomaly was found and the anomaly solved. No anomaly occurs anymore since then.
- **Sea ice flag**: A method has been developed to detect data corrupted by sea ice (see 4.3.2.)
- **Filtered dual-frequency ionosphere correction**: A 300-km low pass filter is applied along track on the dual frequency ionosphere correction to reduce the noise of the correction. This correction is applied up to the cycle 64, after that, it cannot be computed anymore, due to the S-Band Power drop (17th January 2008) the GIM ionospheric correction is then used.
- **Filtered dual-frequency ionosphere correction (bis)**: For cycles 9-40 from the sea state bias (SSB) used to correct the S-Band Range was updated in its right S-Band version. The dual-frequency ionosphere correction was therefore recomputed accounting for the S-Band SSB solution on S-Band range. Before that, both S and Ku-Band ranges used for that correction were corrected from the Ku-Band SSB (Labroue (2004 [40])).

- **Geophysical corrections**: The new geophysical corrections associated with version CMA7 have been updated on the whole data-set in order to have the most homogeneous time series: wind table and SSB, new S1S2 wave model in dry troposphere, GOT00.2 with two extra waves, FES2004, S1 and S2

- **GOT 4.7**: A new tidal model was available during 2009. It was analysed and replaces the GOT00.2 correction in some studies (see 7.3).

- **SSB 2007**: A new SSB model was also available during 2009. It was analysed and validated this year (see 7.4).

- **MOG2D HR**: The new High resolution DAC implemented into the CMA 9.2 from cycle 69 on Envisat (see Table 3) was also updated on the whole data-set.

- **Inverse barometer and dry troposphere corrections**: Pressure values used to compute the inverse barometer and the dry troposphere corrections have been derived from the ECMWF gaussian grids. Indeed, errors due to the topography, up to several centimeters near the coasts, significantly impact the accuracy the so-called Gaussian grids used as input of the Envisat (and Jason-1) ground processing (e.g. Dorandeu et al., 2004b [18]).

- **GIM/IRI ionosphere corrections**: Jason-1 doesn't fly at the same altitude as Envisat which means that ionosphere corrections are not comparable. Moreover, ERS-2 has a mono-frequency altimeter on-board. Therefore it is not possible to use these satellites to assess the Envisat ionosphere path delay. Thus the JPL GPS-based global Ionospheric Maps (GIM) containing the vertical ionospheric total electron content are used here. Note that GIM maps contain the vertical ionospheric total electron content in the 0-1400km altitude range. As Envisat flies around 800km, the International Reference Ionosphere (IRI) model is uses to estimate the GIM correction at the altitude of Envisat:
$GIM_{[0-800]} = GIM_{[0-1400]} \times \frac{IRI_{[800]}}{IRI_{[1400]}}$. Since the S-Band loss (17th January 2008) this correction is used for the SSH computation. Also note that since cycle 41 onwards, this GIM ionosphere correction is available in the GDR products.

- **USO correction**: The range needs to be corrected for the Ultra-Stable Oscillator (USO) clock period variations. From the beginning of the mission it underwent several behaviors and the way it is corrected depends on the cycle. It is detailled hereafter in part 3.2.3..

3.2.3. USO correction's specificities

The USO clock period is used to perform the computation of the Ra-2 window time delay and the range needs to be corrected :
- on the whole period, from a drift due to the aging of the device
- during some periods (detailed in Figure 3), from a strong anomaly detailed hereafter.

Description of the USO anomaly:
On the 1st of February 2006 (12:05:36), at the end of cycle 44, for an unknown reason a change of behavior of the USO device occurred. This anomaly, already observed for a short period during

cycle 30, created a 5.5m jump on the range parameter and oscillations of about 20-30cm of amplitude at the orbital period. The anomaly became permanent on cycle 46 to 56. On the 1st of March 2007, the USO recovered in a non-anomalous mode. Between cycles 56 and 61, Ra2 data was not affected by the anomaly. On the 27th of September 2007 (cycle 62), a new change of behavior of the Ultra Stable Oscillator (USO) clock frequency occurred. A short break in the anomaly occurred between cycles 63 and 64, followed by another one on the 23th of January which was permanent over the whole year 2008. The anomaly and associated correction is detailed in [50]. The quality assessment of these data has been performed using the USO temporary correction provided by ESA. Users are strongly advised not to use the range parameter in Ku and S Band without this correction.

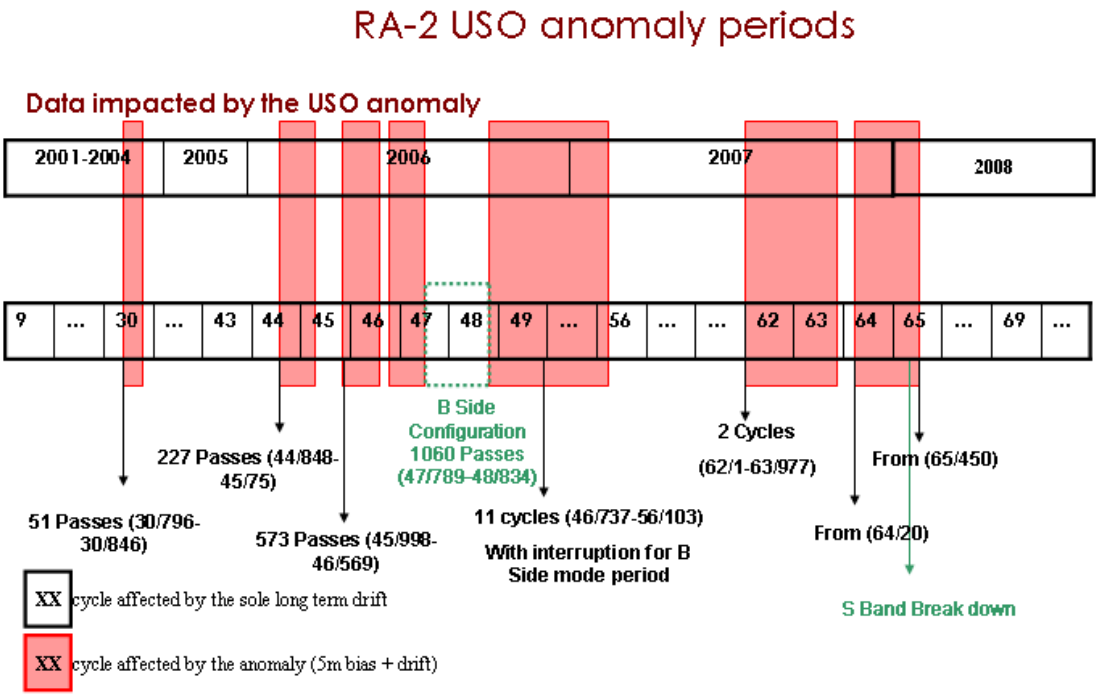

Figure 3: *Chronology of USO Correction anomaly.*

The correction of the Ultra-Stable Oscillator (USO) clock period variation applied to the range depends on the cycle considered. This is detailed hereafter:
For cycle 9 to 40, (outside of the anomaly periods): The method to correct the USO clock period is described in Celani (2002 [14]). The correction is regularly updated in the IPF ground processing via an Auxiliary data file. However, due to an anomaly in the ADF format, the correction was not taken into account (Martini, 2003 [50]) in the products for cycles lower or equal to 40. ESA supplies auxiliary files to allow users correcting their own database (Martini, 2003 [50]) (http://earth.esa.int/pcs/envisat/ra2/auxdata/). The distributed auxiliary corrections containing the drift + bias have to be used. The supplied correction has to be subtracted from the original altimetric range (EOP-GOQ and PCF team, 2005) and consequently added to SSH.
Note that for our database, the distributed auxiliary correction was smoothed over a 1-month

period to filter peaks and short period variations.

For cycle 41 to 45, (outside of the anomaly periods): The USO drift + bias is already taken into account in the products. No additional auxiliary correction has to be used.

After cycle 45, (and for all the previous anomaly periods): ESA supplies auxiliary files to allow users correcting their own database (Martini, 2003 [50]) (http://earth.esa.int/pcs/envisat/ra2/auxdata/). The distributed auxiliary corrections containing the drift + anomaly correction have to be used.

4. Missing and edited measurements

This section mainly intends to analyze the ability of the Envisat altimeter system to correctly sample ocean surfaces. This obviously includes the tracking capabilities, but also the frequency of unavailable data and the ratio of valid measurements likely to be used by applications after the editing process.

4.1. Missing measurements

From a theoretical ground track, a dedicated collocation tool allows determination of missing measurements relative to what is nominally expected. The cycle by cycle percentage of missing measurements over ocean has been plotted in Figure 4. The measurement unavailability over the whole mission is about 6% in average. Eleven cycles have more than 10% of unavailability, notably from cycle 13 to cycle 17. Passes 1 to 452 of cycle 15 have not been delivered because of a wrong setting of RA-2. Several long RA-2 platform events occurred during cycles 13, 14, 16, 17, 22, 34, 51, 53, 55, 56, 59, 62 which resulted in a significant number of missing passes.
An improvement of the data dissemination since May 2008 leaded to decrease the average ratio of missing RA2 measurements over ocean down to 1.3%.

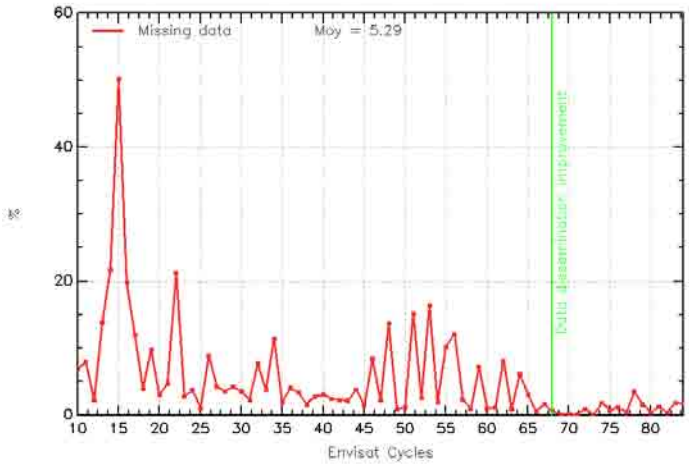

Figure 4: *Monitoring of the percentage of missing measurements relative to what is theoretically expected over ocean*

Figure 5 shows an example of missing measurements for cycle 84. The measurements which are missing over the Himalaya are due to the IF Calibration Mode occurring on ascending passes only. This procedure was not always the same: for cycles prior to 55, it was performed over the Himalaya on both ascending and descending passes and for cycles 56 to 66 it was performed on ascending passes only but on the Rocky Mountains as well as on the Himalaya). Afterwards, it is performed on ascending passes above the Himalaya only.

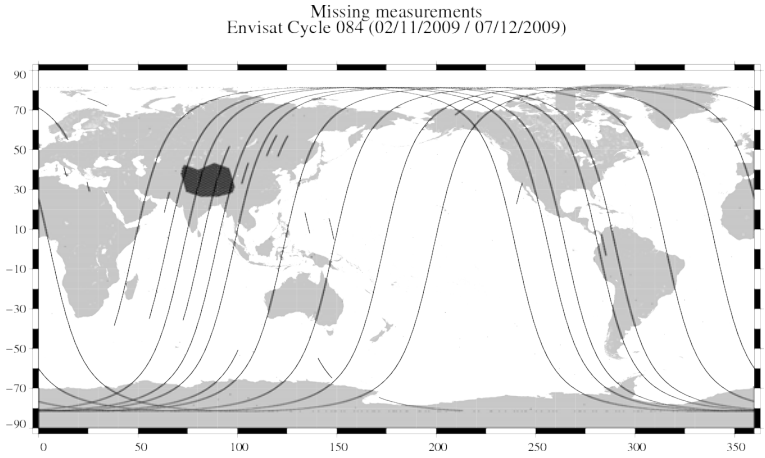

Figure 5: *Envisat missing measurements for cycle 84*

Finally, it has been found that some pass segments were quasi-systematically missing. Figure 6 shows the pass segments missing more than 5 times over the 11 last cycles. Some of them are explained (comparisons to transponders like ESA/Rome or GAVDOS/ Creta), others are not. Apart from that, the data retention rate is very good on every surface observed. This might be due to the tracker used by Envisat Ra-2, the Model Free Tracker (MFT).

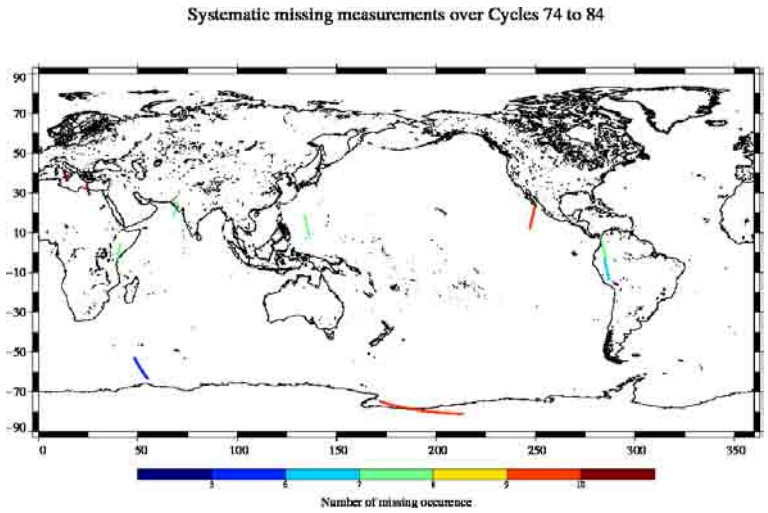

Figure 6: *Pass segments unavailable more than 5 times between cycles 56 and 84. The color indicates the occurrence of unavailability*

Finally, the list of instrument and platform events is available. Apart from instrumental and platform events, up to 3% of measurements can be missing because of data generation problems at ground segment level: LRAC or PDHS level1 data generation problems or ingestion problems on F-PAC side.

4.2. Missing MWR data

The Envisat MWR exhibits nearly 100% (Dedieu et al., 2005) of availability since the beginning of the mission. However, MWR corrections can be missing in the GDRs due to data generation problems at ground segment level. When the Land/sea radiometer flag is set to land over ocean, it means that the radiometer data is missing. The percentage of missing MWR corrections over ocean has been plotted in Figure 7. The radiometer unavailability is not constant: it is greater than 4% for cycles 14 to 19 and for cycles 58 and 60, and lower than 2% elsewhere. Since 2008, the MWR unavailability is very stable and very low around 0.4%.

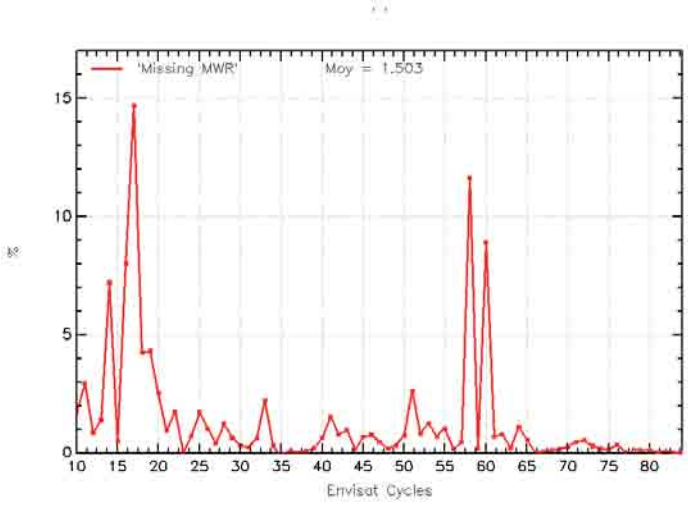

Figure 7: *Cycle per cycle percentages of missing MWR measurements*

4.3. Edited measurements

Data editing is necessary to remove altimeter measurements having lower accuracy. There are 4 steps in the editing procedure. The first step of the editing procedure consisted in removing data impacted by the S-Band anomaly. Note that this step is not necessary anymore from cycle 60 onwards, when the source of the anomaly was solved. Therefore, the first step is now the removal of data corrupted by sea ice. Then, measurements are edited using thresholds on several parameters. The third step uses cubic splines adjustments to the ENVISAT Sea Surface Height (SSH) to detect remaining spurious measurements. The last step consists in removing entire pass where SSH-MSS mean and standard deviation have unexpected value.

4.3.1. Measurements impacted by S-Band anomaly

During the Commissioning Phase, it has been discovered that the RA-2 data are affected by the so-called S-Band anomaly. The anomaly results in the accumulation of the S-Band echo

waveforms (Laxon and Roca, 2002 [43]). It happens randomly after an acquisition sequence and is only stopped by switching the Ra-2 in a Stand-By mode. When this anomaly occurs, the S-Band waveforms are not meaningful. Consequently, all the S-Band parameters and the Dual Frequency ionosphere correction are not reliable. Notably, the S-Band Sigma0 is unrealistically high during these events. Thus applying a threshold of 5 dB on the (Ku-S) Sigma0 differences is very efficient for detecting the impacted data over ocean. The ratio of flagged measurements over ocean is plotted in Figure 8. A method has been developed to flag the impacted data over all surfaces (Martini et al., 2005 [51]). This flag is available in the GDR product since cycle 51 and has been applied in our internal data base from cycle 54 onwards.

Except from cycle 10 where 33% of the data are impacted (before any solution has been found), between 0 and 8% of the data are affected by the S-Band anomaly. From cycle 31 onwards, some modifications have been performed by ESA to decrease the duration of these events: instrument switch-offs (Heater 2 mode) were performed twice a day over the Himalayan and Rocky mountain region. This prevents the S-Band anomaly from lasting more than half a day. Thanks to this procedure the ratio of impacted data decreased from 4.2% (cycles 11 to 30) to 2.2% (cycles 31 to 38). On the 27th of June 2007 (cycle 60) an on-board patch solving the problem has been successfully uploaded. Since then and until the S-Band loss, no occurrences of the anomaly have been detected.

Finally, an algorithm for the S-Band waveform reconstruction has been developped which will enable the recovery of the data affected by the anomaly. The correction will be achieved with the full mission reprocessing campaign scheduled for 2010.

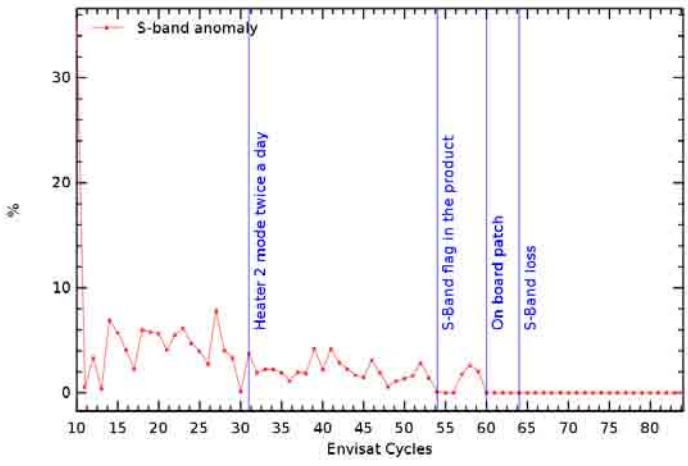

Figure 8: *Cycle per cycle percentages of data impacted by the S-Band anomaly and major events concerning the band.*

4.3.2. Measurements impacted by Sea Ice

Since Envisat operates between 82N and 82S of latitude, sea ice detection is an important issue for oceanic applications. No ice flag is currently available in the Envisat products, therefore alternate

sea ice detection techniques are used in order to retain only open ocean data. A study performed during the validation phase showed that the combination of altimetric and radiometric criteria was particularly efficient to flag most of the data over ice. The method is described in detail in (Faugere et al, 2003 [27]). We employ the Peakiness parameter (Lillibridge et al, 2005 [47]) in conjunction with the MWR- ECMWF wet troposphere difference which appears to be a good means to complement the Peakiness parameter in all ice conditions.

The ratio of flagged measurements over ocean is plotted on Figure 9

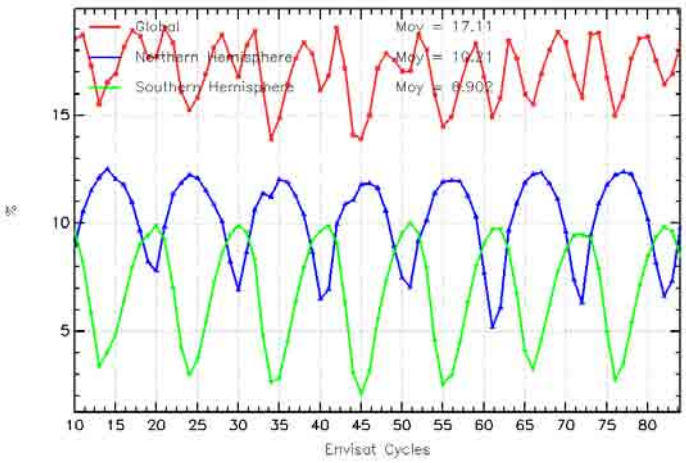

Figure 9: *% of edited points by sea ice flag over ocean*

In September 2007, a record-breaking minimum of flagged data for the Northern Hemisphere zone around cycles 61-63 due to a low ice extend record. This was observed by different Envisat instruments including its altimeter RA2. Indeed, for the first time, an altimeter satellite could observe open ocean surfaces up to 82°N above Siberia in September (see figure 10). This event has had an impact on the global cyclic standard deviation of sea level anomaly (figure 33). Inaccurate Mean Sea Surface or tide models in this area might explain these low SLA performances. See further details on http://www.aviso.oceanobs.com/en/applications/glace/glaces-de-mer/l-etendue-des-glaces-de-l-arctique-vue-par-l-altimetre-d-envisat/index.html.

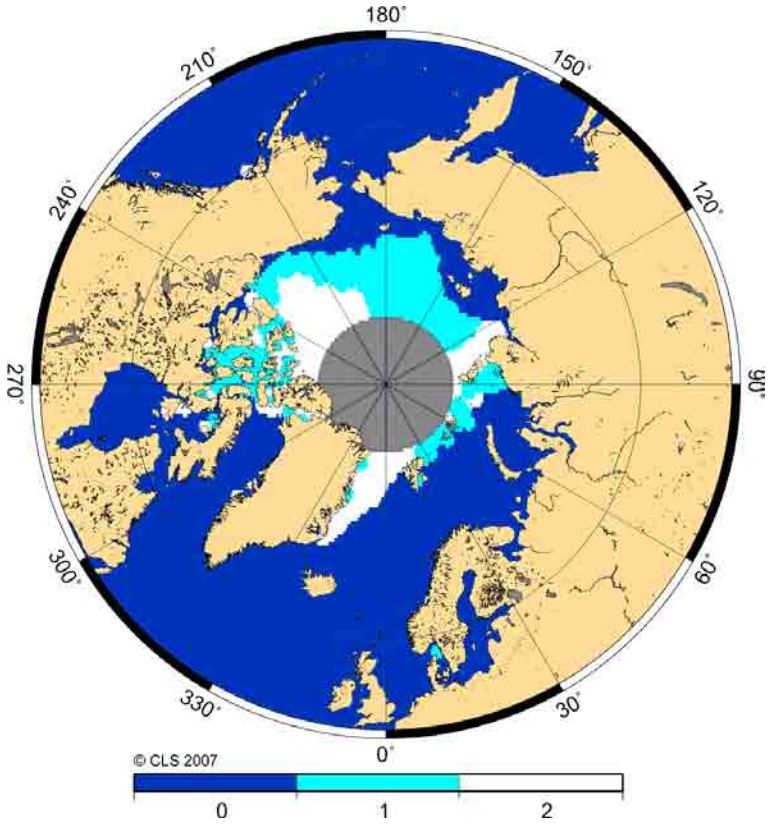

Figure 10: *Sea ice coverage seen by Envisat RA-2, averaged 1° by 1° over September 2007 and compared to an average over the previous years (2003-2006). Dark blue = open ocean, White = usual ice coverage, Light blue = open ocean seen in 2007 where sea ice was observed previously.*

4.3.3. Editing by thresholds

The second step of the editing procedure consists in using thresholds on several parameters. The minimum and maximum thresholds used in the routine quality assessment are given in table 4.

Parameter	Min thresholds	Max thresholds
Sea surface height (m)	−130	100
Variability relative to MSS (m)	−2	2
Number of 18Hz valid points	10	–
Std deviation of 18Hz range (m)	0	0.25
Off nadir angle from waveform (deg2)	−0.200	0.160
		.../...

Parameter	Min thresholds	Max thresholds
Dry troposphere correction (m)	−2.500	−1.900
Inverted barometer correction (m)	−2.000	2.000
MWR wet troposphere correction (m)	−0.500	0.001
Dual Ionosphere correction (m)	−0.200	−0.001
Significant waveheight (m)	0.0	11.0
Sea State Bias (m)	−0.5	0
Backscatter coefficient (dB)	7	30
Ocean tide height (m)	−5	5
Long period tide height (m)	−0.500	0.500
Earth tide (m)	−1.000	1.000
Pole tide (m)	−5.000	5.000
RA2 wind speed (m/s)	0.000	30.000

Table 4: *E*diting criteria

The thresholds are expected to remain constant throughout the ENVISAT mission, so that monitoring the number of edited measurements allows a survey of data quality. The percentage of edited measurements over ocean for the main altimeter and radiometer parameters has been plotted in Figure 11. These ratios are very stable and surprisingly low over the period if compared to other altimeters. The RMS of elementary measurements has the strongest ratio among the altimeter parameters, more than 1% in average. On cycle 47, a special operation was executed to limit RA-2 Chirp Bandwidth to 80MHz. It has impacted this parameter as well as the dual frequency ratio. A slight seasonal signal is visible on the curve, mostly due to sea state seasonal variations. The number of elementary measurements has a surprisingly low ratio, except for cycles 14 and 20 when wrong configuration files were uploaded on-board after a RA-2 event. A slight increase is noticed from cycle 54 onwards due to the use of the product S-Band anomaly flag instead of the criteria based on KU/S Sigma0 difference. The square of the off-nadir angle derived from waveforms leads to very stable editing ratio but with a drop on cycle 41, due to a change of the algorithm in CMA7.1. Variations of this parameter can reveal actual platform mispointing, if any, but can also reveal waveform contamination by rain or by sea-ice. It is indeed computed from the slope of trailing edge when fitting a typical ocean model to the waveforms. No seasonal signal is visible which may prove that the sea-ice detection method is efficient. The dual frequency ratio shows a slight increasing trend between cycles 15 and 28 which cannot be considered as significant, given the scatter of the curve. The Ku-band SWH, sigma0 also present a slight increase, mainly since cycle 41. Concerning MWR ratios it is very stable and low before cycle 41 and still low but more cahotic afterwards. The variations cohincidate with the ECMWF model changes presented further.

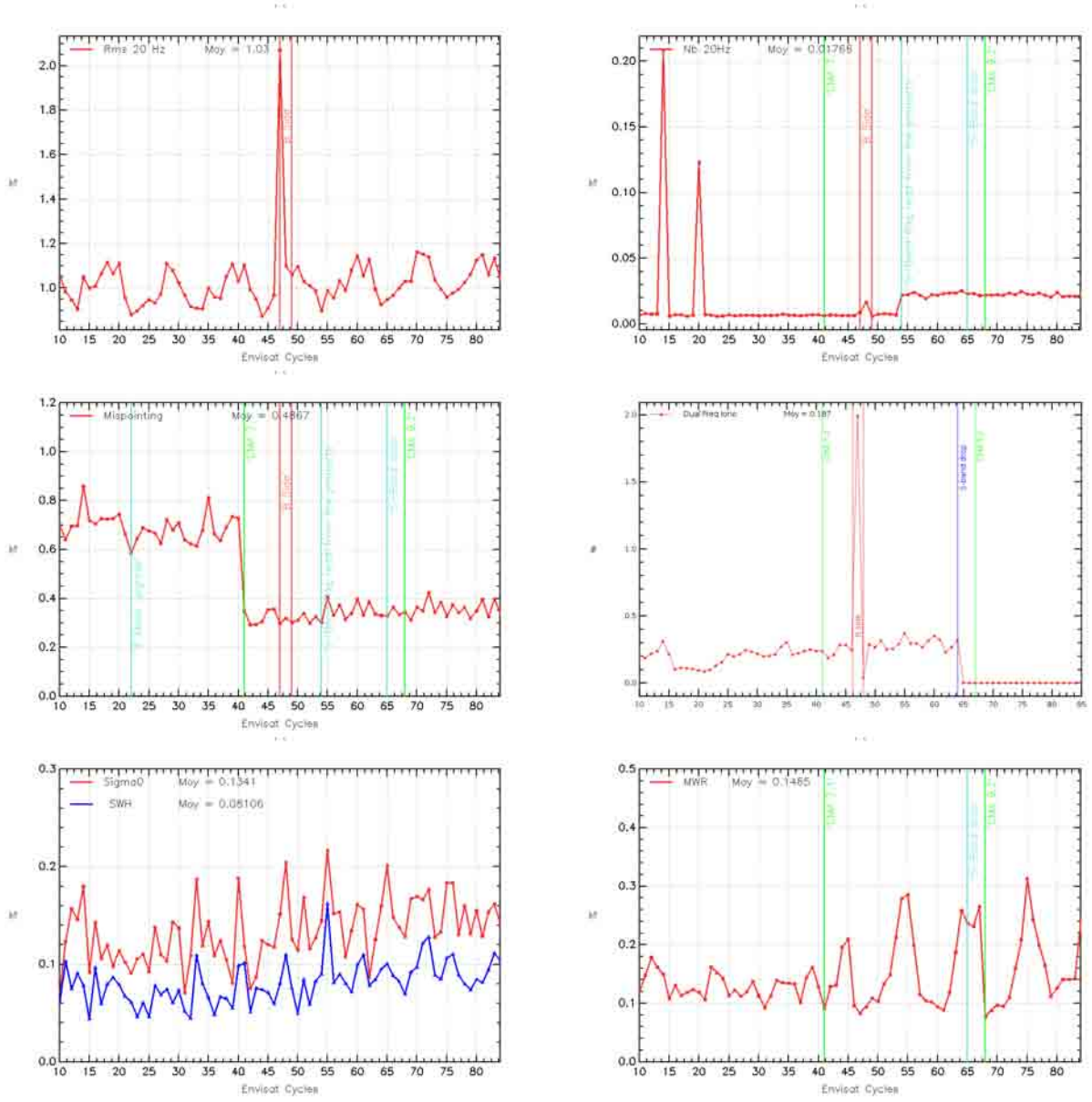

Figure 11: *Cycle per cycle percentages of edited measurements by the main Envisat altimeter and radiometer parameters:* ***Top-Left****) Rms of 20 Hz range measurements > 25 cm,* ***Top-Right****) Number of 20-Hz range measurements < 10,* ***Middle-Left****) Square of off-nadir angle (from waveforms) out of the [-0.2 deg2, 0.16 deg2] range,* ***Middle-Right****) Dual frequency ionosphere correction out of [-40 , 4 cm],* ***Bot-Left****) Ku-band Significant wave height outside > 11 m, Ku band backscatter coefficient out of the [7 dB, 30 dB] range,* ***Bot-Right****) MWR wet troposphere correction out of the [-50 cm, -0.1 cm] range*

4.3.4. Editing on SLA

It has been necessary to apply additional editing criteria on SSH-MSS differences in order to remove remaining spurious data. The first criterion consists in removing measurements with SSH-MSS greater than 2m. The strong value on cycle 30 is due to the first occurrence of the USO anomaly. The second criterion was necessary to detect measurements impacted by maneuvers. Maneuvers are necessary to compensate the effect of gravitational forces but can have a strong impact on the orbit quality. Two types of maneuvers are operated to maintain the satellite ground track within the +/-1km deadband around the reference ground track: in-plane maneuvers, every 30-50 days, which only impact the altitude of the satellite and out-of-plane maneuvers, three times a year, to control the inclination of the satellite (Rudolph et al., 2005). The out-of-plane maneuvers are the most problematic for the orbit computation. The second criterion consists in testing the mean and standard deviation of the SSH-MSS over each entire pass. If one of the two values, computed on a selected dataset, is abnormally high, then the entire pass is edited.

A specific study has been performed to determine how to compute the statistics, and what threshold should be applied. The statistics have to be computed on very stable area. The criteria for selecting the area and the thresholds are detailed as follows:

- The latitude: the range value can be degraded near the ice, despite the use of the ice flag. Moreover, the MSS is less accurate over 66 $^\circ$, as it has been computed without Topex data.
- The oceanic variability: the standard deviation of SLA can be very high because of the mesoscale variability. Areas with high oceanic variability have to be removed to detect the abnormally high standard deviation.
- The bathymetry and distance from the coast: A lot of corrections (tides for example) are less accurate in low bathymetry areas and near the coast (Japan sea).
- The sample: The statistic have to be computed on a significant number of points

All those criteria have been tested and combined as part as a specific study in a previous yearly report. The conclusion is that two criteria are needed:
1st **criteria**:
for small portion of pass (less than 200 points) the sample is not big enough to compute reliable statistic. The selection must not be severe: Selected areas: |latitude|<66 $^\circ$, variability<30cm, bathymetry>1000m, distance to coast>100km Threshold: 30 cm on mean and standard deviation
2nd **criteria**:
for other passes Selected areas: |latitude|<66 $^\circ$, variability<10cm, bathymetry>1000m, distance>100km Threshold: 15 cm on mean and standard deviation

The percentage of edited measurements over ocean for the main altimeter and radiometer parameters has been plotted in Figure 12. On cycles 11, 12, 21 and 26, several full passes have been edited because of bad orbit quality related to out-of-plane maneuver or lack of Doris data (cycle 11).The special operation on RA-2 Chirp Bandwidth mentioned previously impacted the SSH editing ratio on cycle 47. On cycle 56 an USO anomaly recovery, occurred at the beginning of cycle and impacted the SSH statistic editing per pass.The behavior of the Ultra Stable Oscillator (USO) clock frequency on this cycle is chaotic. The transitions between anomaly and normal mode

has been very straight and the USO correction does not allow us to well correct some passes.

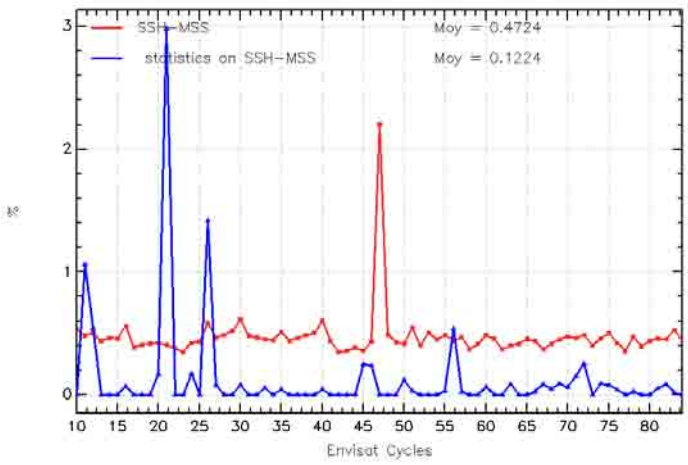

Figure 12: *SSH-MSS out of the [-2, 2m] and edited using thresholds on the mean and standard deviation of SSH-MSS on each pass*

5. Long term monitoring of altimeter and radiometer parameters

All GDR fields are systematically checked and carefully monitored as part of the Envisat routine calibration and validation tasks. The main Ku-band parameters are the most significant in terms of data quality and instrumental stability. However, some significant S-band parameters are also presented here. Furthermore, all statistics are computed on valid ocean datasets after the editing procedure.

5.1. Number and standard deviation of 20Hz elementary Ku-Band data

As part of the ground segment processing, a regression is performed to derive the 1 Hz range from 20 Hz data. Through an iterative regression process, elementary ranges too far from the regression line are discarded until convergence is reached. The mean number and RMS of Ku 20Hz elementary data used to compute the 1Hz average are plotted in figure 13. These two parameters are nearly constant, which provides an indication of the RA-2 altimeter stability. The mean number of Ku 20Hz values over one cycle is about 19.97. This value is very high compared to other altimeters. It is almost not disturbed in wet areas or near the coast. The two drops on the Ku-band on cycles 14 and 20 are due to wrong setting of the RA-2 just after recovery. A slight seasonal signal is visible on the mean RMS of Ku 20Hz. Higher values correspond to higher waves occurring during the austral winter. The mean value is about 9.0 cm. This value represents a rough estimation of the 20 Hz altimeter noise (Zanifé et al. 2003 [79], Vincent et al. 2003a [77]). Assuming that the 20Hz measurements have uncorrelated noise, it corresponds to a noise of about 2 cm at 1Hz. It is consistent with the expected noise values.

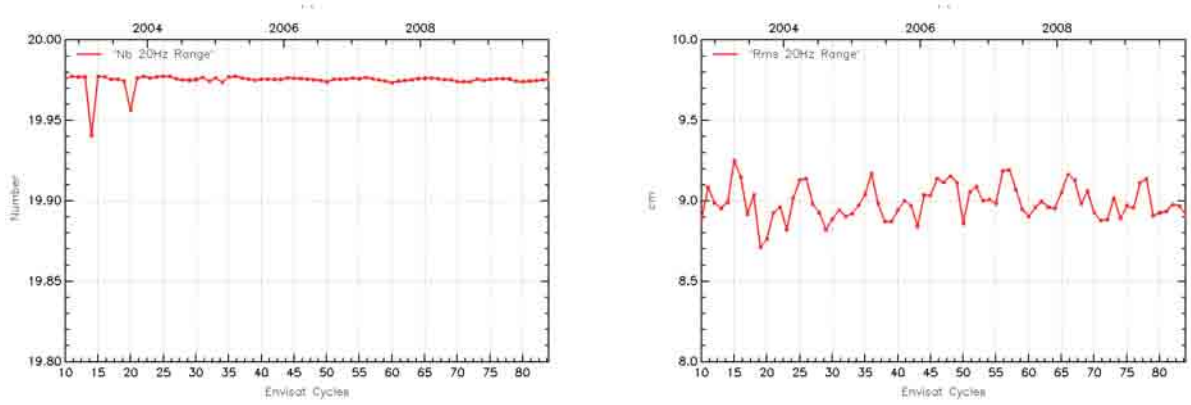

Figure 13: ***left**) Mean per cycle of the number of 20 Hz elementary range measurements used to compute 1 Hz range. **right**) Mean per cycle of the standard deviation of 20 Hz measurements.*

The corresponding S-Band parameters have a less stable behaviour (see figure 14). The S-Band mean number and RMS of 20Hz measurements have respectively an increasing and decreasing trend. Moreover jumps are noticed on the two plots on cycle 41 due to a change in the IPF Level 1 processing chain (Rx dist Fine). Moreover, from this cycle, the ascending and descending values are slightly different on the S-Band mean RMS of 20Hz measurements.

Histogram of RMS of Ku Range on cycle 84is plotted in figure 15.

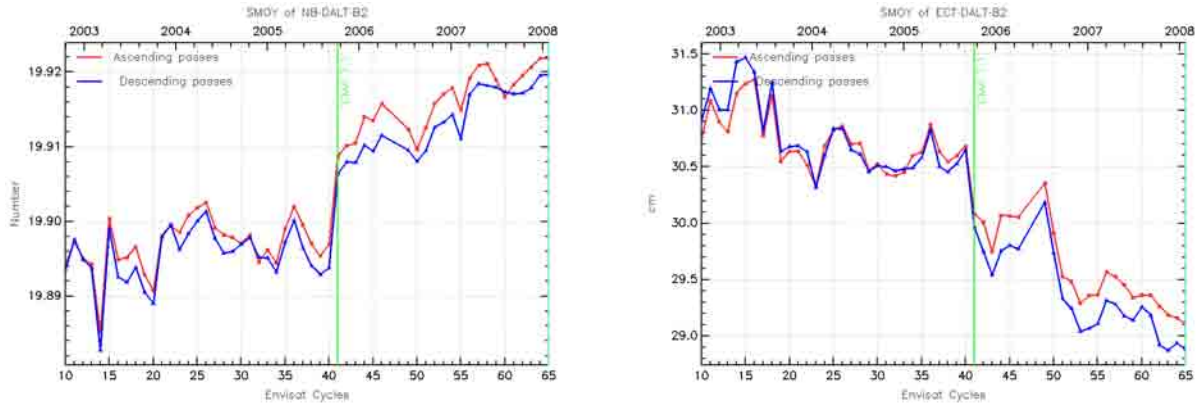

Figure 14: *Mean per cycle of the S-Band number of measurements (left) and standard deviation (right) of 20 Hz measurements separating ascending and descending passes (cm)*

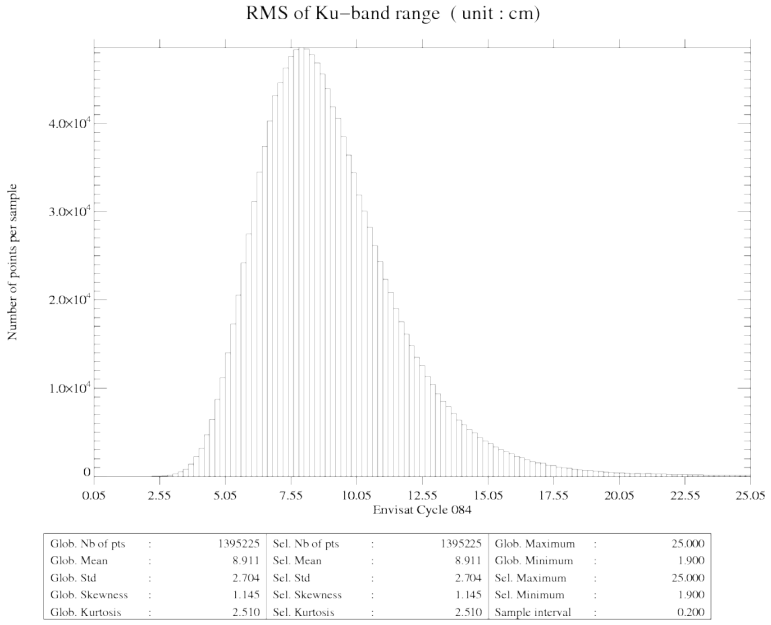

Figure 15: *Histogram of RMS of Ku range (cm). Cycle 84.*

5.2. Off-nadir angle from waveforms

The off-nadir angle is estimated from the waveform shape during the altimeter processing. The square of the off-nadir angle is plotted in Figure 16. The mean value is between 0.02 deg2 and 0.03deg2 before cycle 41. There is a slight rising trend over this period and a 0.005 deg2 jump between cycles 21 and 22 which is due to the upgrade of the IF mask filter auxiliary data file. The mean value observed during this period is not significant in terms of actual platform mispointing. This is due to the way the slope of the waveform trailing edge is computed. On cycle 41, a 0.02 deg2 drop occurs, due to an improvement of the mispointing estimation in IPF 5.02. The mispointing was estimated through the waveform trailing edge slope using an adaptative window that defines the beginning and the end of the slope. To avoid the filter bump effect that leads to high value of the mispointing, an optimum and fixed gate was estimated and

implemented. Note that the rising trend observed previously desappeared. This is probably an effect of the regular update of the IF filter since cycle 41. Finally, a smaller value is noticed for the cycle 48, for which altimeter was turned to its B-Side for a short period (cf. details in part 3).

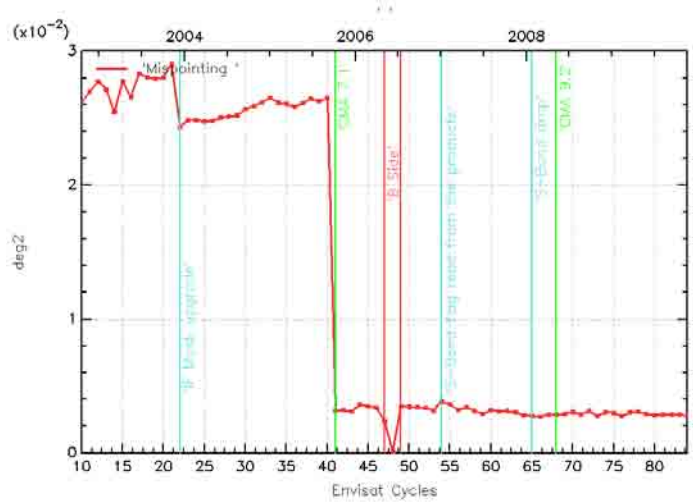

Figure 16: *Mean per cycle of the square of the off-nadir angle deduced from waveforms (deg2).*

The histogram of the squared mispointing is plotted in figure 17.

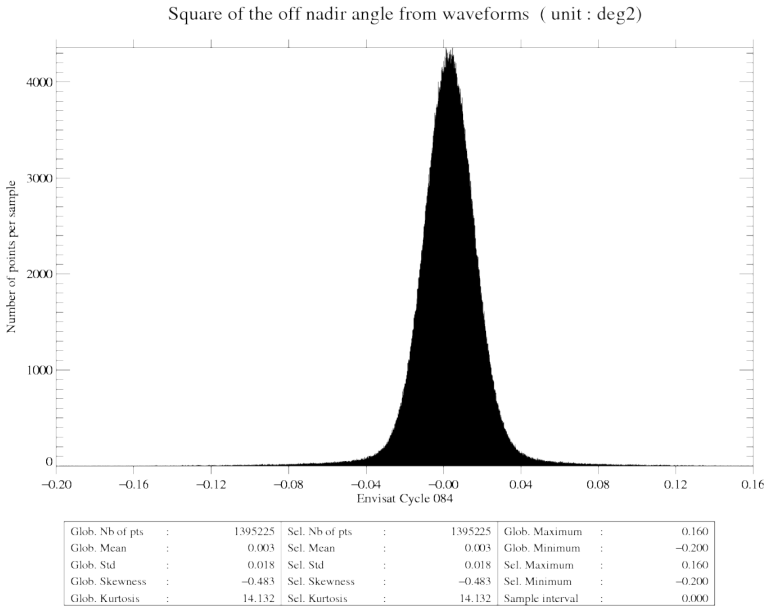

Figure 17: *Histogram of off-nadir angle from waveforms (deg2). Cycle 84.*

5.3. Significant Wave Height

The cycle by cycle mean and standard deviation of Ku and S-Band SWH are also plotted in figure 18. The curve reflects sea state variations. The mean value of Ku SWH is 2.66 m. The S-Band mean SWH is very close, less than 10 cm apart. The cycle by cycle mean of Envisat-Jason-1

differences and ERS-2-Envisat differences are plotted in Figure 18. The data taken into account for Jason-1 are the GDR-B until 233 and GDR-C afterwards. Note that for ERS, data concern the sole North Atlantic ocean (since july 2003, see 3.2.2.). For contractual reasons, they are not monitored anymore after cycle 42. These differences are quite stable. Envisat SWH is respectively 14 cm and 22 cm higher than Jason-1 and ERS-2 SWH. As for range parameters, some strange behaviours on S-Band SWH are also noticed (see Figure 19): jumps occurred during the S-Band time series (cycle 41 and 51) due to a change in the IPF Level 1 processing chain (Rx dist fine), and inconsistencies between ascending and descending passes.

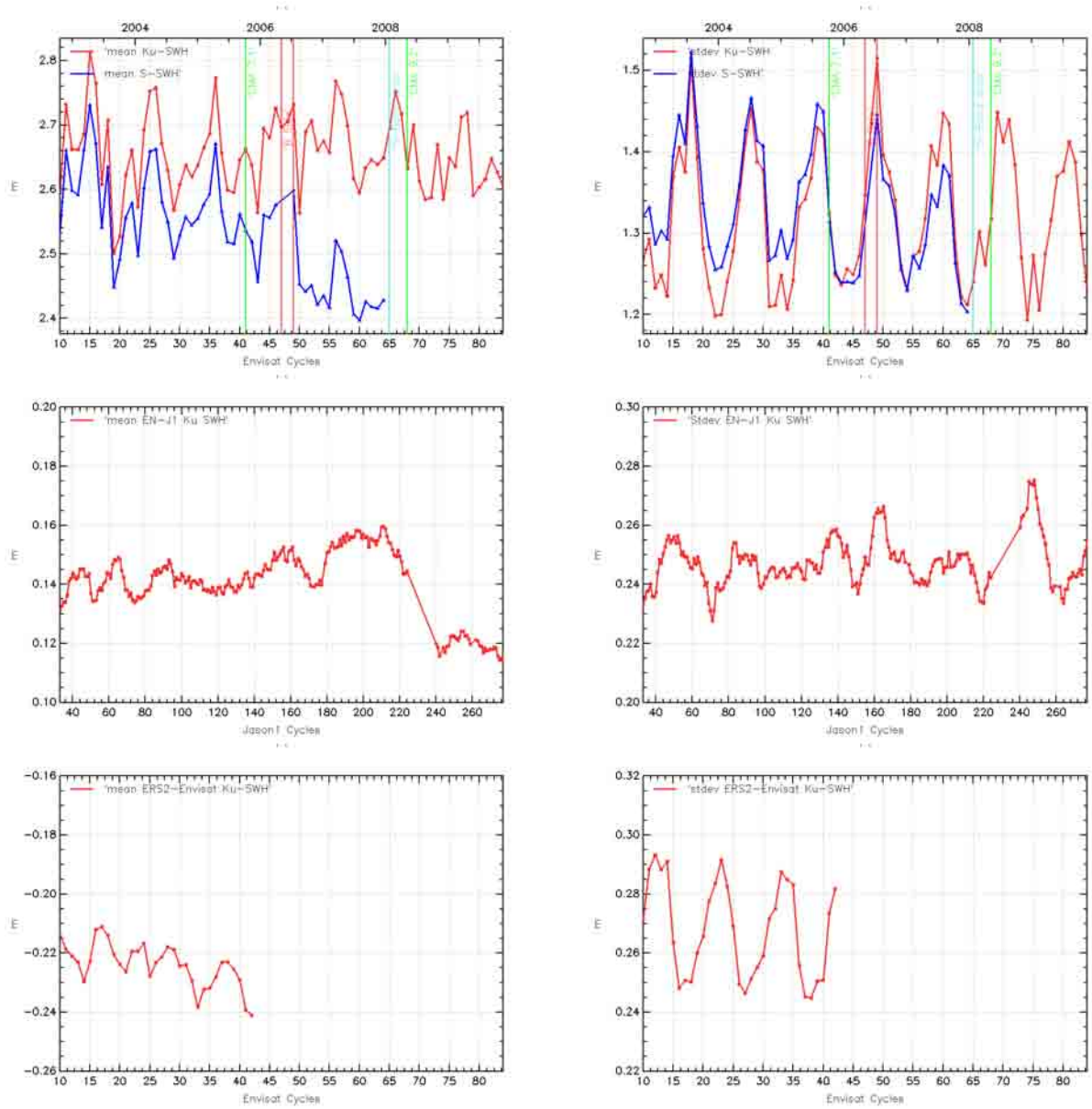

Figure 18: *Global statistics (m) of Envisat Ku and S SWH* ***top****) Mean and Standard deviation.* ***middle****) Mean Envisat-Jason-1 Ku SWH differences at 3h EN/J1 crossovers computed with 120 days running means.* ***bottom****) Mean and Standard deviation of ERS-2-Envisat Ku SWH collinear differences over the Atlantic Ocean.*

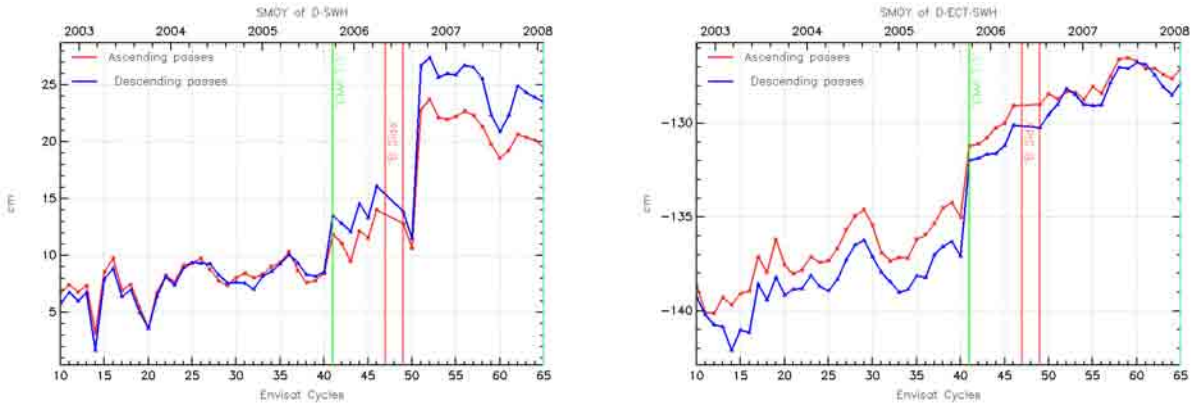

Figure 19: ***left)*** *Mean per cycle of SWH(Ku)-SWH(S).* ***right)*** *Mean per cycle of RMS20Hz[SWH(Ku)]-RMS20Hz[SWH(S)].*

Histogram of Ku SWH is plotted in figure 20. The Ku SWH histogram has a good shape.

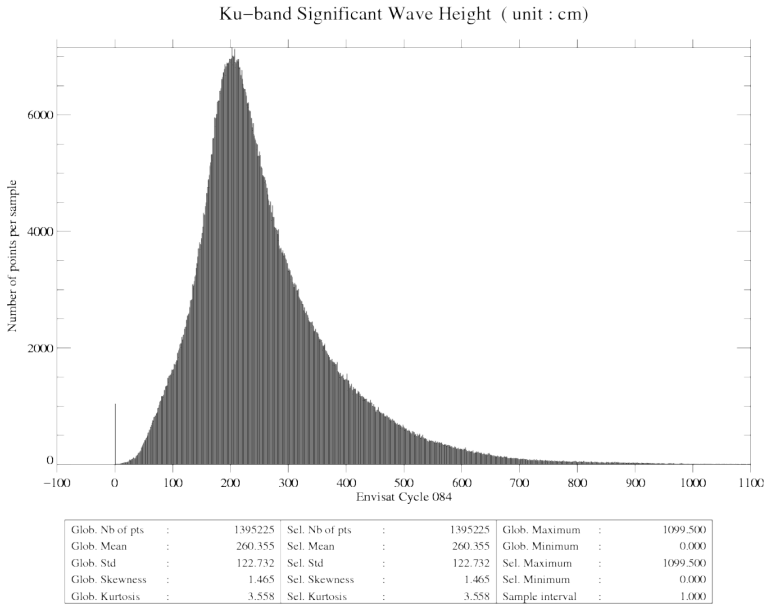

Figure 20: *Histogram of Ku SWH (m). Cycle 84.*

5.4. Backscatter coefficient

The cycle by cycle mean and standard deviation of Ku and S-Band Sigma0 are plotted in Figure 22. Note that a -3.5 dB bias has been applied (Roca et al., 2003 [64]) on the Ku-band Sigma0 in order to be compliant with the wind speed model (Witter and Chelton, 1991 [78]). The mean values in Ku band are stable, around 11.1 dB. Two 0.66 dB jumps are visible on the S-Band on cycles 14 and 22. They are due to a correction of the AGC evaluation. This modification has been included in IPF version 4.56, used from cycle 22 onwards for the current processing and for all the reprocessed cycles. The cycle by cycle mean of Envisat-Jason-1 differences and ERS-2-Envisat differences are plotted in figure 22. The data taken into account for Jason-1 are the GDR-B until 233 and GDR-C afterwards. The difference between Envisat and Jason-1 Ku-band Sigma0 is between -2.9 and -3.02 dB. This high value is explained by the fact that, Envisat Sigma0 value has been biased and not Jason-1. This mean difference has increased by 4.10-2dB/year between cycles 38 and 140 Jason-1 (corresponding to cycle 13 to 41 of Envisat) and remains constant afterwards. This drift was checked to be unchanged after correcting it from the atmospheric attenuation computed with a homogenous reprocessed set of brightness temperature. These sigma0 differences obviously impact the wind consistency between the two satellites. Note that the wind from the ECMWF model, which does not assimilate Jason-1 data, shows a very good agreement with the Jason-1 wind with a slope close to 6 cm/s/yr whereas Envisat wind trend is much lower, 1.3cm/s/year (see [4]. This trend difference could mean that the Envisat wind slightly drifts. This potential trend, though slight, has to be closely monitored.

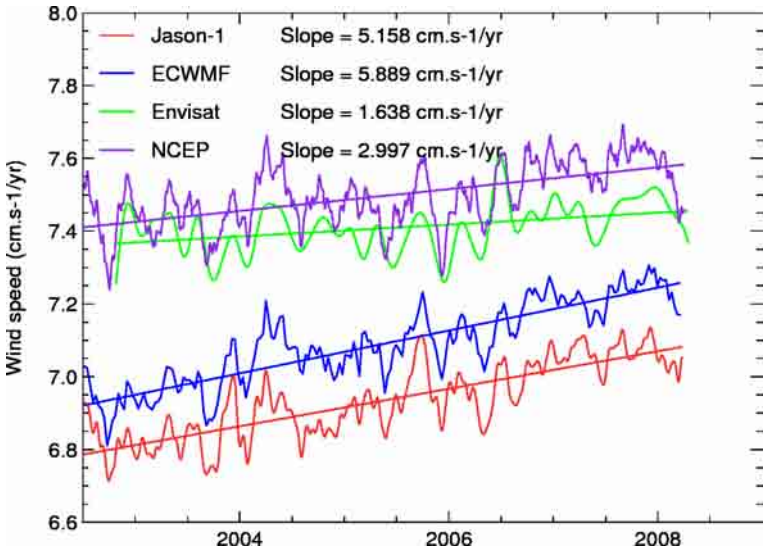

Figure 21: *Wind speed from different sources (EN, J1, ECMWF, NCEP).*

The mean ERS-2-Envisat Ku-band Sigma0 difference is 0.05 dB. However, this mean value accounts for the calibration correction applied in the ground processing to be compliant with the wind speed algorithm (Witter and Chelton, 1991 [78]). The monitoring of (ERS-2 - Envisat) Sigma0 differences exhibits a 0.1 dB jump between cycles 38 and 39. This jump occurs at the end of cycle 38, on the 4th July 2005 11:29 UTC. Since no jump is observed on the Envisat/Jason-1 differences, it may be attributed to ERS-2.

Histograms of Ku Sigma0 is plotted in figure 23. The Ku Sigma0 histogram has a good shape.

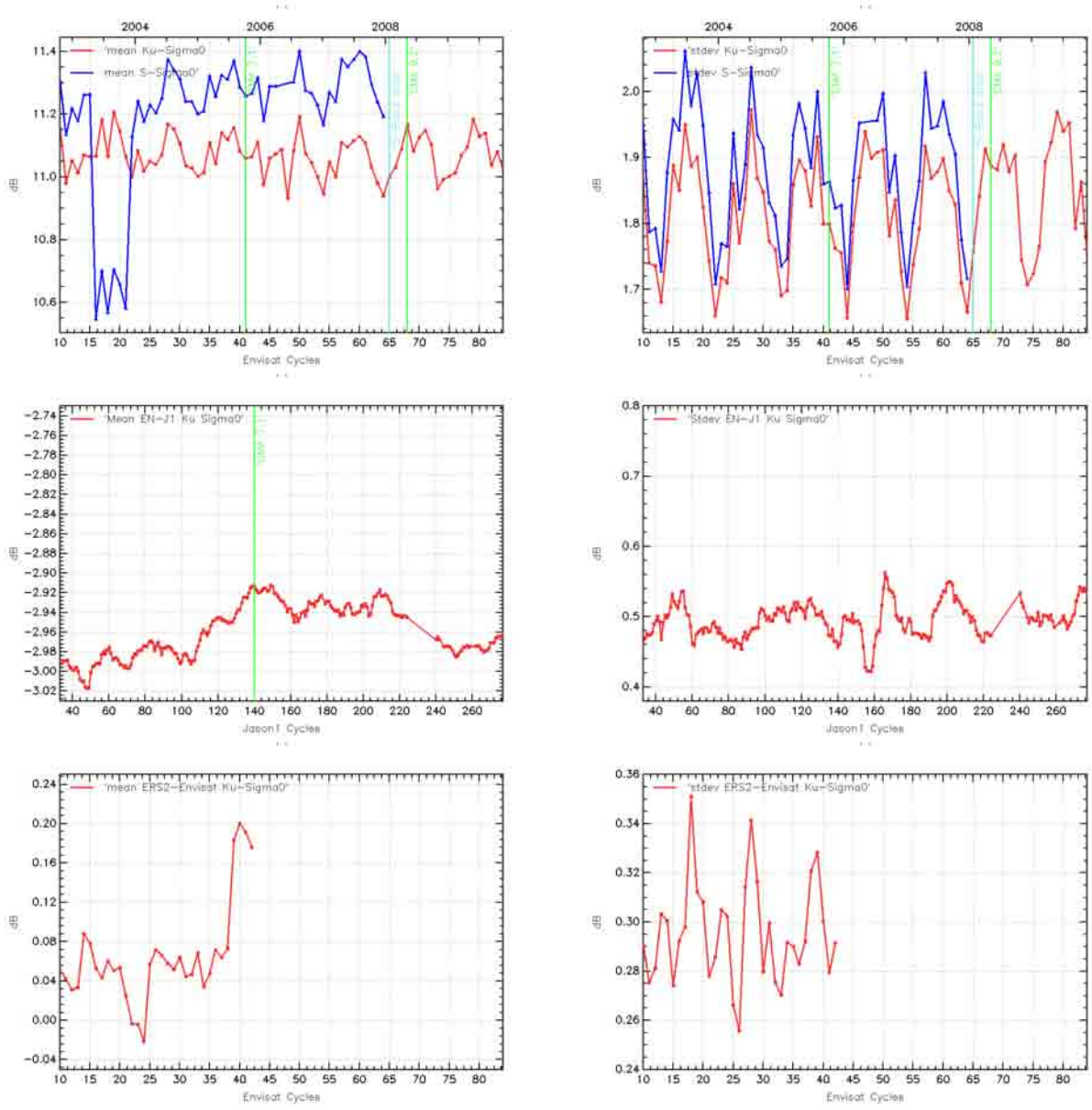

Figure 22: *Global statistics (dB) of* ***top****) Envisat Ku and S Sigma0 Mean and Standard deviation.* ***middle****) Mean Envisat-Jason-1 Ku Sigma0 differences at 3h EN/J1 crossovers computed with 120 days running means.* ***bottom****) Mean and Standard deviation of ERS-2-Envisat Ku Sigma0 collinear differences over the Atlantic Ocean.*

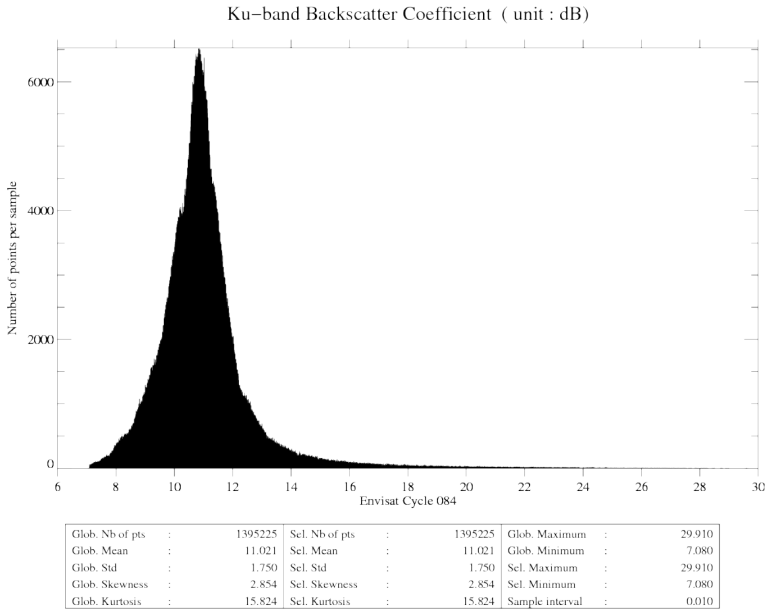

Figure 23: *Histogram of Ku Sigma0 (dB). Cycle 84.*

5.5. Dual frequency ionosphere correction

As performed on TOPEX (Le Traon et al. 1994 [44]) and Jason-1 (Chambers et al. 2002 [15]) it is recommended to filter dual frequency ionosphere correction on each altimeter dataset to reduce noise. A 300-km low pass filter is thus applied along track on the dual frequency ionosphere correction. As previously mentioned, the JPL GIM ionosphere corrections are computed to assess the dual frequency altimeter based ionosphere correction. The cycle by cycle mean of dual frequency and JPL GIM ionosphere correction are plotted in figure 24 (top). The mean value of the two corrections is clearly decreasing since the beginning of Envisat mission due to inter-annual reduction of the solar activity. The mean differences (GIM-Dual frequency), plotted in figure 24 (bottom), is stable around -0.8 cm. It is stronger in absolute value for high ionosphere corrections, for descending passes (in the daytime). The standard deviation of the difference is also plotted in figure 24 (bottom right). Low values, less than 2 cm, indicate a good correlation between dual-frequency and GIM corrections (note that the low value <0.5 cm is obtained for cycles 47-48 for which the switch between SideA-SideB happenned). Notice that, in the GDR products, the same sea state bias (SSB) has been used to correct the Ku and S-Band Ranges for cycles 9-40 (Sep 2002-Sep 2005). Since cycle 41, a suitable Ku and S-Band SSB correction is used on the two bands before computing the dual frequency ionosphere correction from Ku and S-Band ranges (Labroue 2004 [40]). In this analysis, the sea state bias (SSB) used to correct the S-Band Ranges for cycles 9-40 is updated in its right S-Band version. The differences with the GDR correction are very small with no impact on the global statistics and only small geographic variations between -1 mm and +1.5 mm (Labroue 2004 [40]). However, the update was done because the impact was shown to be significant in the Mean Sea Level Trend estimation of around 0.4 mm/year (see Ollivier et al, 2009 **??**).

Since the S-Band loss, this correction is not available anymore. As written before, the GIM Ionospheric correction is used instead. The same GIM model is used to compute the iono corrections on Envisat and Jason-1. The quality of Envisat's ionosphere correction can thus be assessed by monitoring the dual-frequency-GIM based ionosphere correction on Jason-1. The cycle by cycle mean of dual frequency and JPL GIM ionosphere correction are also plotted in figure 24. Different trends are observed on the two curves.
Concerning the discrepencies between both missions, note that, in terms of noise, the higher noise for Jason-1 is due to a higher noise in the C band (used for Jason-1 bifrequency ionosphere) than in S-Band (used for Envisat one). The filtering step applied on both ionospheres from the products enables to have comparable noise level for both missions. In terms of bias, differences are likely due to the difference of altitude for both missions, but the stability of Envisat ionosphere difference (Bifrequency-GIM) can also be seen as an anomaly at the beginning of Envisat mission (before cycle 22), reducing the dependancy between the absolute value and the bias on this correction (observed on Jason-1). This would deserve more investigation.

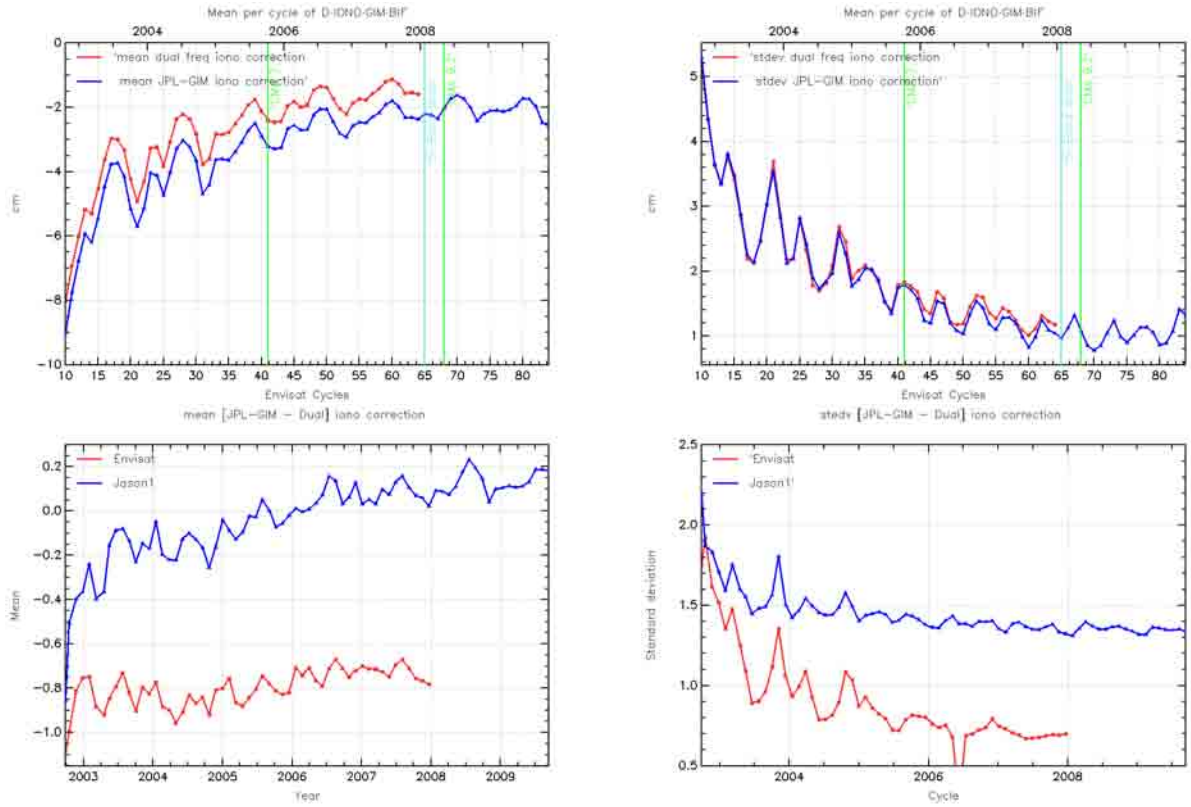

Figure 24: *Comparison of global statistics of Envisat dual-frequency and JPL-GIM ionosphere corrections (cm).* ***top****) Mean and standard deviation per cycle of Dual Frequency and GIM correction.* ***bot****) Mean and standard deviation of the differences for Envisat and Jason-1*

5.6. MWR wet troposphere correction

A neural network formulation is used in the inversion algorithm retrieving the wet troposphere correction from the measured brightness temperatures (Obligis et al., 2005 [57]). As an example, the scatter plot of MWR correction according to ECMWF model for cycle 84is given in figure 25.

Since the beginning of the mission, the instrumental parameters at 36.5 GHz have been drifting and investigations are in progress to identify the source for these drifts. In particular, different behavior is observed depending on the brightness temperature values. Mean and standard deviation of (MWR-ECMWF model) differences are plotted in figure 27. The difference is not really stable, though the global mean remains small. It rises by 3mm between cycles 11 and 27 (19300-19850), which corresponds to 1.8 mm/year. Then, it decreases by 2mm between cycle 27 and 46 (20525). Finally, an annual signal of about 1.5mm of amplitude seems to appear on cycle 47. This annual signature was previously attributed to successive jumps on the ECMWF side as explained into S. Abdalla's presentation (QWG 2008), because similar paterns could be seen when comparing the difference of correction radiometric - model on Jason-1 (see 27). On the plot, the main model changes are marked out by vertical lines (see ECMWF web site [20]). Today, the hypothesis of a real annual cycle is rehabilitated. Actually, this signal becomes really clear and uncorrelated to the ECMWF updates when separating Ascending and Descending tracks (see 28). Furthermore, selections per values of wet troposphere also enlights this annual signal. Therefore,

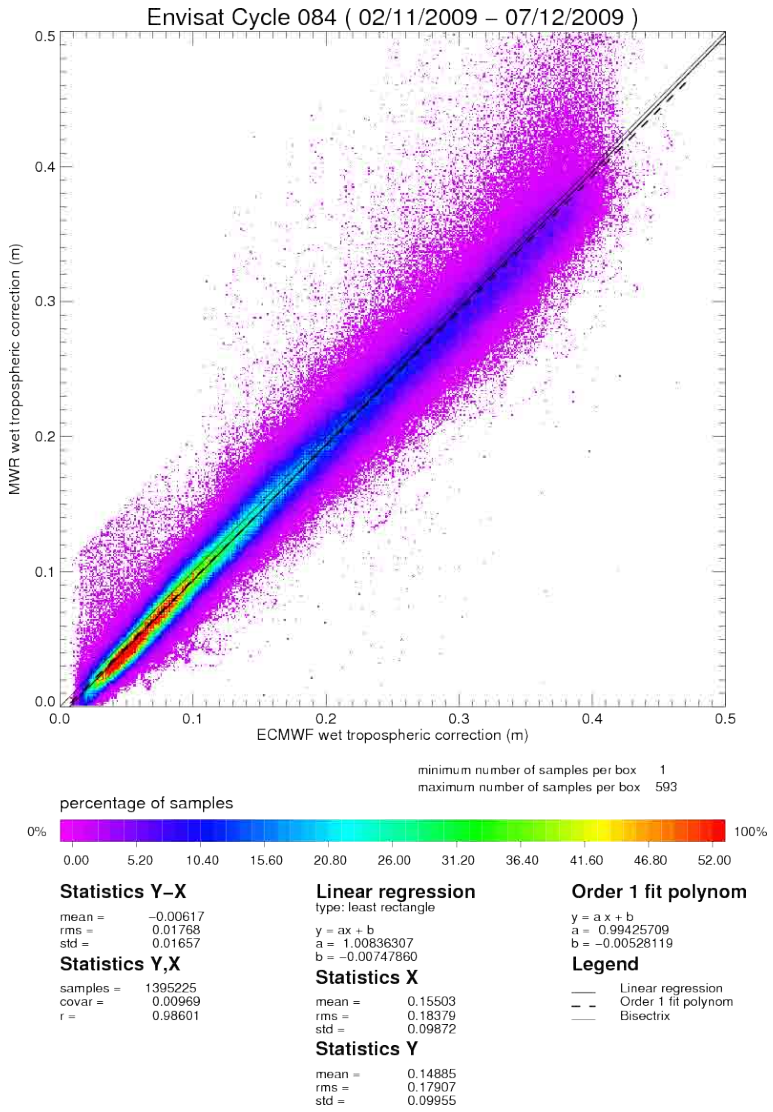

Figure 25: *Scatter plot of MWR correction according to ECMWF model (m)*

it would likely be a difference of behavior between model and radiometer in some conditions. This signal is currently under investigation.
The standard deviation is also very variable throughout the mission. It drops down by 2 mm from cycle 13 (19370), decreases afterwards linearly from cycles 14 to 41 (20350) and adopts a cahotic behavior until cycle 65 (21190) where it stabilizes around 1.5 cm. This decrease cohincidates with another change of model but because MWR seems to undergo a bigger jump than ECMWF series, it could also be due to a larger amount of data taken into acount at the end of the mission (see part 4.3.4..)
A complete monitoring of all the radiometer parameters is available in the cyclic Envisat Microwave Radiometer Assessment available at http://earth.esa.int/pcs/envisat/mwr/reports/ ([61]).

The (ERS-2 -Envisat) cyclic 23.8 GHz brightess temperatures differences over the Atlantic area are plotted on figure 29. The ERS-2 drift proposed by Eymard et al., 2003 [23] is applied. The correction of the drift proposed by Scharroo et al., 2004 [70], should decrease the mean difference by 0.8K as described in Mertz et al., 2004 [54]. Nevertheless, the mean

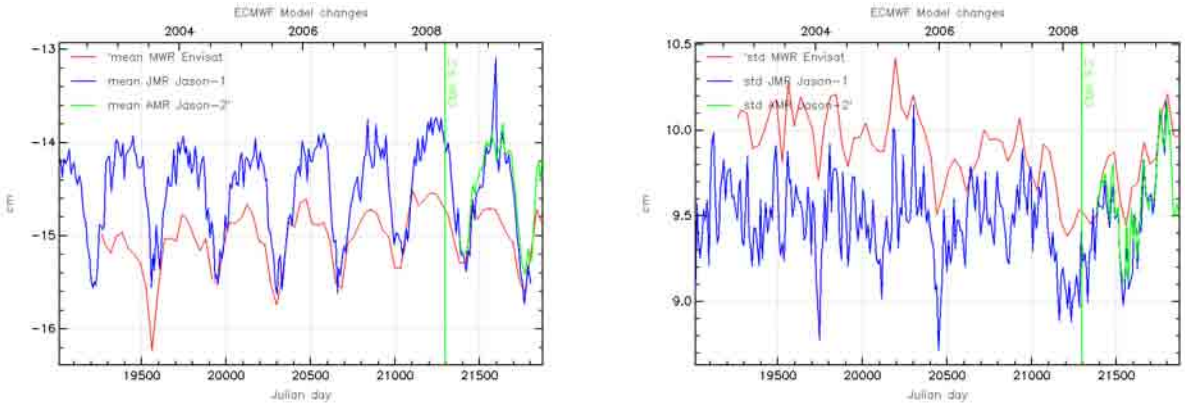

Figure 26: *Comparison of global statistics of wet troposphere corrections (cm). Mean (**left**) and standard deviation (**right**) of MWR EN, JMR Jason-1 and AMR Jason-2 corrections.*

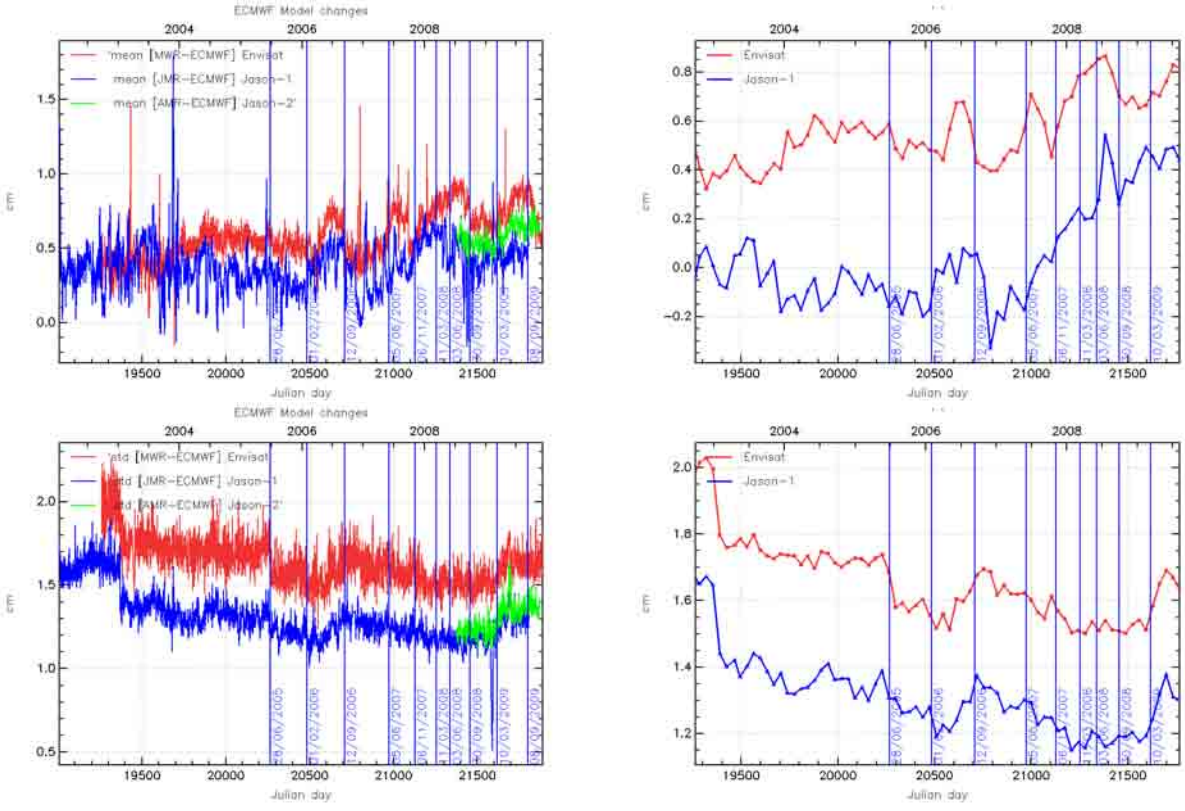

Figure 27: *Comparison of global statistics of Envisat MWR/Jason-1 JMR and ECMWF wet troposphere corrections. Mean per day (**left**) and mean per cycle (**right**) of the differences of correction. Blue vertical lines represent the major changes of ECMWF model.*

difference variations are more steady for the period after cycle 21. The (ERS-2 -Envisat) TB36.5 GHz values are also reported in figure 29. The differences before and after cycle 18 have a different behaviour: one observes a great decrease from -2 to -4 K between cycles 13 and 17 whereas the curve seems to be steadier after cycle 18. This is not an impact of the coverage of the data since in the restricted area, the statistics reveals the same features. They also

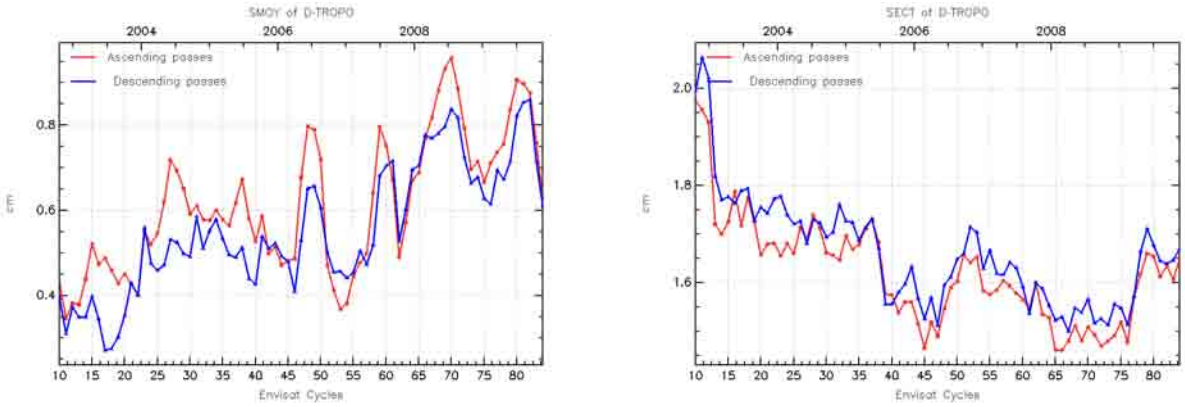

Figure 28: *Comparison of global statistics of Envisat MWR and ECMWF wet troposphere corrections separating ascending and descending passes (cm). Mean (**left**) and standard deviation (**right**) per cycle of MWR and ECMWF corrections.*

show an unusual behaviour of the TB values during that period. Note that this behaviour is not visible on hottest or coldest values but mainly on the mean values. The impact of the drift of the TB36.5 on (ERS-2 -Envisat) wet troposphere correction differences is visible in figure 30.

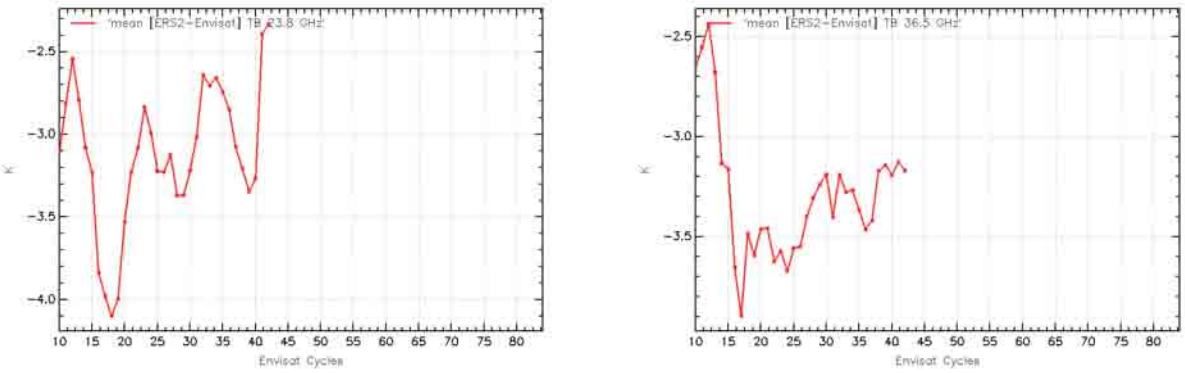

Figure 29: *Monitoring of the (ERS-2 - Envisat) brightness temperatures*

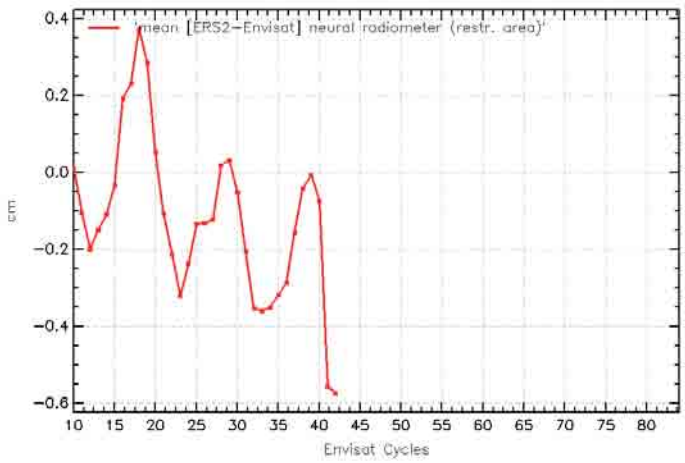

Figure 30: *Monitoring of the (ERS-2 - Envisat) wet troposphere correction*

6. Sea Surface Height performance assessment

One of the main objectives of the Calibration and Validation activities is to assess the performance of the whole altimeter system. This means that the quality of each parameter of the product is evaluated, in particular if it is likely to be used in the Sea Surface Height (SSH) computations. Conventional tools like crossover differences and repeat-track analyses are systematically used in order to monitor the quality of the system.

6.1. SSH definition

The standard SSH calculation for Envisat is defined below.

$$SSH = Orbit - Altimeter\ Range - \sum_{i=1}^{n} Correction_i$$

$$\begin{aligned}\sum_{i=1}^{n} Correction_i &= Dry\ troposphere\ correction : new\ S1\ and S2\ atmospheric\ tides\ applied \\ &+ Combined\ atmospheric\ correction :\ MOG2D\ and\ inverse\ barometer \\ &+ Radiometer\ wet\ troposphere\ correction \\ &+ Filtered\ dual\ frequency\ ionospheric\ correction\ /GIM\ model\ after\ cycle\ 64 \\ &+ Non\ parametric\ sea\ state\ bias\ correction \\ &+ Geocentric\ ocean\ tide\ height,\ GOT\ 2000 :\ S1\ atmospheric\ tide\ is\ applied \\ &+ Solid\ earth\ tide\ height \\ &+ Geocentric\ pole\ tide\ height\end{aligned}$$

As said in 3.2.1., the new geophysical correction associated with version CMA7 have been updated on the whole data-set in order to have the most homogeneous time series. For Envisat, the only discontinuities existing in our dataset are :

- Between cycle 40 and 41 and between 68 and 69 due to the orbit, computed using:
  - GRIM5 gravity model for cycles 9 to 40
  - EIGEN-CG03C from cycle 41 to 68
  - a time variable gravity field after 69.
- Between cycle 40 and 41 due to the retracking (IF monthly estimations from cycle 41 onwards).

The USO auxiliary correction distributed by ESA is used in Envisat SSH computation.

6.2. Single crossover mean

SSH crossover differences are computed on a one-cycle basis, with a maximum time lag of 10 days, in order to reduce the impact of ocean variability which is a source of error in the performance estimation. The mean of crossover differences represents the average of SSH differences between ascending and descending passes. This difference can reflect orbit errors or errors in geophysical corrections. The fact that Envisat is Sun-synchronous can play a role since the ascending passes and descending passes respectively cross the equator at 10pm local time

and 10am local time. Thus all the parameters with a daily cycle can induce errors resulting in ascending/descending differences. The error observed at crossovers can be split into two types: the time invariant errors and the time varying errors.

The analysis of the time invariant errors has been performed last year by comparing local averages of crossover differences over cycles 10 to 40 and 41 to 72 (Ollivier et al, 2009 **??**, section 6.2). On the 10-40 map, systematic differences between ascending and descending passes are observed in some areas. Mean ascending/descending differences are locally higher than 4 cm (Southern Pacific and Southern Atlantic). These patterns, called geographically correlated radial orbit errors, are induced by errors in the gravity models used in the orbit computation. On the 41-72 map the geographically correlated orbit errors are almost fully removed thanks to the use of EIGEN-CG03C gravity model. Small signals remain in Indian and Pacific Oceans.
Besides the systematic ascending-descending errors, a time varying error can also be observed at crossovers. The cyclic mean ascending-descending SSH differences at crossovers shows this error in Figure 31. The cyclic mean crossover differences have been plotted in three different configurations: full data set, deep ocean data, and deep ocean data with low variability, and excluding high latitudes. A strong annual signal is evidenced on the 3 curves. Its amplitude is approximately 1 cm.

A specific study has been carried out in order to analyse deeply this signal. The results of this study are available in Ollivier et al, 2009 **??**. The main results of this study is first that the amplitude is geographically dependent, and second that the geographical patterns depend on the oceanic tide model used in the SSH.

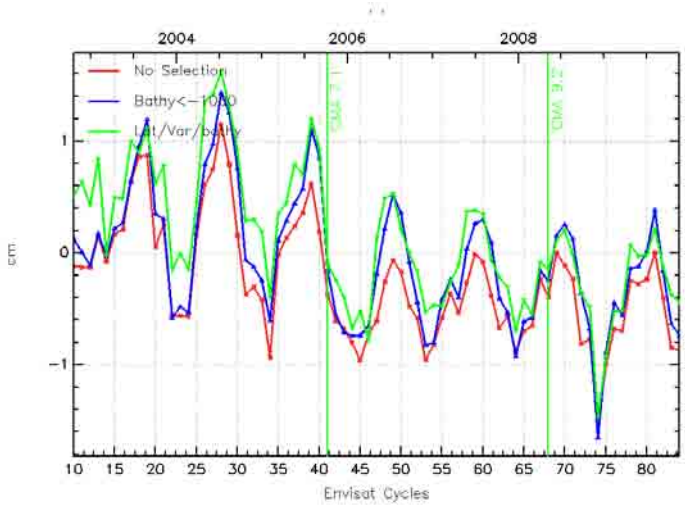

Figure 31: *Time varying 35-day crossover mean differences (cm). Cycle per cycle Envisat crossover mean differences. An annual cycle is clearly visible. Blue: shallow waters (1000 m) are excluded. Green: shallow waters excluded, latitude within [-50S, +50N], high ocean variability areas excluded*

Thanks to this year reprocessing, another plot could be performed see figure 32: comparing GDRC standards for J1 and for Envisat's POE to the previous standards and the annual signal is much decreased for Envisat. On the contrary a periodic signal seems to appear on Jason-1 time series. This very good result is further investigated in part .

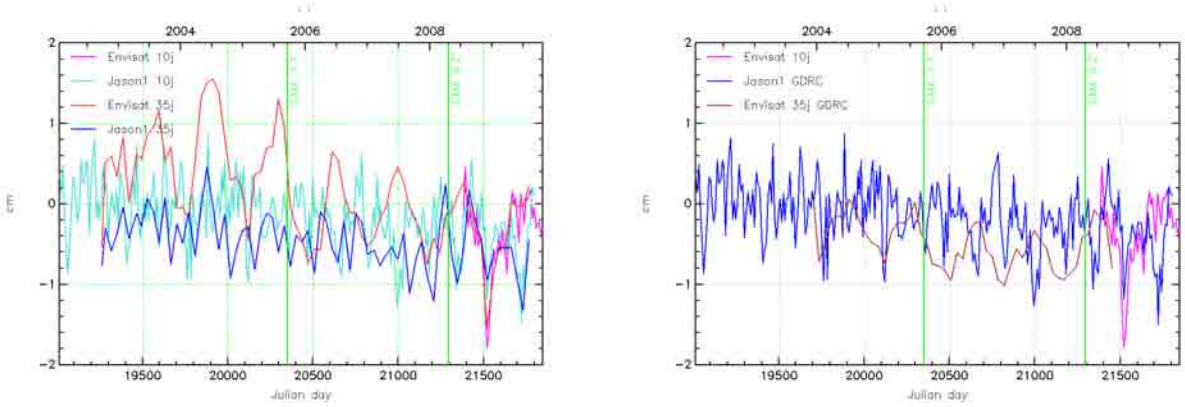

Figure 32: *Time varying crossover mean differences (cm) using Envisat GDR-A-B-C (red 35-day / pink 10-day) and Jason-1 GDR- B(blue 35-day / turquoise 10-day) (left). Same plot using GDRC standards: the annual signal is much decreased for Envisat. On the contrary a bi-annual signal seems to appear on Jason-1 time series.*

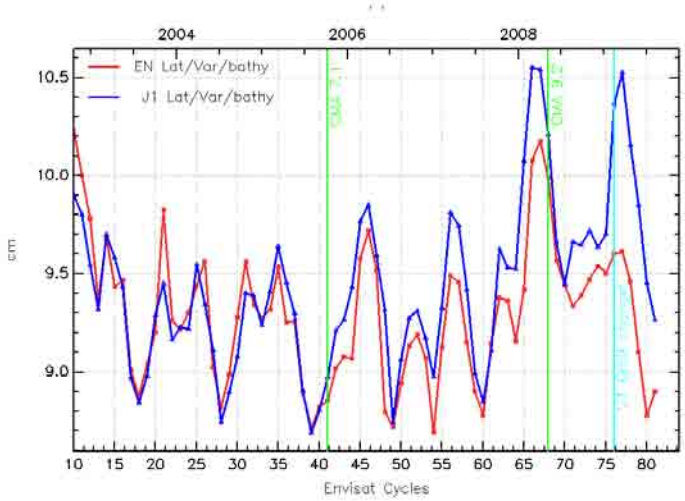

Figure 33: *Standard deviation of along track SLA (m), shallow waters excluded, latitude within [-50S, +50N], high ocean variability areas excluded*

Figure 33 is another way to show that both altimeters have very similar performances. It shows that Envisat and Jason-1 have similar Standard deviation of along track SLA before cycle 41 and that Envisat's curve stands around 1mm under Jason's afterwards until reaching 2 to 3 mm for cycle 80. This improvement is due to the CMA/IPF now version. Note that the relative position of Envisat below Jason-1 was shown to be to the different geographic density of points, which is over estimated at high latitudes for Jason-1 compared to Envisat. To avoid that, statistics averaged per boxe will be provided in the future. Also note that looking at the along track performance enables to enlight the seasonnal Grace gravity model, wich cannot be seen with the cross over analysis only.

Figure 34 shows a good consistency after mid 2005. Note that the 2 last points are slightly higher (5mm) than the others. More data are needed though to be able to drow any conclusion.

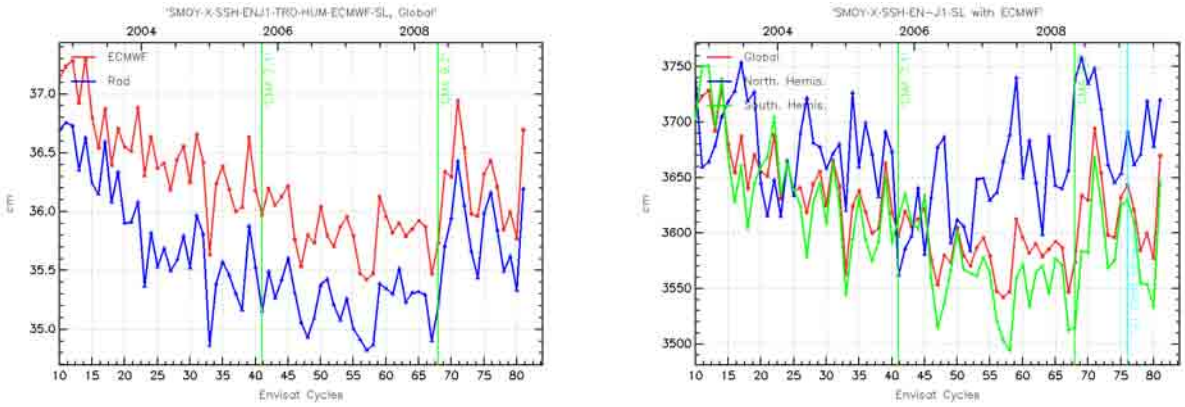

Figure 34: *Mean EN-J1 SSH differences at dual crossovers (cm) for Envisat on global ocean (**left**), and separating Northern and Southern hemispheres (**right**).*

6.3. Variance at crossovers

The variance of crossover differences conventionally gives an estimate of the overall altimeter system performance. Indeed, it gathers error sources coming from orbit, geophysical corrections, instrumental noise, and part of the ocean variability. The standard deviation of the Envisat SSH crossover differences has been plotted in Figure 35, depending on three data selection criteria. Without any selection, a seasonal signal is observed because variations in sea ice coverage induce changes in ocean sampling by altimeter measurements. When only retaining deep ocean areas, excluding high latitudes (higher than 50 deg.) and high ocean variability areas, the standard deviation then gives reliable estimate of the altimeter system performances. In that case most of the cycles have a standard deviation between 7.5 and 7.7 cm. But there are some exceptions that can be explained. Cycles 15 and 48 are strongly different because of the low number of crossover points. There are less than 10000 crossovers whereas other cycles lead to more than 20000. Cycles 21 and 26 have higher values because of bad orbit quality over a few passes related to out-of-plane maneuvers. Cycle 21 has a strong value (8.5 cm) because of the combined effect of 2 maneuvers, intense solar activity between these 2 maneuvers, and lack of laser measurements between these two maneuvers. Cycle 11 has a relative high value because of missing Doris data. No degradation of the performances have been noticed since the beginning of the USO anomaly on cycle 46. This shows that the correction provided by ESA allows Envisat Ra2 data to maintain the same level of quality.

Similarly, no degradation of the performances have been noticed since the S Band power drop, thanks to the efficiant use of the GIM ionospheric correction instead of the missing bifrequency correction. To avoid any jump, the GIM correction is applied with a 8mm bias computed on the last 40 days of SLA difference with GIM and bifrequency corrections. Therefore, the GIM ionospheric correction can be considered to have a good quality for this period of low solar activity. Further studies should be made to evaluate its impact on a higher solar activity period.

In order to compare Envisat and Jason-1 performances at crossovers, Envisat and Jason-1 crossovers have been computed on the same area excluding latitude higher than 50 degree, shallow waters and using exactly the same interpolation scheme to compute SSH values at crossover locations. Performances at crossovers are compared, for the two satellites on Figure 36. The standard deviation of Envisat/Envisat and Jason-1/Jason-1 SSH crossover differences are respectively 6 cm and 5.7 cm.

The use of MLE4 retracking on Jason-1 leads to slightly lower than Envisat standard deviation at crossovers. A slight decrease is visible on Envisat plot at cycle 41, thanks to the new standards used for the POE orbit. From cycle 41 onwards, the performances of the two missions are very close.

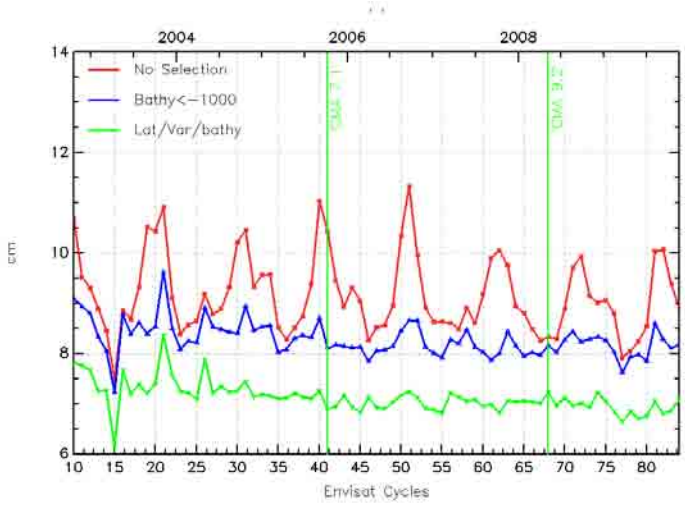

Figure 35: *Standard deviation (cm) of Envisat 35-day SSH crossover differences depending on data selection. Red: without any selection. Blue: shallow waters (1000 m) are excluded. Green: shallow waters excluded, latitude within [-50S, +50N], high ocean variability areas excluded.*

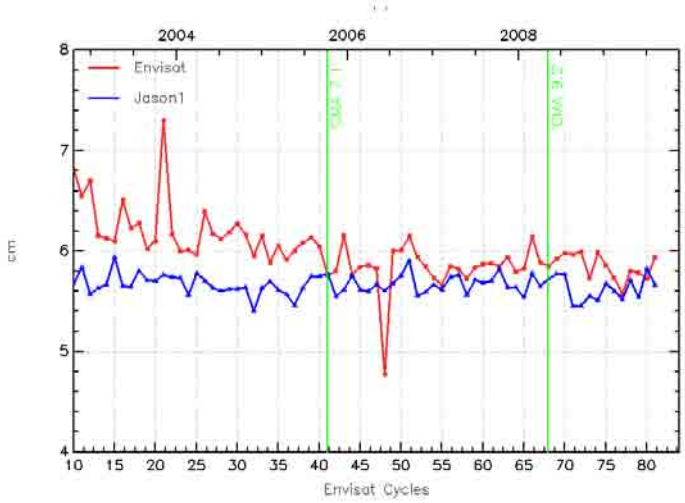

Figure 36: *Comparison of standard deviation (cm) of Envisat (red) and Jason-1 (blue) 10-day SSH crossover differences*

7. Particular Investigations

7.1. GDR-C Orbit analysis and validation

7.1.1. Introduction

A new GDR-C (and further GDR-C') standard orbit is computed at CNES simultaneously for Jason-1 and Envisat.

This standard was/will be used for Jason-1/Envisat reprocessing. It is also being used in advance for the new 2010 MSS computation as well as for DUACS off line new generation products. Prior to the complete Envisat reprocessing, an extensive study was performed to quantify the orbit quality in terms of :

- geographical biases
- data availability and maneuver management
- long term impact on Mean Sea Level, notably on ascending/descending descrepencies

For a deeper analysis, this orbit was compared to Jason-1 solution and to a similar GDR-C like standard computed at ESOC (version V4).
The aim is to validate the orbit prior to the reprocessing and to better understand discrepencies between both solutions and their impact on different missions.

7.1.2. Comparison of Envisat CNES to Jason-1 CNES and Envisat ESOC-V4 GDR-B/C evolution

7.1.2.1. Cartography of the average differences GDRC - GDRB

Figure 37 and 38 show the mean difference of GDRC -GDRB orbits for Envisat over the period concerning cycles 41 to 69 (CNES and ESOC) and for Jason-1 (cycles 1 to 239).

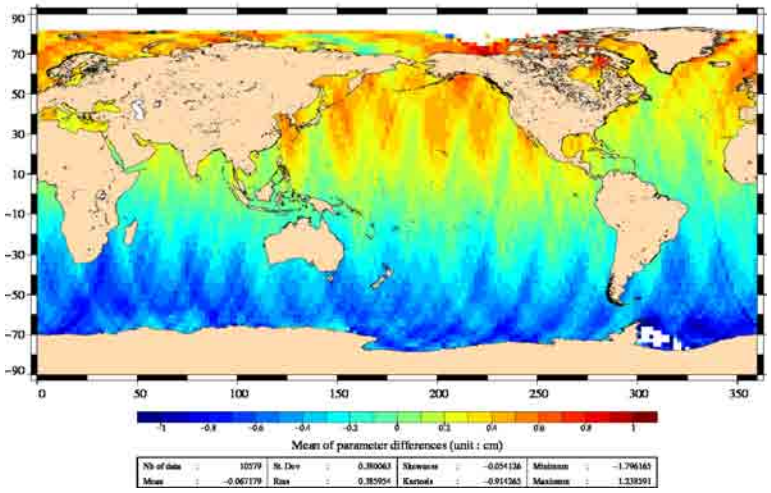

Figure 37: *Mean differences for Envisat over cycles 41 to 69 (GDRC -GDRB).*

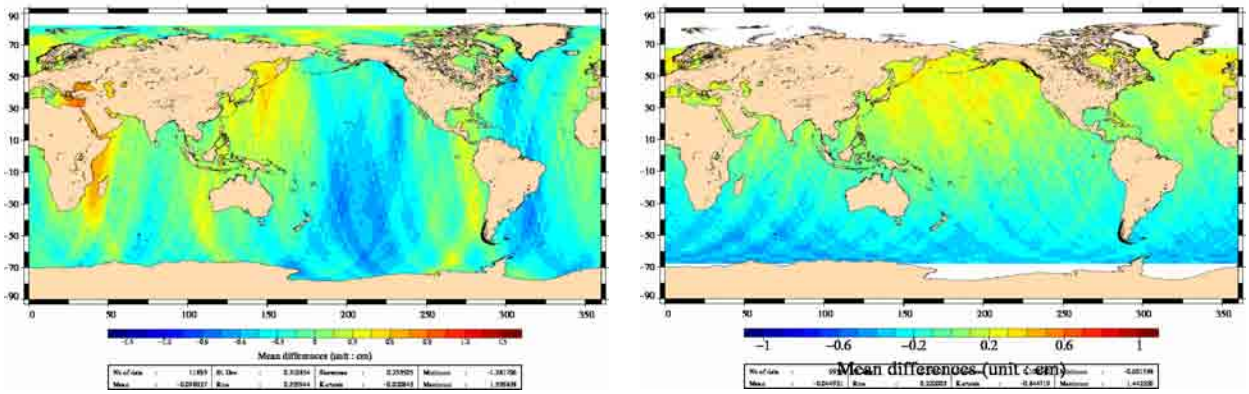

Figure 38: *Mean differences for Envisat over cycles 41 to 69 ESOC V4 -GDRB (left)/ J1 CNES GDRC (right).*

The same evolution can be observed on CNES side for both Envisat orbits (after cycle 41) and J1: a North/South signature due to the new ITRF evolution between GDRB and C (ITRF 2000 to 2005).
Contrarily, evolution on ESOC side for Envisat (after cycle 41 as well): a Basin scale signature due to the new ITRF evolution and to the gravity field variation.

7.1.2.2. Cartography of SLA variance differences

Figures here after show the SLA variance gain (compared to GDRB) from cycles 41 to 69 for Envisat CNES (Figure 39) and for ESOC V4 and Jason-1 CNES GDRC (Figure 40).

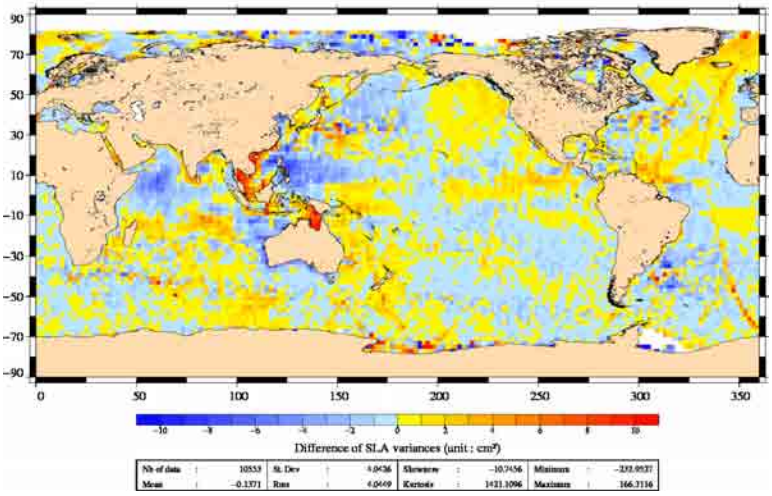

Figure 39: *VAR(CNES GDR-C orbit - CNES GDR-B Orbit), Cycles 41-69*

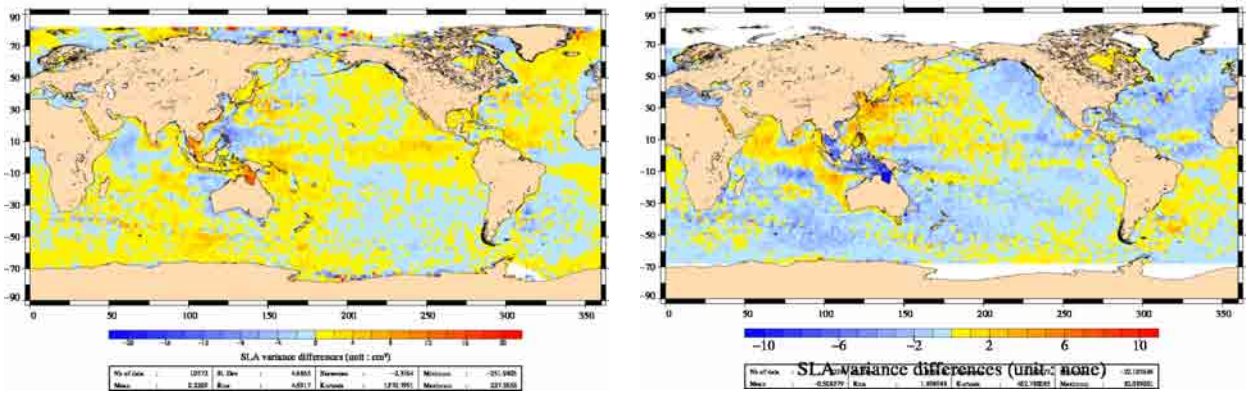

Figure 40: *left: VAR(Envisat ESOC V4 - CNES GDR-B orbit), right: VAR(CNES GDR-C - CNES GDR-B) for Jason-1.*

Surprisingly, on Jason-1, the structures observed on the SLA variance reduction/increase are inverted compared to Envisat's structures (both for CNES and ESOC solutions). This could be due to the gravity field impact on the data and should be analysed further.

7.1.2.3. Cartography of SSH variance gain at crossovers

Figures hereafter show the variance gain at crossovers (compared to GDRB orbit) for cycles 41 to 69 for Envisat CNES (Figure 41) and ESOC V4 and Jason-1 CNES GDRC (42).

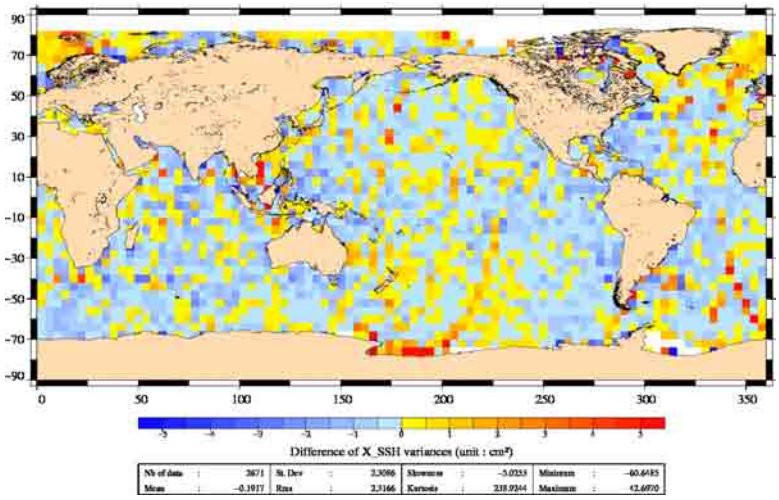

Figure 41: *Envisat CNES GDR-C orbit variance gain Cycles 41-69*

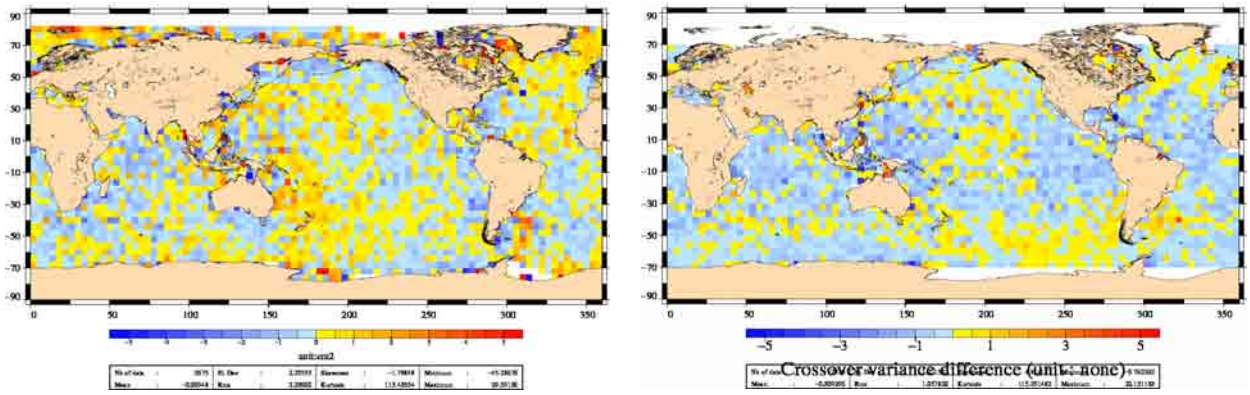

Figure 42: *Envisat ESOC V4 Orbit Cycles 41-71 (left), Jason-1 CNES GDR-C orbit(right)*

At crossovers, GDRC are seen to improve GDRB for all versions and for both missions except for 2 days listed in the editing part (cycles 44 and 68, see section 4.3) and for which tracks appear on the map. Though, better improvement is observed with CNES version (without gravity field trend) than for the ESOC version (with gravity field trend). Similar results are observed for Jason-1.

7.1.2.4 Statistics of SSH differences at crossovers : MEAN(X_SSH with CNES GDR-C orbit), MEAN(X_SSH with CNES GDR-ABC Orbit)

These figures show the mean of SSH differences at crossovers for CNES GDR-C orbit and CNES GDR-ABC Orbit per cycle.
The left hand Figure refers to the standard 10 days crossovers selection, while the right hand Figure refers to the LatBathyVar (SL2) selection ; this selection has the same time criterion, but requires moreover that : |LAT| < 50deg, BATHY < -1000m and VAR_OCE < 0.2m

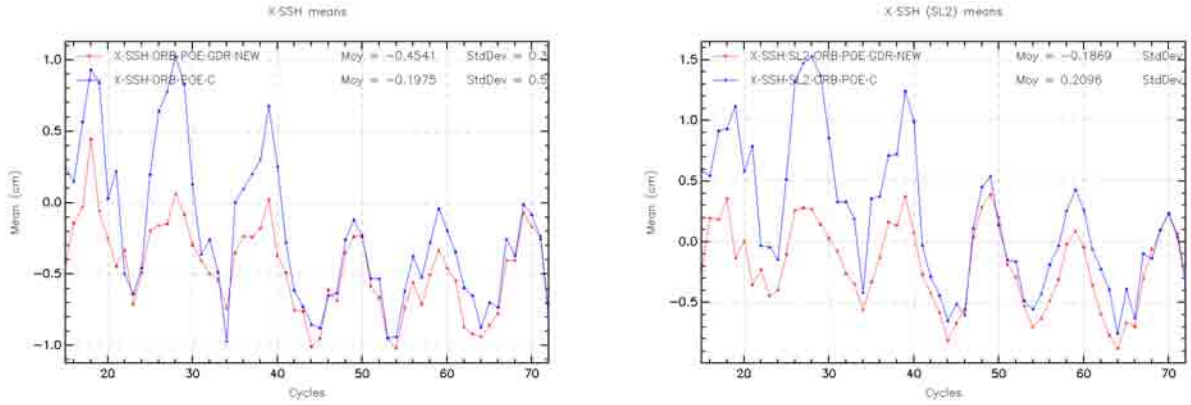

Figure 43: *X_SSH Variance with no selection (left) and Open ocean Selection (right). ORB_POE_C stands for CNES orbit GDR-ABC*

On both monitorings above, the known annual signal observed on the mean differences at crossovers for Envisat is observed.
For both selections, the new GDRC orbit is seen to reduce significantly the amplitude of this signal, mainly for the GDRA period (before cycle 41 around $3cm^2$ gain) but also afterwards (around $0.2cm^2$ gain). This is a good result, enlighted on Figure 44 for both EN and J1 missions as well as for both ESOC and CNES solutions.
Note that for Envisat, a slight annual signal can be observed on the GDR-B part.
Also note that for ESOC V4 solution during the GDR-B period (Cycles 41 to 69), the improvement is not striking and a degradation is even noticed alternatively to the improvements following an annual signal.

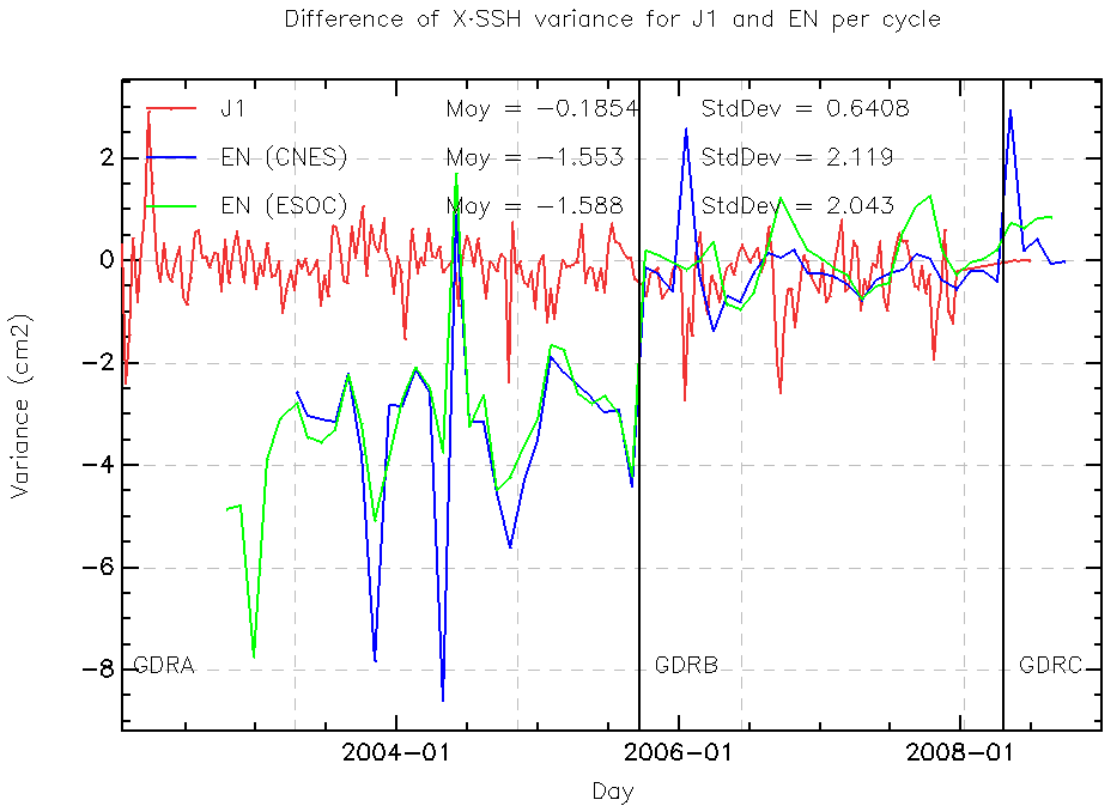

Figure 44: *X_SSH Variance Gain*

7.1.2.5 Difference of variances of SLA : VAR(SLA CNES GDR-C orbit) - VAR(SLA CNES GDR-ABC Orbit)

Figures 45 shows the difference of variances of SLA with CNES GDR-C orbit and CNES GDR-ABC Orbit per cycle. Like for SSH differences at crossovers per cycle, a significant improvement is observed on the SLA variance gain.
This gain is periodically (annual signal) very significant (up to 3 or 4cm^2) for both EN and J1 missions as well as for both ESOC and CNES solutions.
Note that for both missions and solutions, a degradation is periodically noticed (up to 2cm^2) following an annual signal. These degradations should be analysed further.
Also note that for ESOC V4 solution, a slight drift is observed of the SLA variance gain monitoring, in addition to the annual signal. This could also be observed on a preliminary version of Jason-1 GDRC and is due to the 1st order trend modelled in the time variable gravity field. It is cancelled on both Envisat and Jason-1 operationnal GDRC.

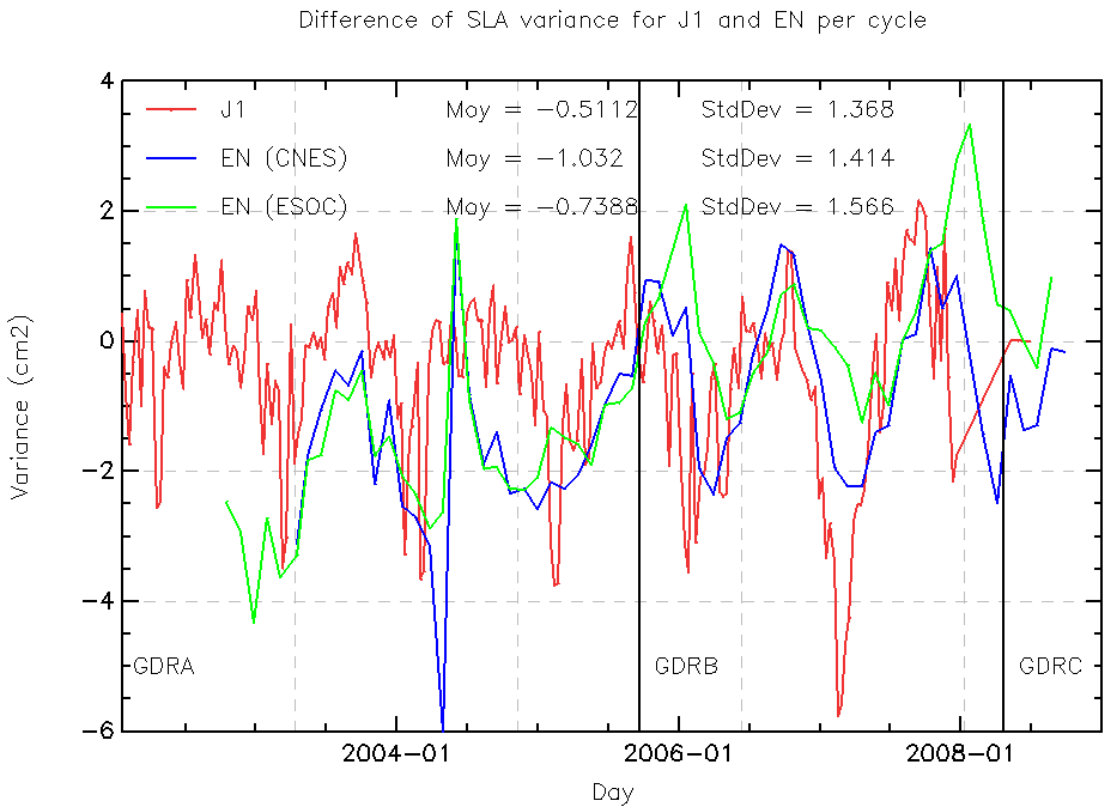

Figure 45: *SLA Variance Gain*

7.1.3. Fine Validation of data quality and availability

To complete the study about the new GDRC orbit, an analysis of the editing with this orbit is carried out.
Firstly, the editing is explained.
Secondly, a comparison of the number of edited measurements with the two different orbits all over the period is analysed precisly.
Finally, particular cases of degradation or of improvement are detailed and explained.

7.1.3.1. Editing principle

Data editing is necessary to remove spurious altimeter measurements.
First, there is an editing using flags. Compared to the GDR product, an additional flag is computed:
The ice flag to detect sea ice measurements. A measurement is set to ice if, at high latitudes ($> |50|$ deg), one of the following criteria is valid:
- Number of 20Hz measurement < 17
- |MWR - ECMWF| wet tropospheric correction > 10cm
- Peakiness > 2

Then, measurements are edited using thresholds on several parameters. These thresholds are expected to remain constant throughout the Envisat mission, so that monitoring the number of edited measurements allows a survey of data quality.
The following table gives for each tested parameter, minimum and maximum thresholds.

Parameters	Minimum	Maximum
Sea surface height (cm)	-130	100
Variability relative to MSS (m)	-2	2
Number of 18Hz valid points	10	-
Std. deviation of 18Hz range (m)	0	0.25
Off nadir angle from waveform (deg2)	-0.2	0.16
Dry tropospheric correction (m)	-2.5	-1.9
MOG2D correction (m)	-2	2
MWR wet tropospheric correction (m)	-0.5	-0.001
GIM Ionospheric correction (m)	-0.4	0.04
Significant wave height (m)	0	11
Sea state Bias (m)	-0.5	0
Backscatter coefficient (dB)	7	30
GOT00 ocean tide height (m)	-5	5
Long period tide height (m)	-0.5	0.5
Earth tide (m)	-1	1
Pole tide (m)	-5	5
RA2 wind speed (m/s)	0	30

Another editing is then performed on corrected sea surface height, using a spline fitting procedure. A final editing is then performed on corrected sea surface height, to remove whole tracks having out of thresholds statistics (mean and Std over the track).

7.1.3.2. Number of Edited Measurements over the whole period

Figure 46 shows the number of edited measurements per cycle with each orbit GDR-ABC and GDR-C orbits (left) and the difference between the number of edited measurements with the two orbits (right).
The data quality of both orbits is globally close except for some cycles. The following cycles have been particularly investigated: 16, 21, 24, 26, 44 and 68:
- Cycles 16,21,24 and 26 have more edited measurements with the previous orbit than with the new orbit.
- Whereas it is the contrary for cycles 44 and 68.
These particular cycles are detailed in the next parts.

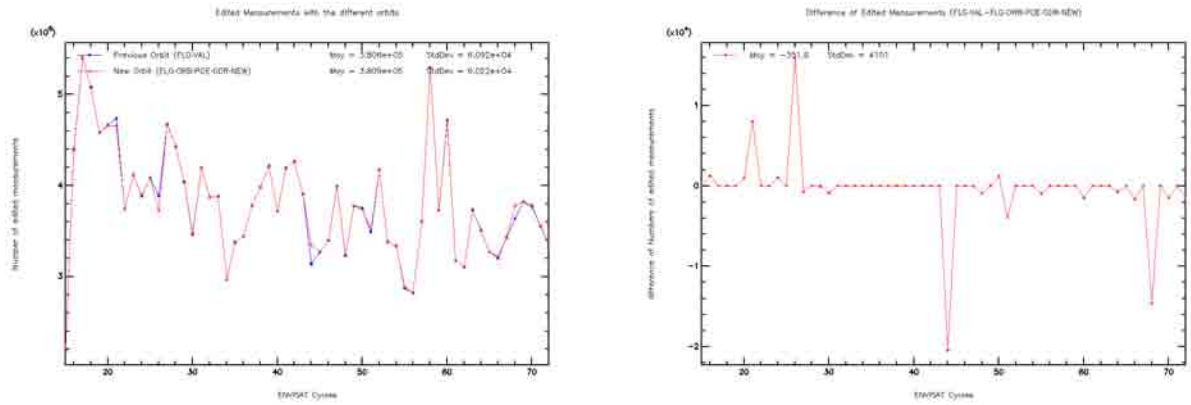

Figure 46: *Number (left) and Difference of Numbers (right) of Edited Measurements*

7.1.3.3. Particular cases (Cycles 16, 21, 24, 26, 44 and 68)

For the cycles enlighting a difference of editing with both orbits, along trak SLA are superimposed on plots hereafter:
- In blue for SLA computed with the previous orbit (GDR-ABC)
- In red for SLA computed with the new GDRC orbit.

To enlight the difference of edited data all data are plotted:
- In light colors (light blue and light red) for edited data
- In dark colors (blue and red) for valid data

7.1.3.4 Under-edited measurements : Cycle 16,21,24 and 26

For these cycles, the SLA using the new orbit is no longer edited (compared to the previous one) and its quality seems good (within the current values) as seen on figures 47 and 48.
The differences occur during manoeuvers which dates and corresponding cycles/arcs are listed in the synthetic table 5.
For these cases, the new orbit seems to be more robust to maneuvers.

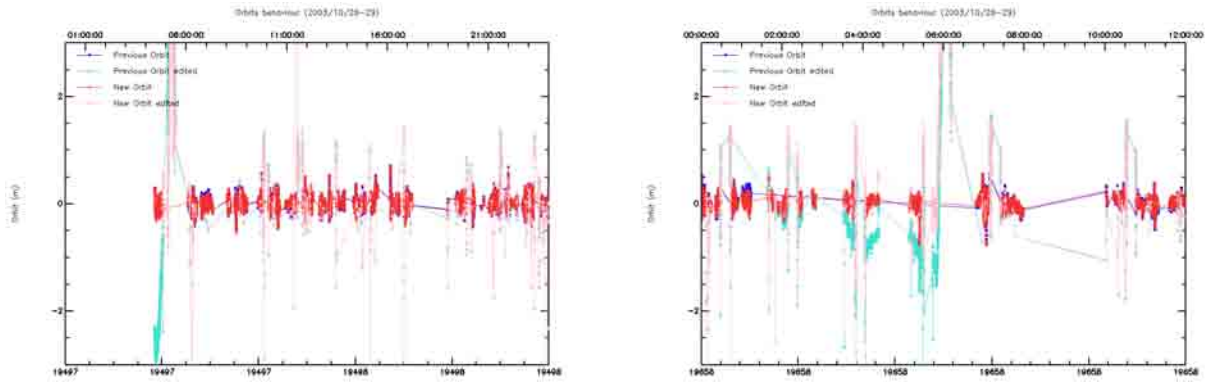

Figure 47: *SLA behavior during the manoeuver left (Cycle 16) right (Cycle 21)*

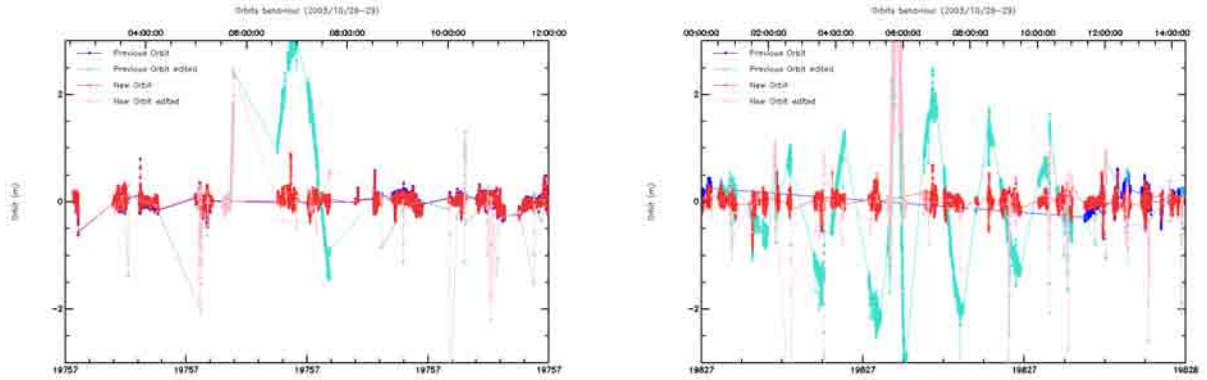

Figure 48: *SLA behavior during the maneuver left (Cycle 24) right (Cycle 26)*

7.1.3.5. Over-edited measurements :Cycle 44 and 68

Unlike previous cycles, those manoeuvers have a greater impact on data with the new orbit than with the previous one. SLA gets out of threshold for those cases as seen on the Figures 49 and listed in table 5.

7.1.3.6. Conclusion on quality and editing

Globally, the results of editing using the both different orbits are close. Nevertheless some particularities are detected and explained in this present report. These particularities are mainly due to maneuvers managing. The following table summarizes improvements and degradations brought by the new orbit CNES POE GDR_C compare to the previous orbits GDR_A and GDR_B.

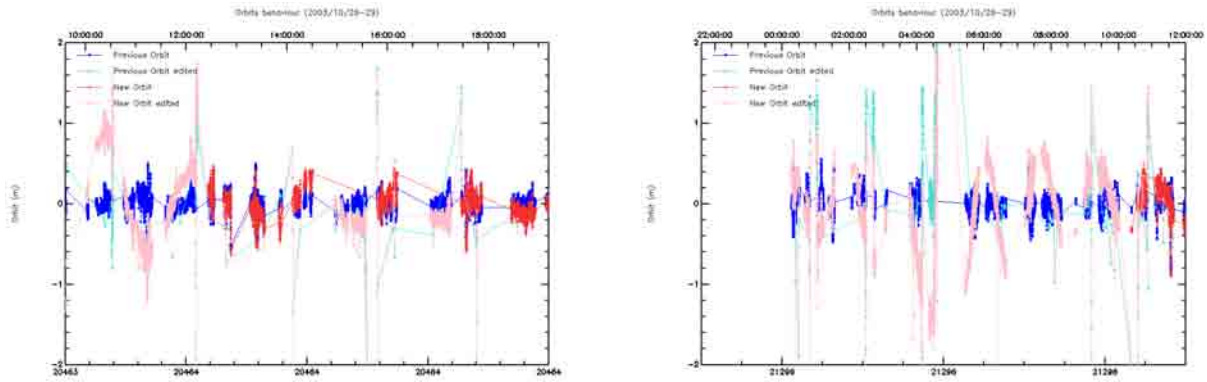

Figure 49: *SLA behavior during the maneuver left (Cycle 44) right (Cycle 68)*

Date (Julian Day) of the Maneuver	Cycle / Arc	Editing of GDR-C/GDR-ABC	Better SLA Quality before editing?	SLA Illustration
20/05/2003 (19497)	Cycle 16/ Arc 49	less	YES	Fig.47 (left)
28/10/2003 (19658)	Cycle 21/ Arc 73	less	YES	Fig.47 (right)
04/02/2004 (19757)	Cycle 24/ Arc 86	less	YES	Fig.48 (left)
11-14/04/2004 (19827)	Cycle 26/ Arc 95-96	less	YES	Fig.48 (right)
10/01/2006 (20463)	Cycle 44/ Arc 187	more	NO	Fig.49 (left)
22/04/2008 (21296)	Cycle 66/ Arc 306	more	NO	Fig.49 (right)

Table 5: *M*aneuvers managing for GDR-ABC and GDR-C orbits

7.1.4. Impact of the orbit on the Mean Sea Level trends

Homogenising the orbit solution is an essential step for MSL computation. Generating a GDR-ABC MSL is sensless because it introduces bias at transition and potential change of behavior.
Since 2007, we gathered orbits from different solutions: DELFT, different versions of ESOC (V2, V3, V4) and finally the new operational CNES GDR-C homogeneous orbit.
Results are the following:
The orbit solution DEOS have an impact on the MSL trend and particularly on the Ascending/Descending discrepancies observed on Envisat.

7.1.4.1. Monitoring of statistics per cycle

7.1.4.2 Means of SLA : MEAN(SLA with CNES GDR-C orbit), MEAN(SLA with CNES GDR-ABC Orbit)

These figures show the means of SLA with CNES GDR-C orbit and CNES GDR-ABC Orbit per cycle. The left hand figure refers to the standard 10 days crossovers selection, while the right hand figure refers to the LatBathyVar (SL2) selection ; this selection has the same time criterion, but requires moreover that : |LAT| < 50deg, BATHY < -1000m and VAR_OCE < 0.2m

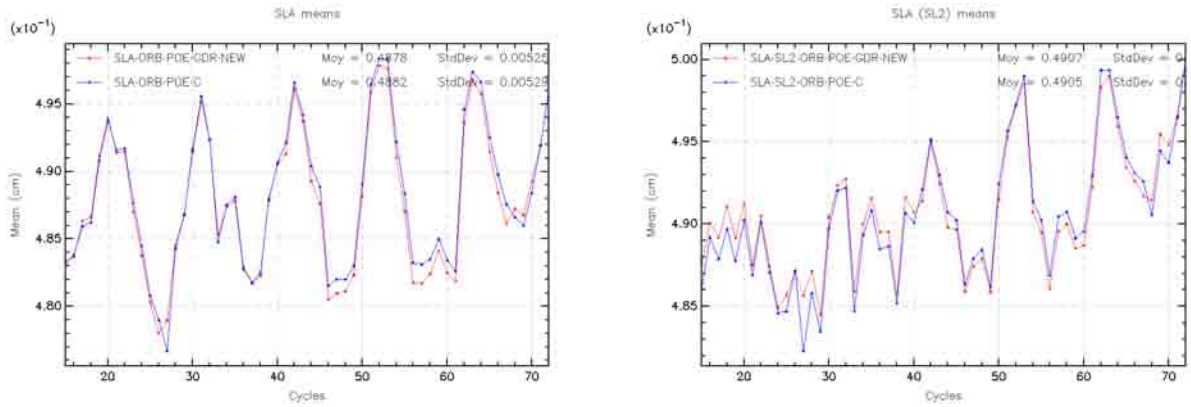

Figure 50: *SLA mean with no selection (left) and Open ocean Selection (right). ORB_POE_C stands for CNES orbit GDR-ABC*

The SLA using both orbits are not much different. The anomalous decrease and lack of annual signal observed prior to cycle 22 is observed on both curves. This drives us to compute the msl trends from cycles 22 onwards in this part.

7.1.4.3. MSL trends and Ascending/Descending discrepencies

The GDRC orbit has 2 main impacts on the MSL.

Concerning the global trend, the difference between Jason-1 and Envisat is reduced to 0.7mm/year, whereas it is slighly bigger with other solutions (see Table 6 and Figure 55) .

Concerning the Ascending/Descending discrepencies, it is reduced to the order of difference observed on Jason-1 (0.7mm/year) with CNES GDRC orbit whereas it is larger for ESOC V2, V3 and V4: between 1.4 and 2.4mm/year (see Table 6 and Figure 51 and 52).

The reason of such reduction of discrepencies remains uncertain however differences between the different versions are rather weak. The possible reasons are:
- the choice of ITRF solution (2000/2005) is different between GDRB and GDRC. However, it is the same on both ESOC V3 and V4, therefore it probably does not explain everything.
- the Gravity field model is also different between GDRB and GDRC. It contains a unique constant value for ESOC V3, an Annual variation + a 1st order trend for ESOC V4 and the sole Annual variation for GDRC. On both CNES GDRC and ESOC V3 the gravity field model does not have any variation at the yearly level (only seasonnal) and should not impact long term drifts...
- Finally, a DORIS preprocessing was applied on the whole series for the CNES GDRC solution and not on the others, for which it is only applied after cycle 41 (September 2005). This could be a possible source of difference on the long term behaviors.

	ESOC V2	ESOC V3	ESOC V4	CNES GDR-ABC	CNES GDR-C	J1
ITRF	2000	2005	2005	2000	2005	2005
Gravity field	Constant	Constant	Annual variation + trend	Constant	Annual variation	Annual variation
DORIS preprocessing	No	No	No	No	Yes	-
First EN Cycle	22	22	22	22	22	22
Last EN Cycle	58	58	63	74	74	74
Asc	2.2	1.9	2.3	3.2	2.2	2.3
Desc	-0.2	0.2	0.9	0.8	1.5	2.9
Desc-Asc	2.4	1.7	1.4	2.4	0.7	-0.6
All tracks	1.1	1.2	0.96	1.7	1.9	2.6

Table 6: MSL trends from cycle 22 (in mm/year)

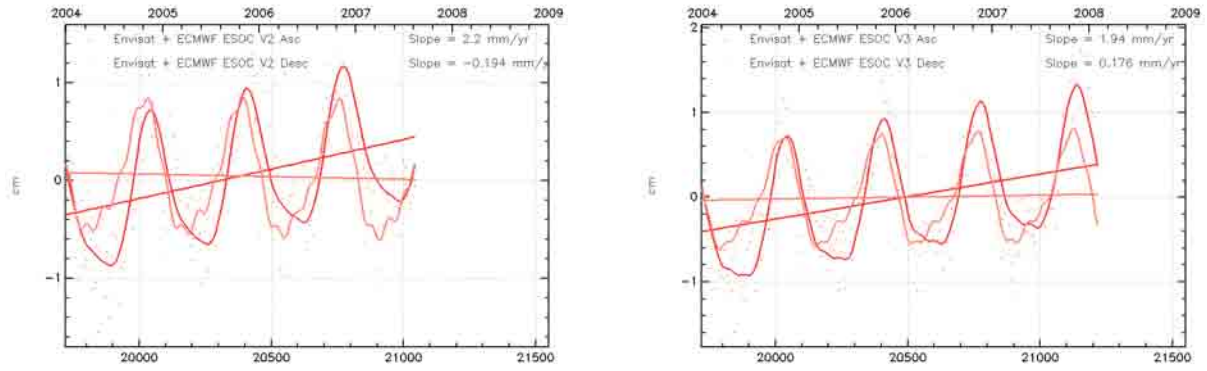

Figure 51: *Ascending/Descending discrepancy for filtered (6months filtering) MSL for Envisat using ESOC V2 solution (left) and ESOC V3 solution (right).*

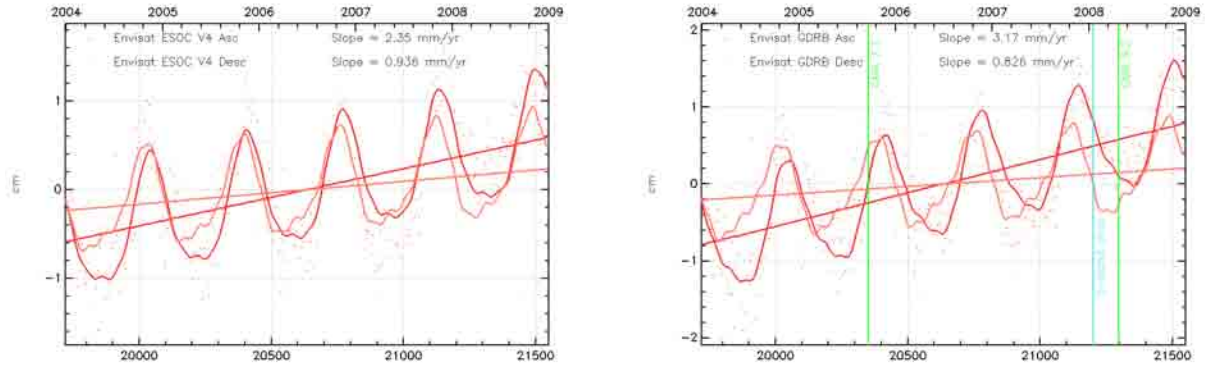

Figure 52: *Ascending/Descending discrepancy for filtered (6months filtering) MSL for Envisat using ESOC V4 solution (left) and CNES GDR-ABC solution (right).*

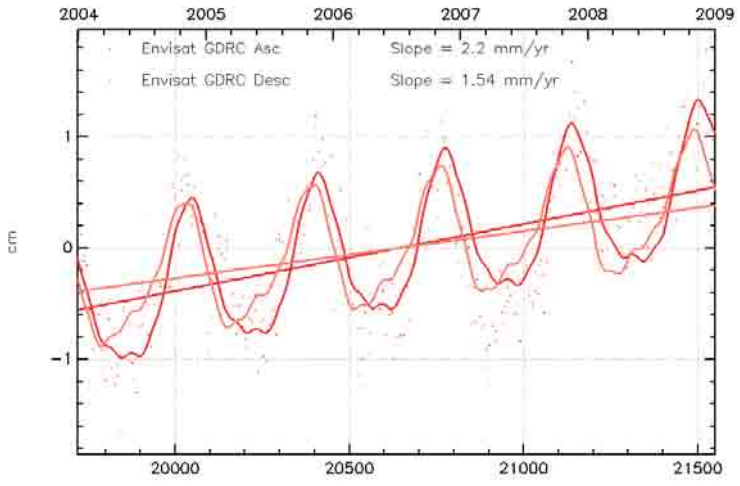

Figure 53: *Filtered MSL using GDRC Orbit*

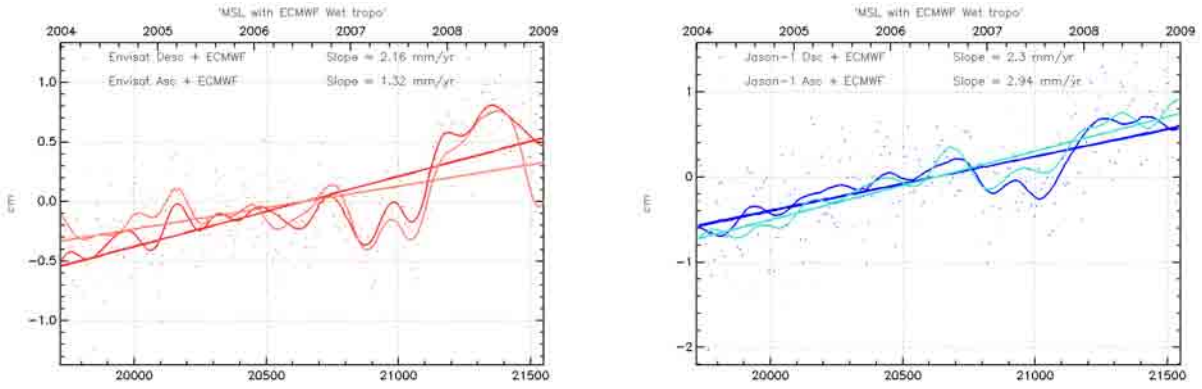

Figure 54: *Ascending/Descending discrepancy for filtered (6months filtering + annual signal removed) MSL using GDRC Orbit for Envisat (left) and for Jason-1 (right).*

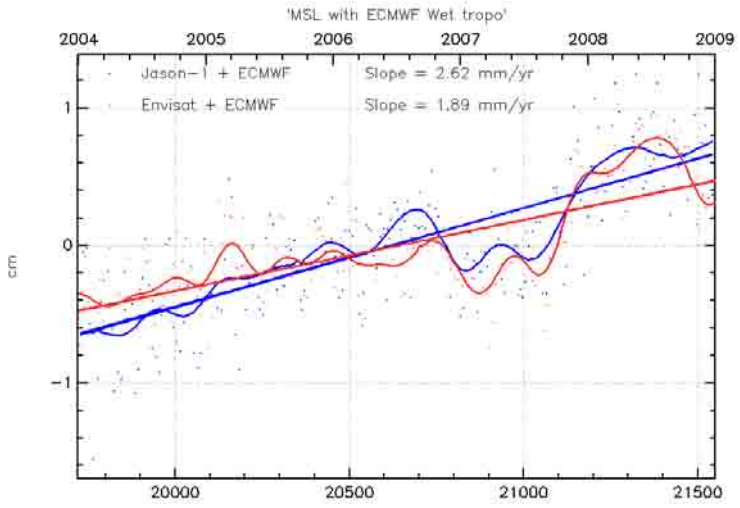

Figure 55: *Filtered (6months filtering + annual signal removed) MSL using GDRC Orbit for Envisat and Jason-1 since 2004.*

7.1.5. General Conclusions

The quality of the new orbit is generally very good and presents a significant improvement of altimetric data compared to both GDRA and GDRB versions. This improvement is observed on several criteria concerning general performances:
- Respectivelly 3cm^2 and 0.2cm^2 variance gain on Variance at crossovers.
- Reduction of the annual signal observed on Envisat's Mean difference at crosovers
- Periodic improvement (up to 3 or 4cm^2) and degradation (down to -1cm^2) for both EN and J1 missions as well as for both ESOC and CNES solutions, related to the time gravity field intensity modelled into the GDRC orbit solution.
- The SLA quality after editing is generally better around maneuvers with the new GDRC orbit compared to the old GDR-ABC one except for some rare degradations. All major differences are listed in the document and presents a base for the cyclic analysis of reprocessing.
- Finally, an additionnal study was performed to analyse the impact of the new orbit on the mean sea level trend. This shows good results mainly concerning the reduction of the Ascending/Descending discrepency is reduced to the order of difference observed on Jason-1 (0.7mm/year) which eliminates a possible source of error suspected on Envisat. The reason of such reduction of discrepencies remains uncertain and should be understood but this result is still very encouraging for further MSL studies using Envisat.

7.2. Cross-Calibration with Jason-2, Orbital point of view

7.2.1. Seattle OSTST oral presentations

7.2.1.1. Jason-2 cross-calibration with Jason-1 and Envisat

SERVICE ALTIMETRIE & LOCALISATION PRECISE

Jason-2 cross-calibration with Jason-1 and Envisat

A. Ollivier, Y. Faugère, S. Philipps - CLS
N. Picot, E. Bronner - CNES, P. Femenias - ESA

Introduction

- Since Envisat was launched, Cross Calibration studies with the Jason-1 mission are performed to assess the data quality and performances of both missions.
- A precise altimetric mission as Envisat can help to understand the observed differences between Jason-1 and Jason-2 by giving a third reference
- This presentation aims at showing the cross-calibration between Jason-2 and Envisat, compared to Jason-2 / Jason-1 and Jason-1 / Envisat results.

Overview

In this presentation, we will focus on :

1. Short overview of Envisat mission : *A precise and complementary altimetric mission.*
   - ➔ Systems comparison
   - ➔ Comparison method: small precautions needed
2. Envisat / Jason-1 / Jason-2 : *Performance and correlation estimations*
   - ➔ Dual and Monomission statistics monitoring
3. Envisat / Jason-1 / Jason-2 : *Three very similar missions*
   - ➔ New results using GDR compared to IGDR time series
   - ➔ Geographically correlated biases and variability

1. Envisat mission :
A precise and complementary altimetric mission.

Envisat GDR status

- 7 years of data availability

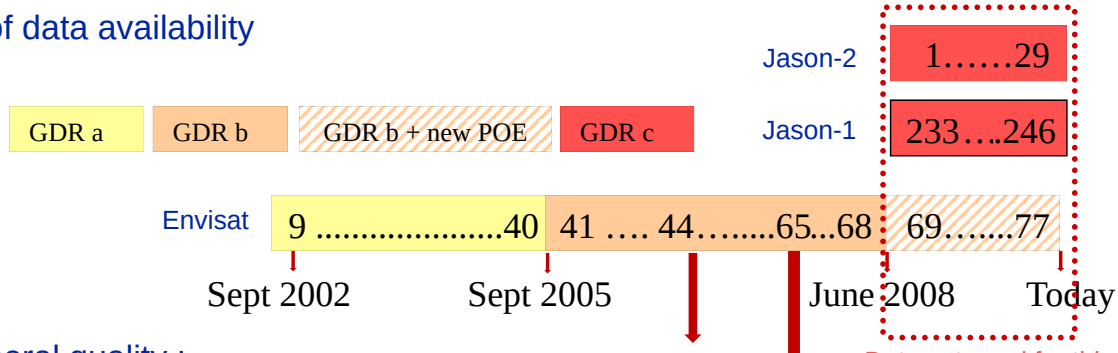

- Good general quality :
  - Very good availability of data.
  - **USO anomaly**: In February 2006, the RA-2 Ultra Stable Oscillator (USO) clock frequency underwent, for an unknown reason, a strong change of behavior.
    ➔ Altimeter range can be corrected from this anomaly by users, thanks to **auxiliary files** distributed by ESA since mid 2006
  - **Loss of the S-Band**: On the 17 January 2008, a drop of the RA2 S-band transmission power occurred. There is thus no more dual frequency altimeter both in A and B-Sides.
    ➔ GIM ionospheric correction is available in the IGDR and GDR products
  - **Reprocessing** of the whole Ra-2 Envisat GDR in version C will start in 2009

Method used for SSH at crossovers comparison

• Statistics are computed on a J2 cyclic basis (10 days)

• An average per boxes is performed, prior to the statistics in order to allow us to have homogeneous sampling of the ocean for the 3 satellites (statistics slightly different from the J1/J2 presentation).

• Sea Surface Heigh formula used:

SSH_Common = Orbit –Range – ECMWF Dry Tropo (Gaussian grids) – MOG2D High Frequency – GOT00 tide – Solid tide – Polar tide-SSB

SSH_J2 = SSH_Common – AMR Wet Tropo - Filtered Bifrequency Ionospheric correction
SSH_J1 = SSH_Common – JMR Wet Tropo- Filtered Bifrequency Ionospheric correction
SSH_EN =SSH_Common – USO correction - MWR Wet Tropo- GIM Ionospheric correction

• Selections are applied on the crossovers to consider only those for:
- Lat < 50° (N/S) to avoid ice zones
- Mean ocean variability < 20cm
- Bathymetry > 1000m to avoid known errors near coasts

2. Envisat / Jason-1 / Jason-2 :
Performance and correlation estimations using GDR

Standard deviation of the SSH differences at cross-overs

GDR Monomission cross-overs

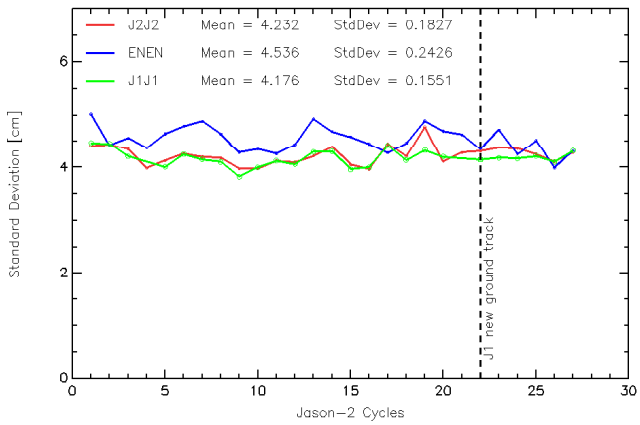

GDR Dual cross-overs

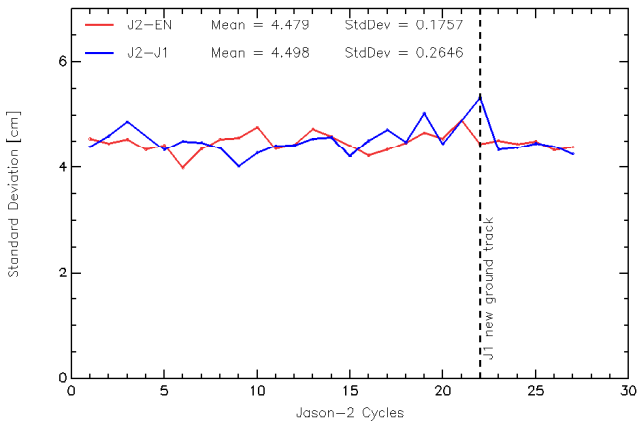

- Standard deviation of SSH crossover difference cycle per cycle shows:
  - ➔Good consistency for the three missions for the whole period
  - ➔ Slightly better performances for Jason-1 and -2 (4 cm) than for Envisat (4.5cm).
  - ➔ The covariance of Jason-2 with Envisat and with Jason-1 is similar, even though the missions are different!

Average bias of SSH differences at crossovers

GDR Monomission cross-overs

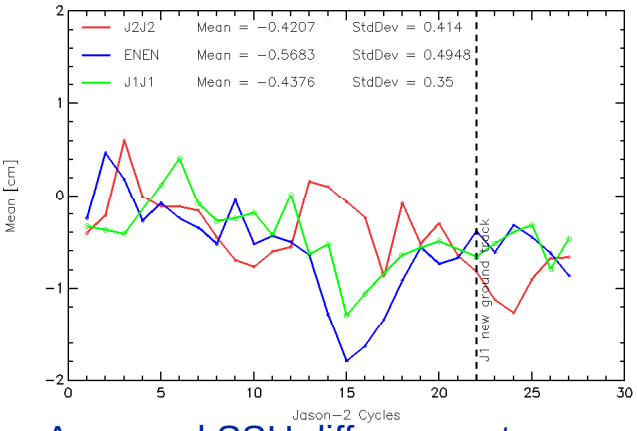

GDR Dual cross-overs

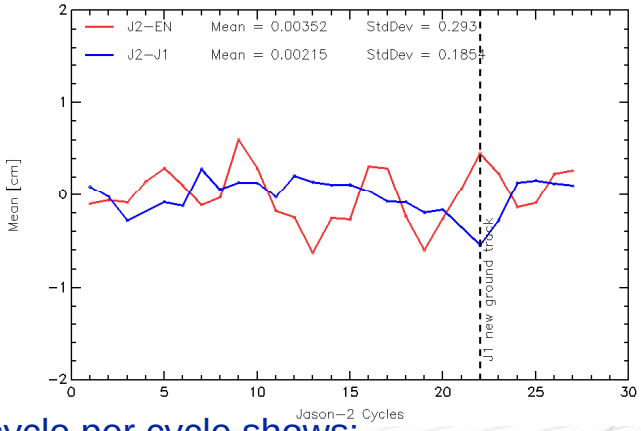

• Averaged SSH difference at crossover cycle per cycle shows:

➔ Good agreement between Ascending and Descending tracks for the 3 missions in GDR.

➔ Known annual signal on EN appearing.

➔ Good stability.

➔ **Geographic behavior detailed in the Orbit session presentation and poster**

➔ Very good agreement/ stability between the 3 missions in GDR.

➔ **Geographic behavior detailed hereafter…**

2. Envisat / Jason-1 / Jason-2 :

Three very similar missions

IGDR improving GDR

Cyclic evolution of J2/EN average Crossovers

Near Real Time, IGDR

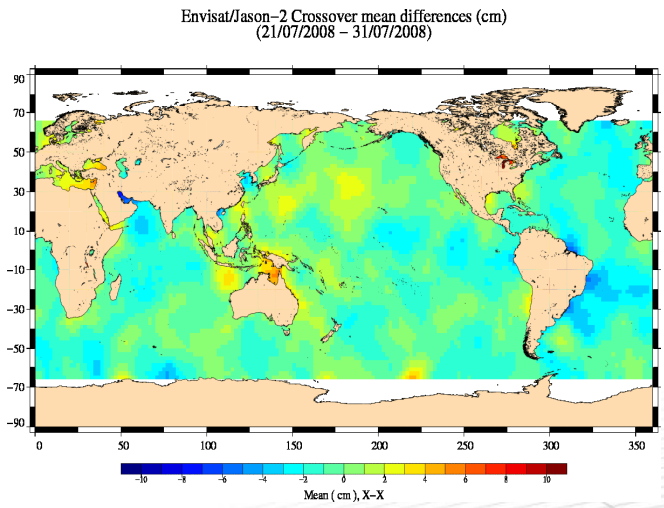

Delayed Time, GDR

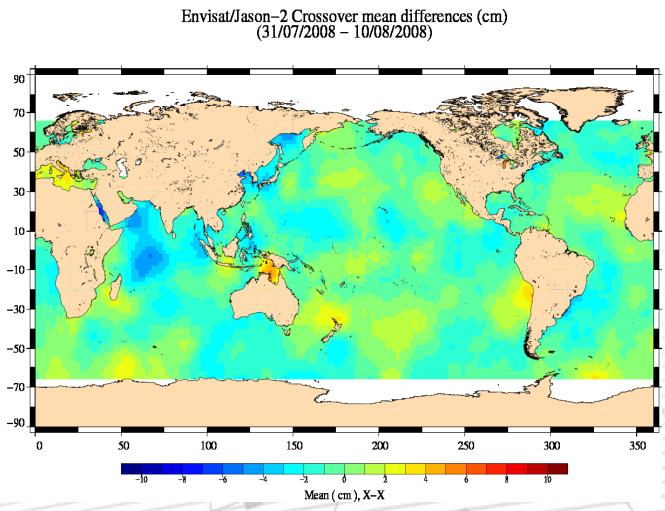

Cycles 1 to 25:
Consistency between both missions improved in GDR compared to IGDR.

J2/EN dual crossovers

Near Real Time, IGDR

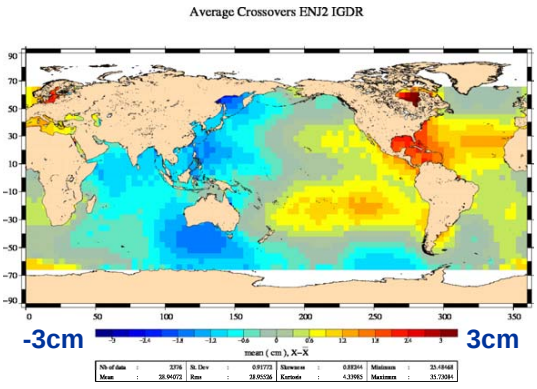

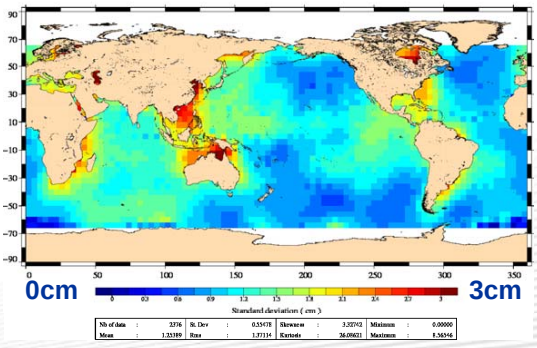

Mean:
Apart from the **bias** (due to the AMR radiometer shift between IGDR and GDR), no major differences are noticed on the geographical patterns

Standard deviation of the Smoothed average per cycle:
- Variability well decreased in GDR
- Mean Std:
←1.2 cm / 0.9 cm→

Delayed TimeGDR

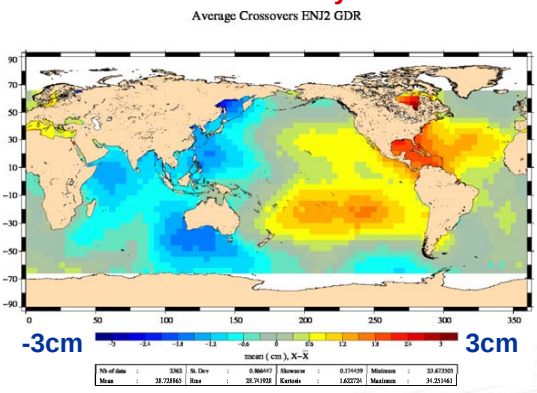

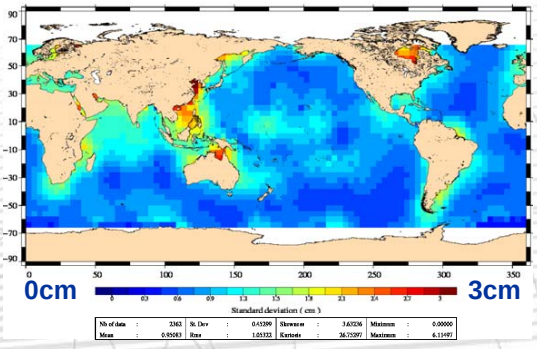

J1/EN multimission crossovers

Near Real Time, IGDR

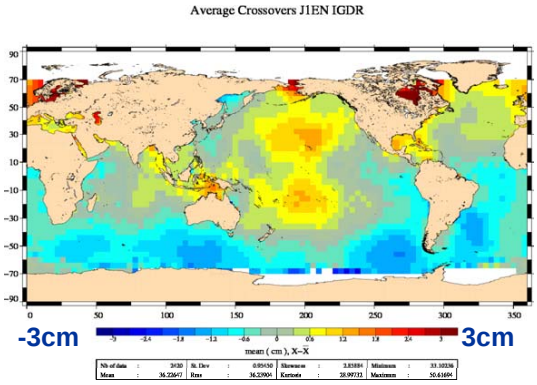

Delayed TimeGDR

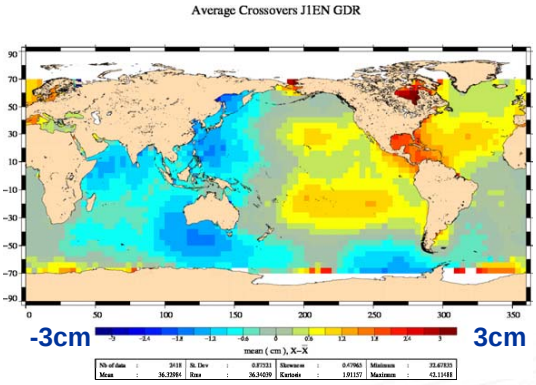

Mean:
the geographical paterns in IGDR are moved and reduced on the GDR map: induced by J1 POE improvement / MOE

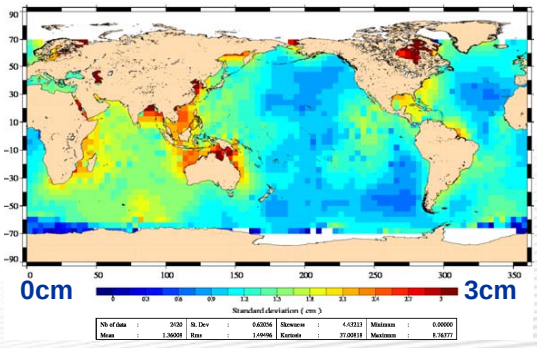

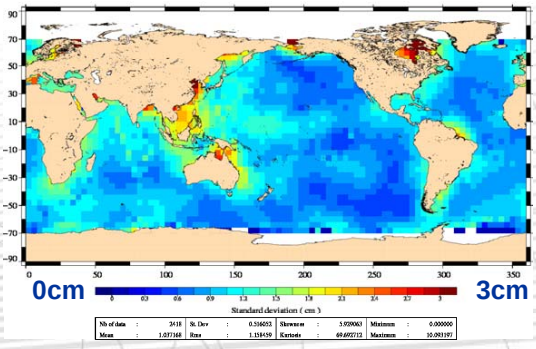

Standard deviation of the Smoothed average per cycle:
-Variability well decreased in GDR
- Mean Std:
←1.4 cm / 1.1 cm→

Conclusion

- **Geographic / temporal coverage difference**
  - ➔ The performances of the 3 missions can be compared after averaging by boxes
  - ➔ Can also be completed by crossing results from 10 days cyclic observation (based on J2 cycles) to 35 days observations (based on EN cycles). Further results using this formalism are developed in Y.Faugere et al. Poster.
- **Envisat /Jason-2/Jason-1 are very precise missions**
  - ➔ Standard deviation of monomission cross-over differences around 4 cm (GDR), which enables a precise cross calibration
- **Jason-1 and -2 comparisons with Envisat GDR are very consistent**
  - ➔ The geographical biases observed on IGDR products disappears in the GDR thanks to the POE improvement compared to MOE.
- **In GDR, Jason-2 / Envisat has the same level of consistency as Jason-2/Jason-1**
  - ➔ This consistency is even more relevnt considering that its orbit configuration is different from the Jason-1 and 2
  - ➔ making Envisat a very precious input to quantify Jason-2 altimetric performances

Further results showing orbit orientated results are developed in A.Ollivier et al. Poster and presentation.

Backup slides

Variance and covariance of the SSH differences at crossovers

The SSH difference at cross-over gives information on the error of a system.
2 different measurements over the same points contains:

➔ Variability due to the system error/noise

➔ Variability of the ocean during the period between the two measurements

Selections are applied on the crossovers to consider only those for:

- Lat < 50° (N/S) to avoid ice zones
- Mean ocean variability < 20cm
- Bathymetry > 1000m to avoid known errors near coasts

Monomission / Dual missions statistics are complementary on these aspects:

Monomossion

$$Var^2(S_{J2}) = Var^2(Oce(< 10days) + Var^2(Noise_{J2})$$

Dual mission (J2 and M (J1 or EN))

$$Var^2(S_{J2} - S_M) = Var^2(S_{J2}) + Var^2(S_M) - 2\,CoVar(S_{J2}S_M)$$

Method used for Jason-2 / Envisat comparison

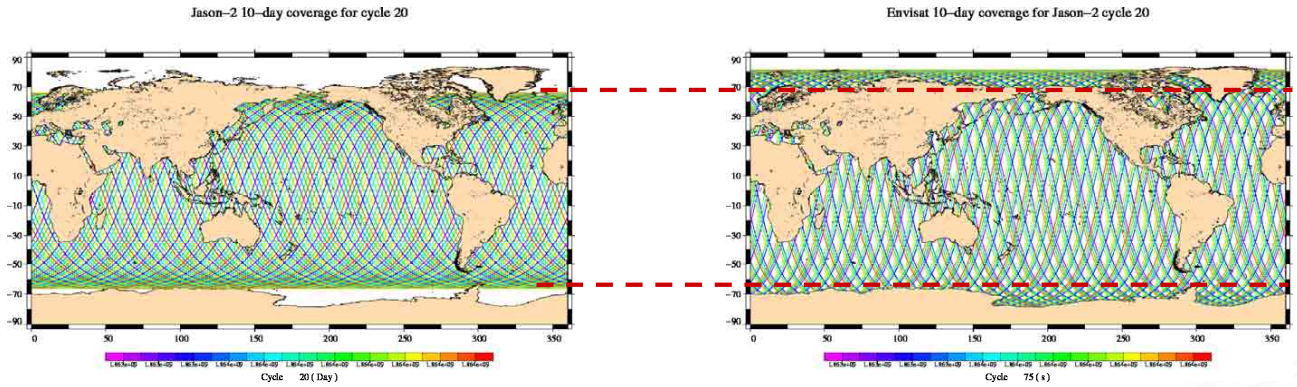

Statistics are computed on a J2 cyclic basis (10 days)
An average per boxes is performed, prior to the statistics in order to allow us to have homogeneous sampling of the ocean for the 3 satellites (statistics slighly different from the J1/J2 presentation).

SSH_Common = Orbit –Range – ECMWF Dry Tropo (Gaussian grids) – MOG2D High Frequency – GOT00 tide – Solid tide – Polar tide-SSB

SSH_J2 = SSH_Common – AMR Wet Tropo - Filtered Bifrequency Ionospheric correction
SSH_J1 = SSH_Common – JMR Wet Tropo- Filtered Bifrequency Ionospheric correction
SSH_EN =SSH_Common – USO correction - MWR Wet Tropo- GIM Ionospheric correction

7.2.1.2. Assessment of Jason-2 orbit quality using SSH cross-calibration with Jason-1 and Envisat

SERVICE ALTIMETRIE & LOCALISATION PRECISE

Assessment of Jason-2 orbit quality using SSH cross-calibration with Jason-1 and Envisat

A. Ollivier, S. Philipps, M Ablain, Y Faugere- CLS
N. Picot, E. Bronner - CNES, P. Femenias - ESA

Introduction

- CalVal exercise performed on the Sea Level Height (SSH) is a complementary way of enlighting geographically related patterns or particular behaviors signing on the ocean altimetric observations.

- For this purpose, monomision SSH cross-over analysis are analysed for the three precise altimetric missions:

➔Jason-1
➔Jason-2
➔Envisat

Near Real Time products using official IGDR MOE

Delayed time products: using official GDR POE

Overview

In this presentation, results are analyzed in terms of :

1. Geographically correlated mean biases
   - ➔ Average maps of SSH cross-over differences over Jason-2 life time
   - ➔ Cyclic monitoring of bias statistics at cross-over.

2. Time Variability of those biases
   - ➔ Standard deviation of SSH cross over differences maps over Jason-2 life time
   - ➔ Cyclic monomission statistics monitoring at cross-over

1. *Geographically correlated biases*

Orbit POE – MOE for the 3 missions over 220 days

Along track average over 22 J2 cycles:
J1: +/- 2 cm geographic biases
➔Centimetric discrepancies
EN: +/- 1mm geographic biases
➔ Very similar
J2: +/- 2.5 mm geographic biases
➔ Good consistency

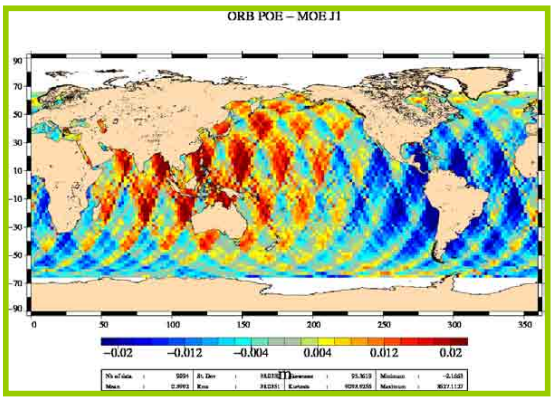

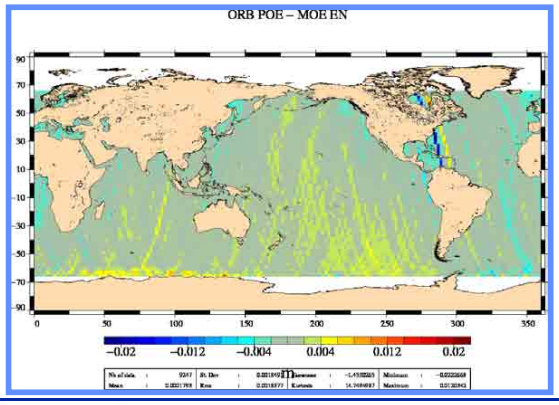

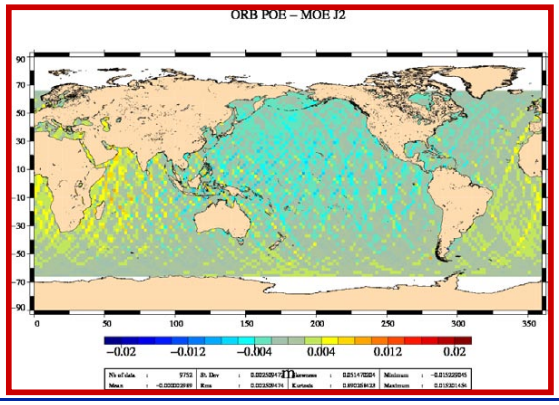

SLA Performances and Consistency

From S.Philipps presentation J2 System Performances

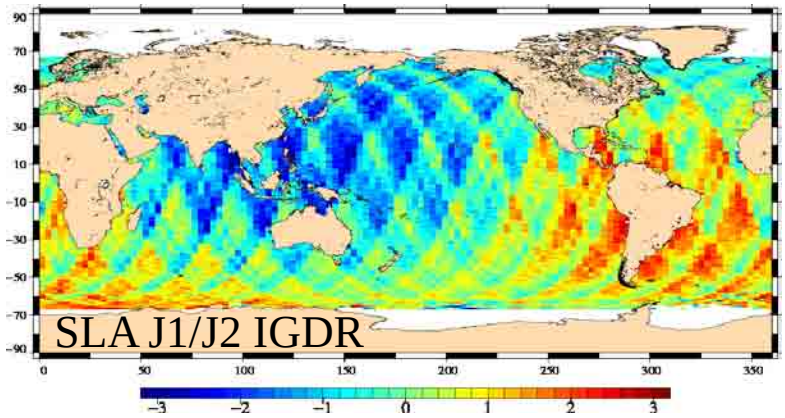

Map of mean JA1/JA2 SLA (orbit – range - mss) differences over cycles 1 to 20

- For IGDR: Geographically correlated patterns (+/- 3cm amplitude)
- For GDR: very good consistency, though
- Small hemispheric bias (+/- 1 cm) is visible -> likely due to slight orbit calculation differences

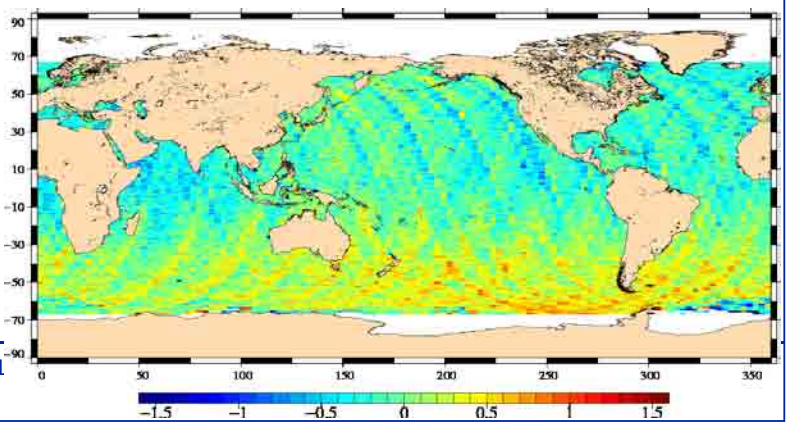

Average at cross-overs using IGDR SSH (with MOE)

Maps display the asc/dsc SSH differences for IGDR → include the orbit error impact on the SSH.

- → J1: +/- 3 cm geographic biases
- → EN: +/- 1cm weak geographic biases
- → J2: +/- <1cm very weak geographic biases

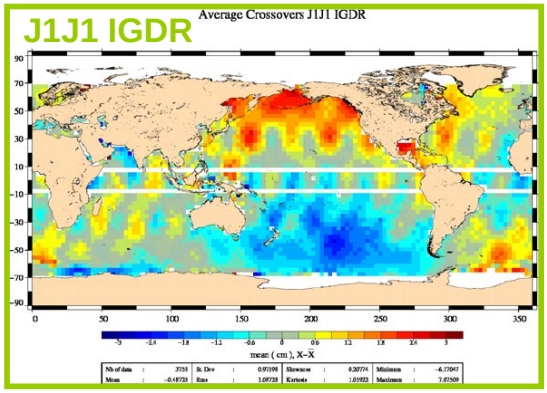

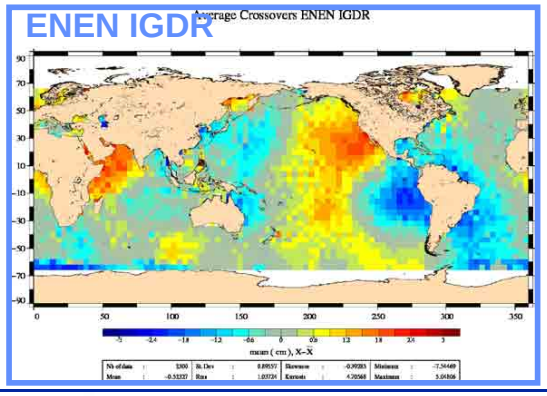

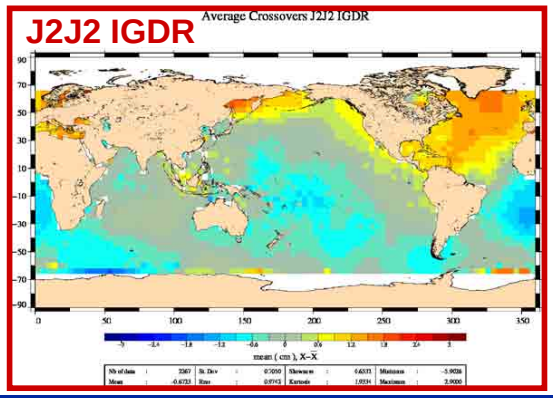

Average at cross-overs using GDR SSH (with POE)

➔Jason-1 Strong improvement in terms of geographical biases: weaker biases than with MOE
➔Jason-2 and Envisat weak impact

All missions present very weak geographically correlated biases (below 1cm)

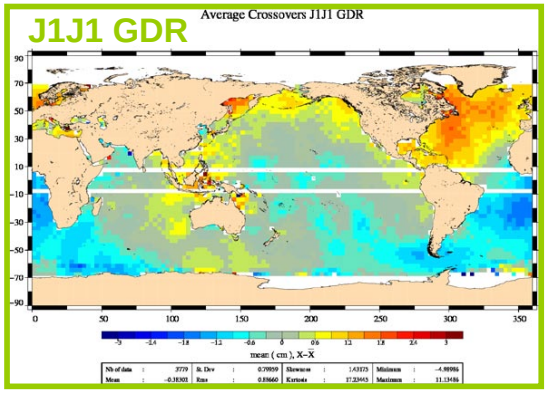

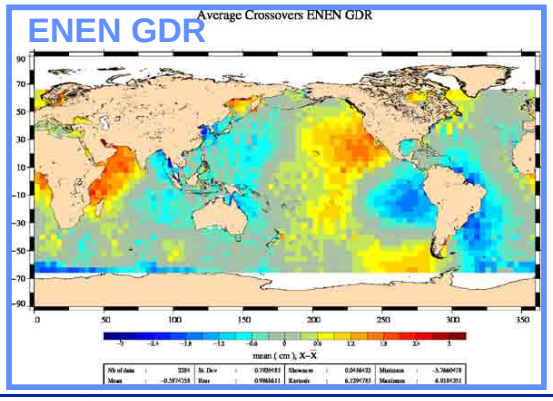

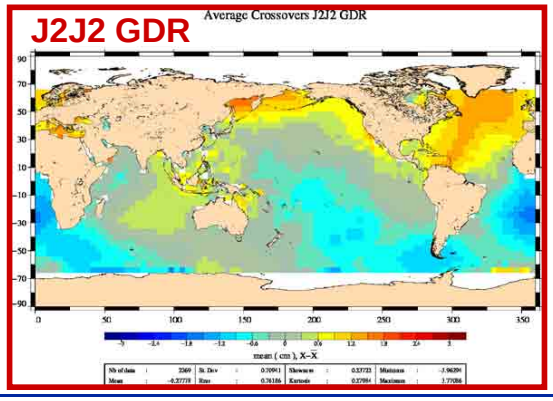

2. *Geographical and temporal stability of the biases*

Temporal variability of the biases

Mean Asc-Desc Monomission SSH at cross-overs over ocean for IGDR and GDR:

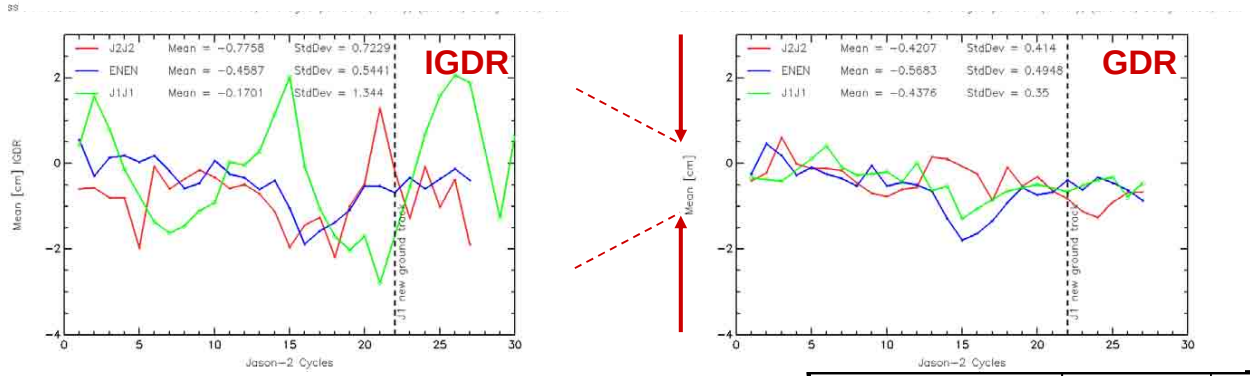

Weak biases (all slightly negative) varying in time:

➔J1: Beta cycle (120 Days) in IGDR reduced in GDR (could be reduced by the SAA model now applied on IGDR)

➔EN: Best stability with MOE not so much improved in GDR (the known annual signal can be observed on these data)

➔J2: good stability slightly improved in GDR

Standard deviation of the cyclic average	IGDR	GDR
J1	1.3 cm	0.35 cm
EN	0.54 cm	0.49 cm
J2	0.72 cm	0.41 cm

Geographic variability of the biases

Standard deviation of the cyclic mean SSH differences at cross-overs over ocean

J2J2 IGDR

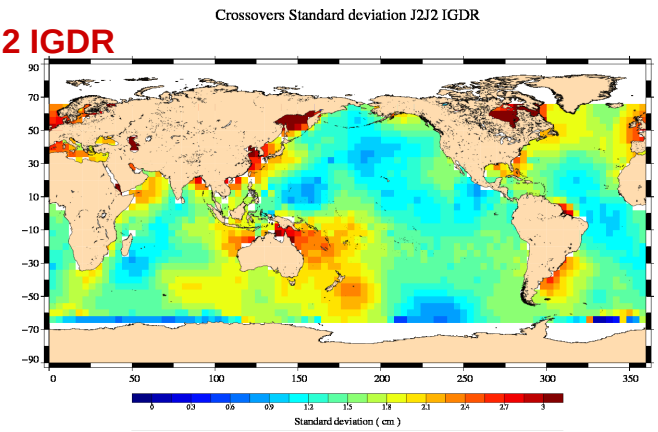

J2J2 GDR

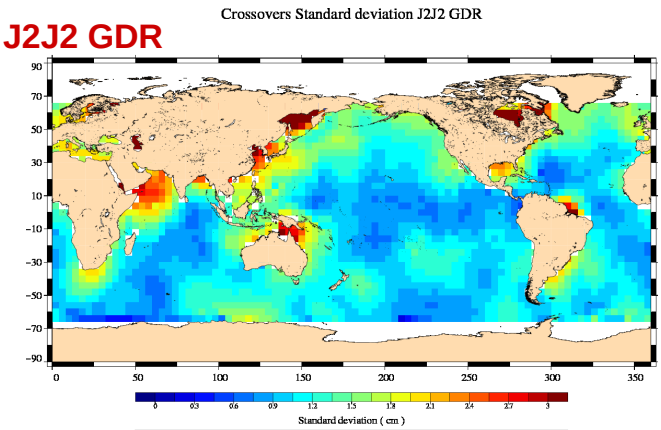

Computed on 22 cycles.

A smoothing is also applied in order to identify the long wave length variations (and not the one linked to the ocean variability)

Geographic Mean Standard deviation	IGDR	GDR
J1	1.9 cm	1.4 cm
EN	1.4 cm	1.3 cm
J2	1.6 cm	1.2 cm

Conclusion

- Centimetric precision is reached for all orbits.
- Jason-1 POE improvement (weaker bias per basin and better time stability) compared to the MOE can be seen on the SSH cross-over analysis
- Envisat MOE and POE have very similar quality with still some weak geographical biases observed between ascending and descending tracks.
- Jason-2 POE and MOE both give homogeneous (geographically) and stable (temporally) Asc/Dsc discrepancies. **Jason-1 and 2 are very consistent using POE orbits.**
- More results about Envisat altimetric data and on the dual cross calibration between missions in « Calval session » presentations and posters

Additionnal slides

Standard dev at cross-overs using IGDR SSH (with MOE)

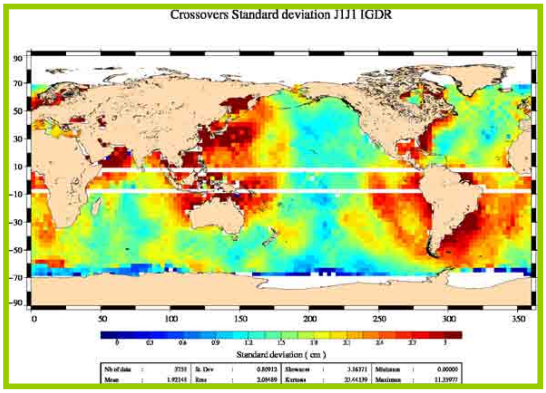

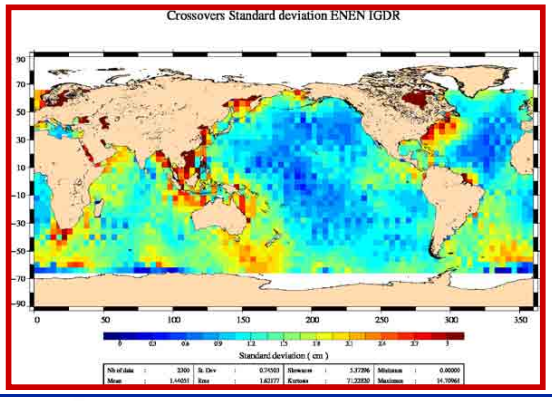

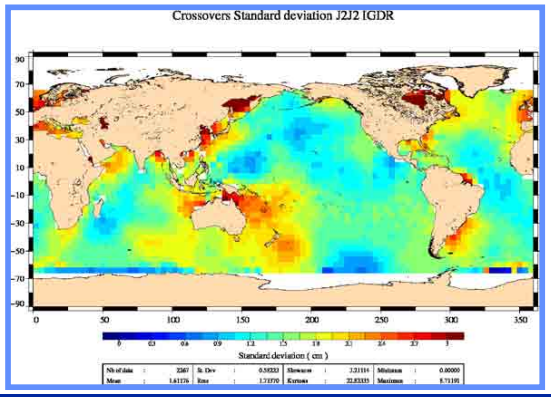

Standard dev at cross-overs using GDR SSH (with POE)

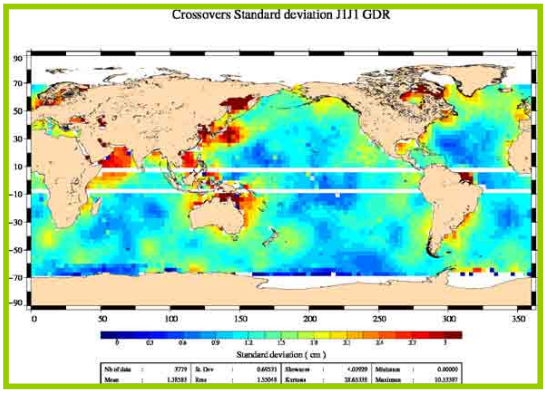

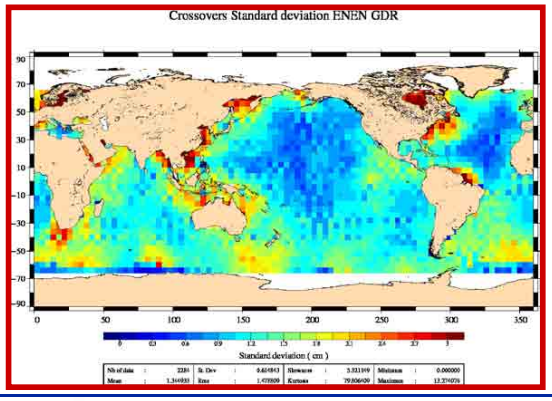

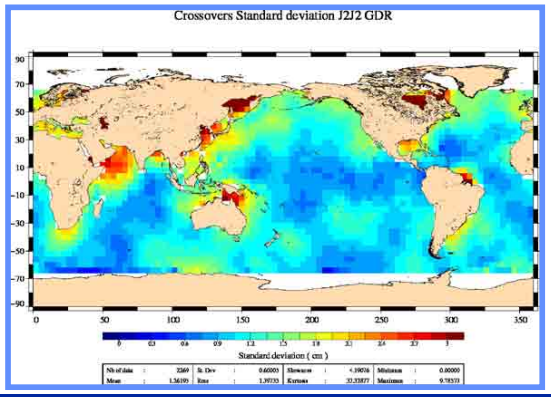

Ascending/Descending descrepencies for the difference Orbit POE – MOE

Jason-1:

➔ Discrepancies on both ascending and descending tracks

Cycles 239-260

Even tracks ORB POE – MOE J1

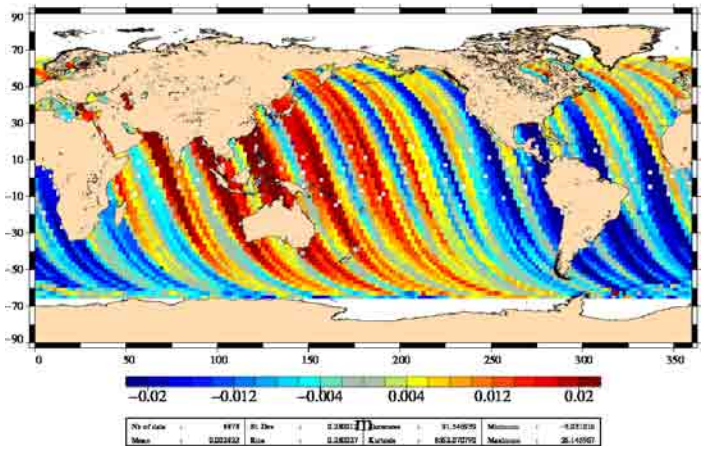

Odd tracks ORB POE – MOE J1

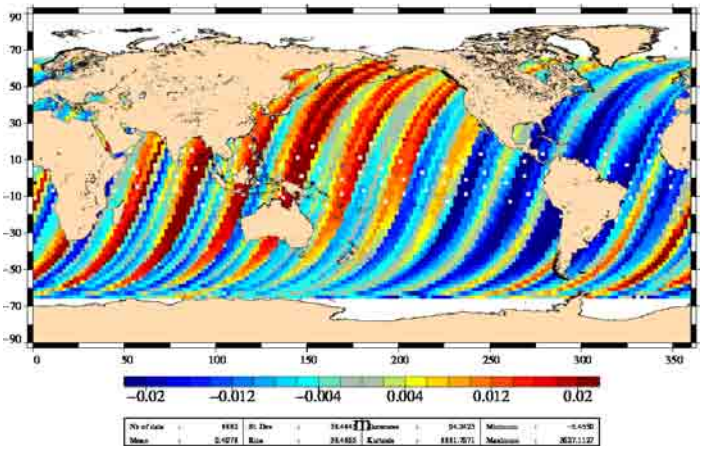

SAA introduction effect

Strong reduction effect on the POE-MOE Jaons-1difference

Cycles 257-260

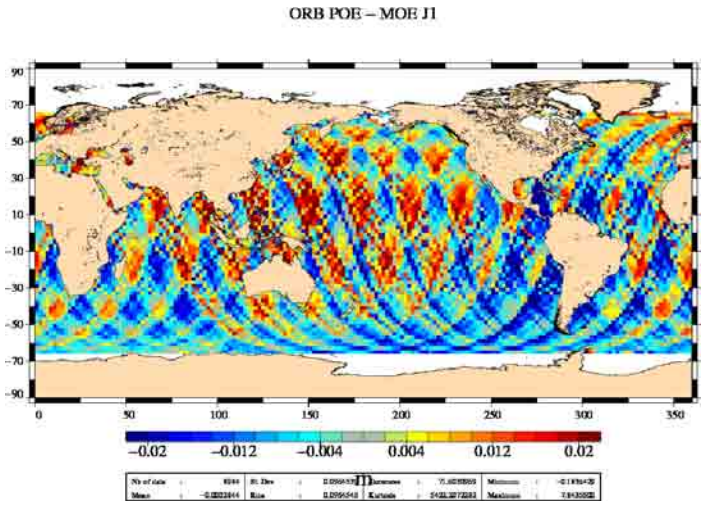

Cycles 267-270

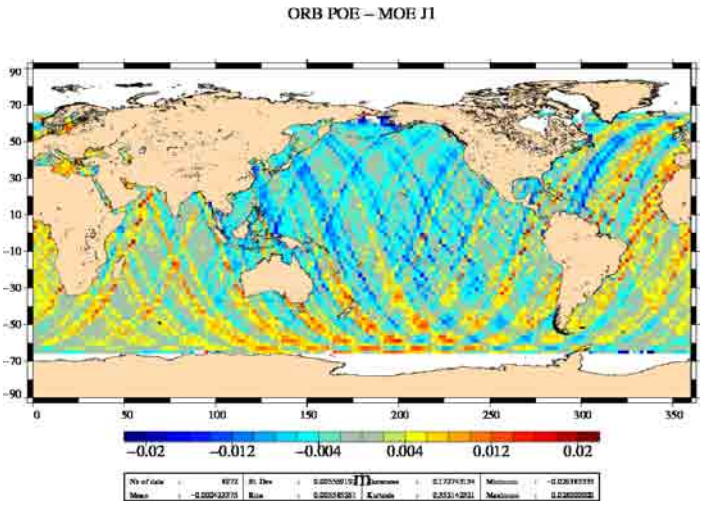

Cycles 257-260

Even tracks ORB POE – MOE J1

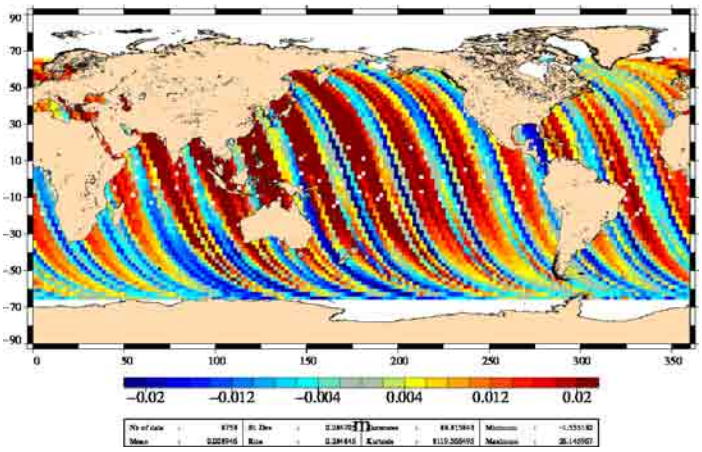

Odd tracks ORB POE – MOE J1

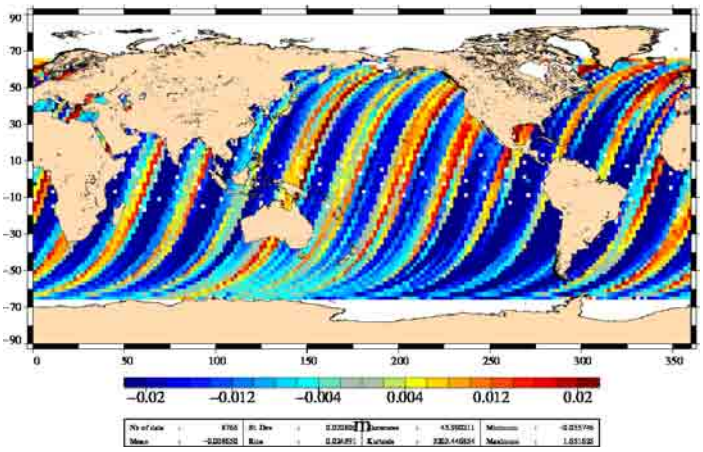

Cycles 267-270

Even tracks ORB POE – MOE J1

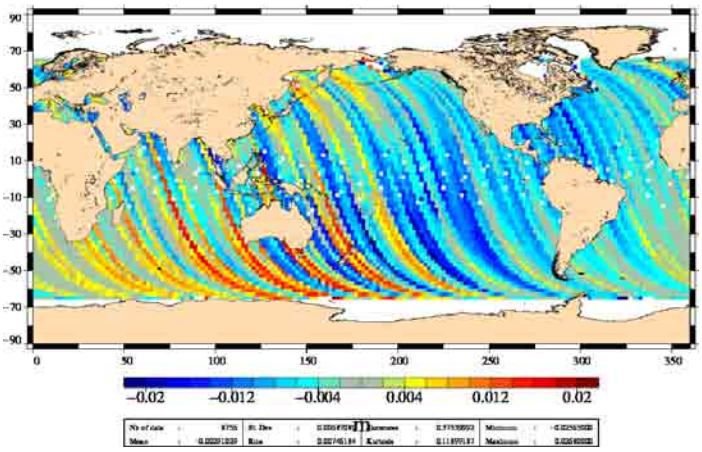

Odd tracks ORB POE – MOE J1

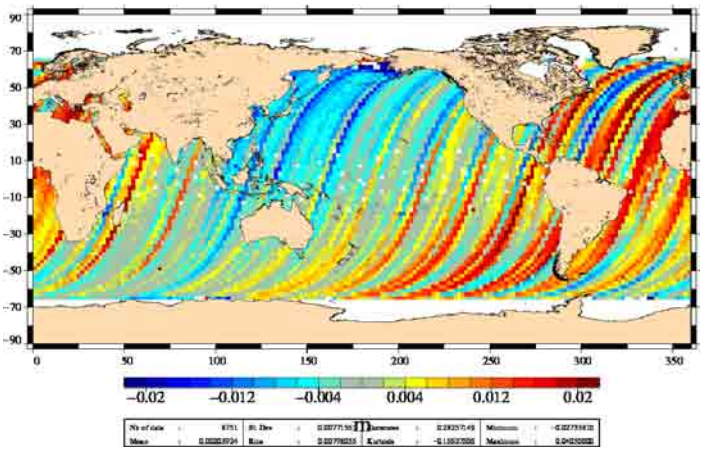

Ascending/Descending descrepencies for the difference Orbit POE – MOE

Jason-2:

➔ Around 4mm bias between Ascending and descending tracks (due to MOE, cf Average X_SSH GDR/IGDR)

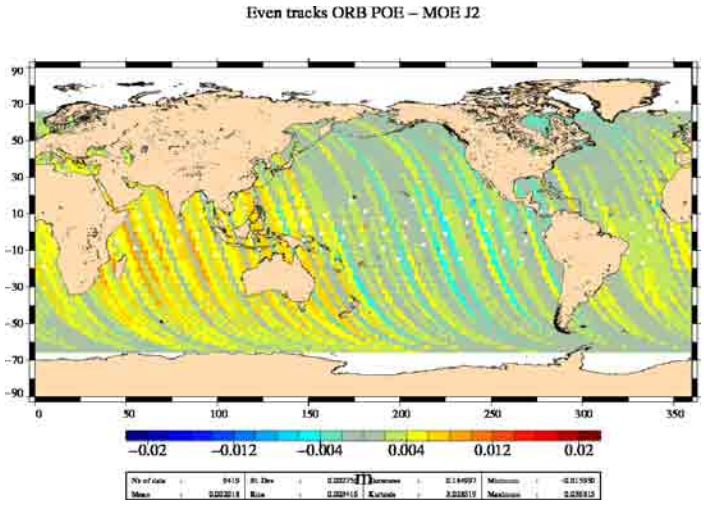

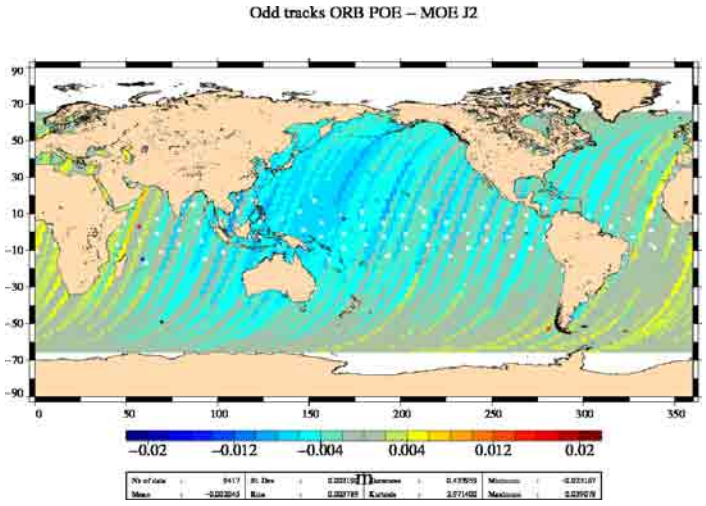

Ascending/Descending descrepencies for the difference Orbit POE – MOE

Envisat:

➔ Very good consistency both on Ascending and descending tracks

Even tracks ORB POE – MOE EN

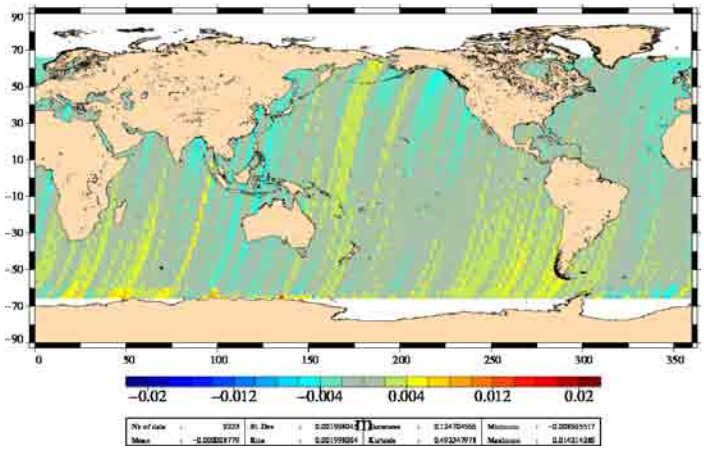

Odd tracks ORB POE – MOE EN

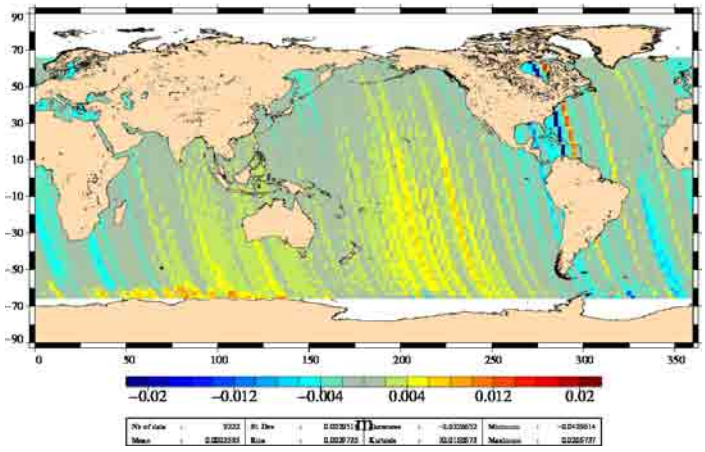

7.2.2. Seattle OSTST posters

7.2.2.1. Jason-2 cross-calibration with Jason-1 and Envisat

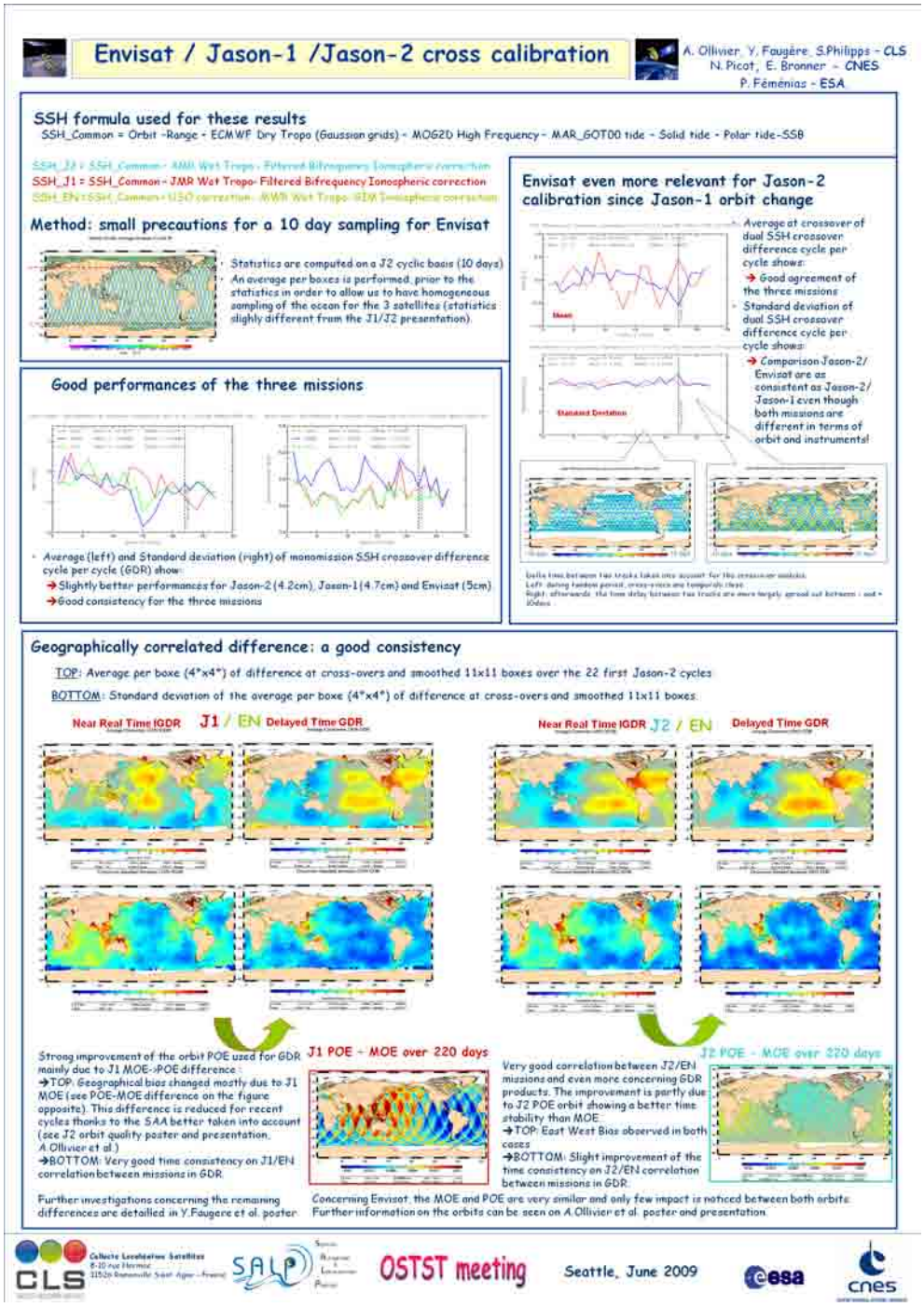

7.2.2.2. Assesment of Jason-2 orbit quality using SSH cross-calibration with Jason-1 and Envisat

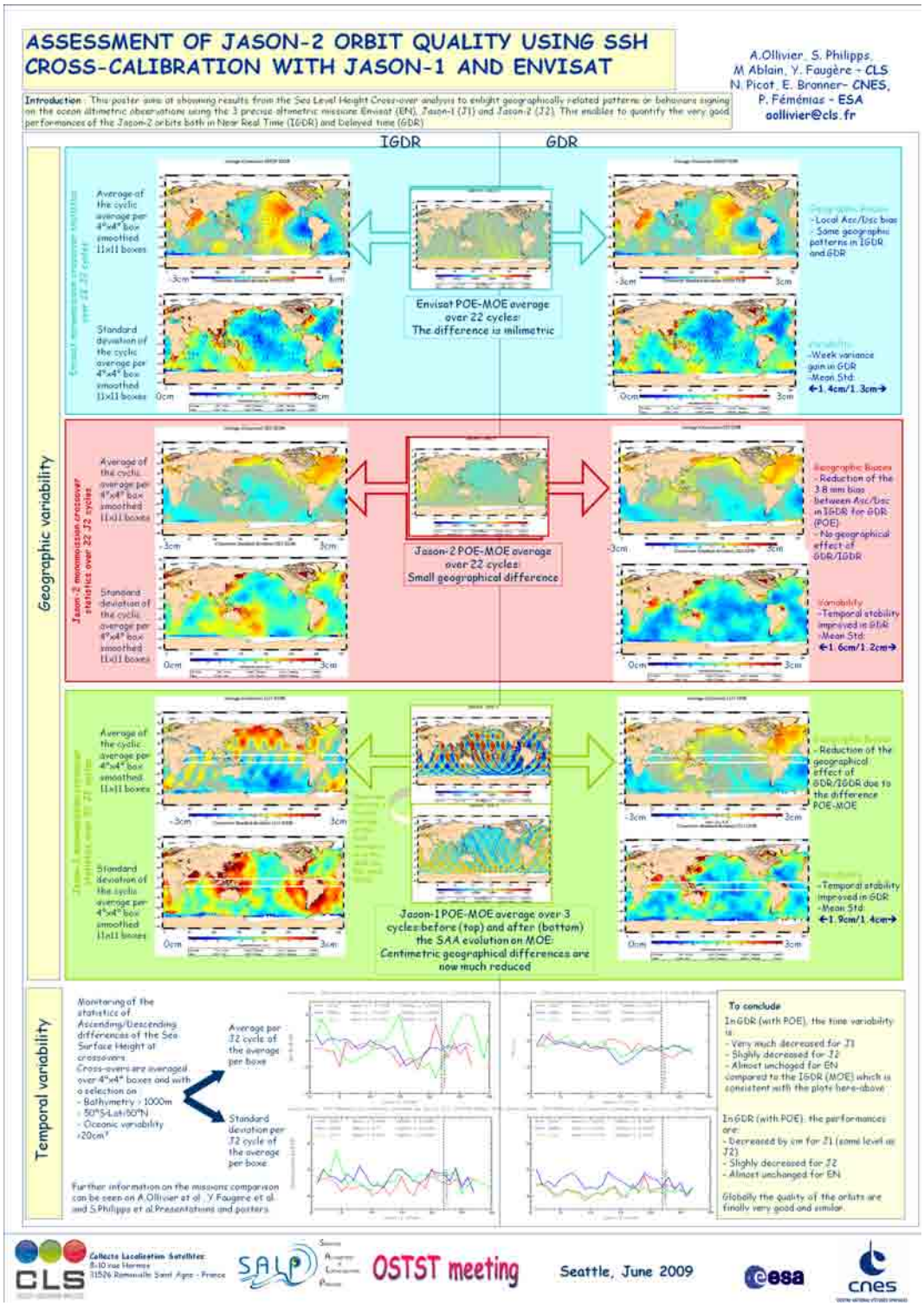

7.2.2.3. Envisat/Jason-1 cross-calibration

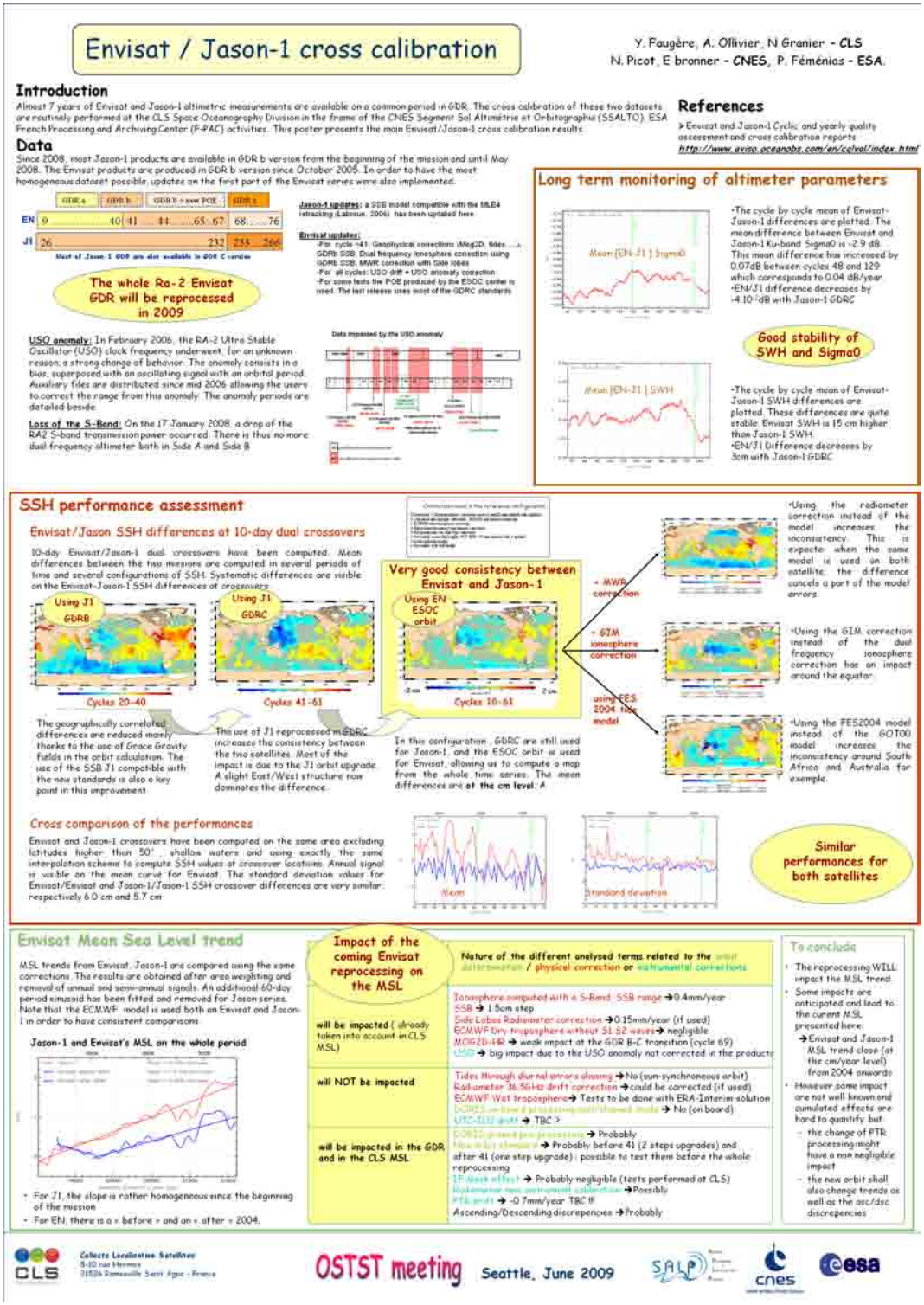

7.3. GOT 4.7 tide model validation

7.3.1. GOT 4.7 tide model analysis on Envisat and Jason-1 (in French)

The analysis performed (by Jean-Francois Legeais) on the new tide correction shows, through a global statistic analysis and a tide gage comparison analysis that the new correction is:
- better than the previous one (GOT00V2) near coasts
- less accurate in the Hudson Bay and North of the Bering strait
- identical in open ocean zones.

1. Introduction

L'objectif de cette note technique est d'évaluer l'impact de la nouvelle correction de marée GOT4.7 (R. Ray, Washington 2008) par rapport à la version précédente GOT00V2.

Nous travaillons pour cela dans un premier temps avec les missions Jason-1 (J1) et Envisat (EN) sur la période 2004-2005. Une approche statistique globale permet d'abord de localiser les différences entre les deux corrections, puis l'étude statistique du gain en variance de la différence de SSH aux points de croisement permet de quantifier et préciser si la nouvelle correction apporte une amélioration ou pas. Nous analysons ensuite l'évolution du gain en variance de la différence de SSH aux points de croisement en fonction de la distance à la côte.

Dans un deuxième temps, nous estimons le gain en variance en comparant les valeurs de SLA altimétriques utilisant les deux corrections de marées testées avec des valeurs de SSH issues de mesures marégraphiques.

2. Statistiques sur les corrections

2.1. Cartographie de la variance des différences

La Figure 1 présente la variance des différences des deux corrections de marée pour les années 2004-2005 de la mission Envisat. Cela indique qu'aucun changement n'est apporté dans le domaine hauturier et que les différences n'ont lieu que dans le domaine côtier. On observe en particulier une forte variance dans la baie d'Hudson et sur tous les plateaux continentaux. La même analyse sur la mission Jason-1 fournit des résultats similaires mais avec les informations aux hautes latitudes en moins puisque l'inclinaison de l'orbite est plus faible (66°).

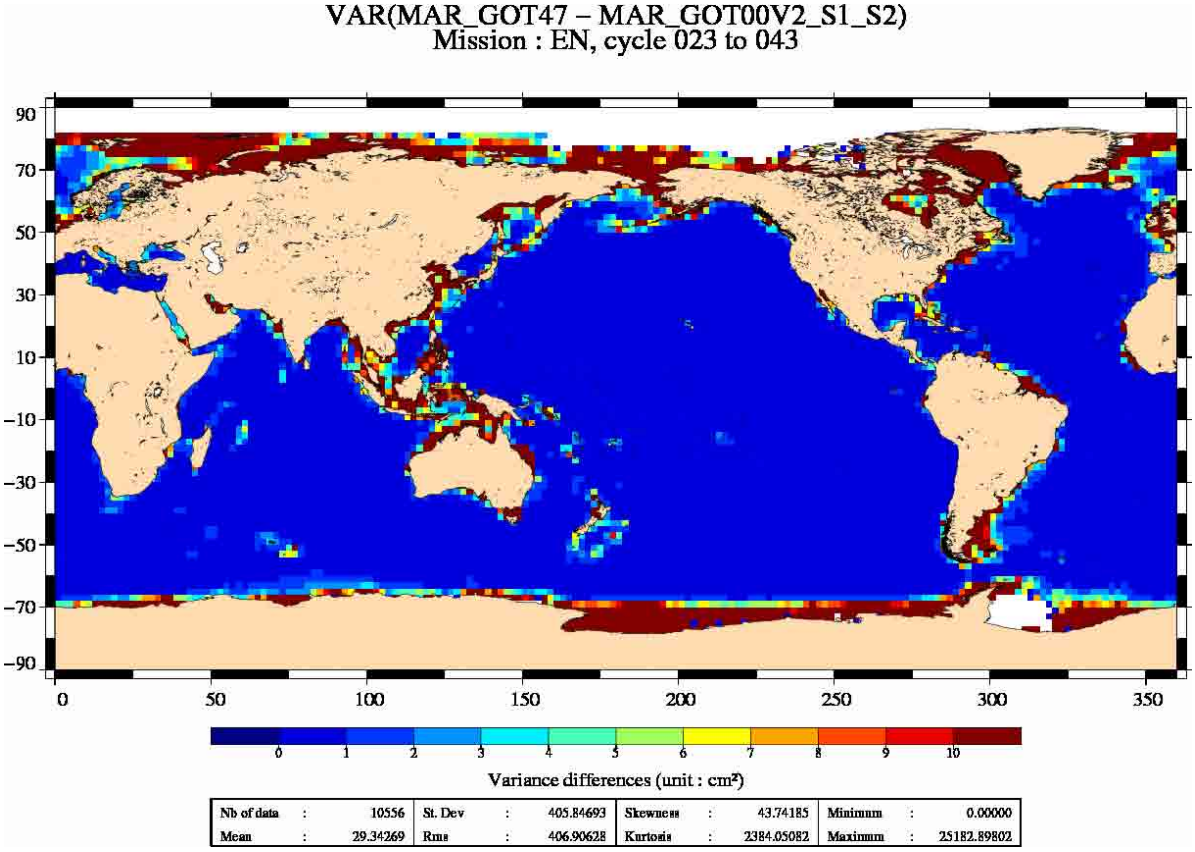

Figure 1 : Variance de la différence des corrections GOT4.7 et GOT00V2 sur les années 2004-2005 pour la mission Envisat

2.2. Suivi des statistiques par cycles

La Figure 2 présente l'évolution de la moyenne des différences (moyennes par cycle) entre les deux corrections de marée sur la période 2004-2005 pour les missions Jason-1 et Envisat.

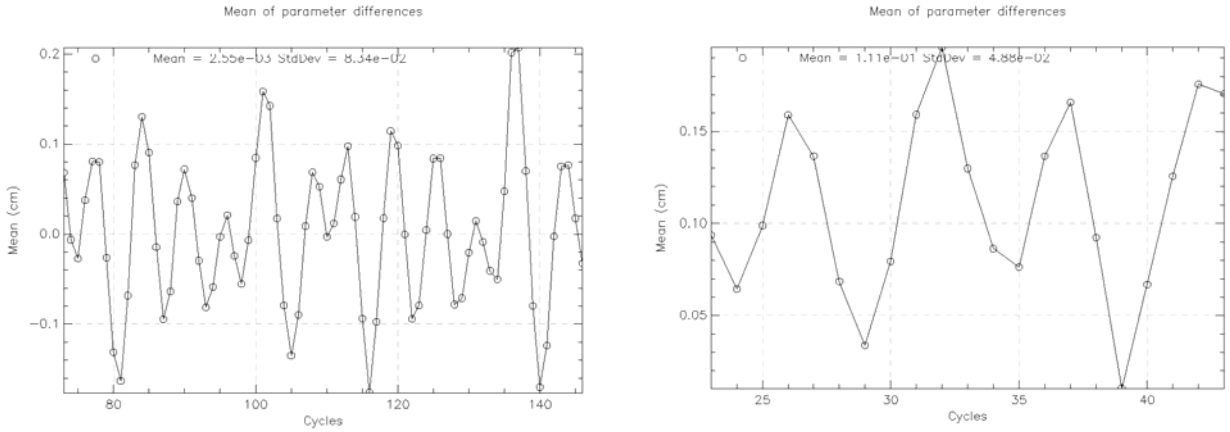

Figure 2 : Statistique par cycles de la moyenne des différences entre les corrections GOT4.7 et GOT00V2 pour Jason-1 (gauche) et pour Envisat (droite) pour les années 2004-2005

On remarque que ce paramètre varie autour de zéro pour Jason-1, alors qu'il est positif dans le cas d'Envisat : cette différence est probablement due à l'héliosynchronisme du satellite EN qui ne peut observer la variabilité de certaines ondes comme S2 (une seule observation par jour à la même heure), ce qui se traduit par un biais en terme de moyenne. Les amplitudes de ces variations restent faibles, de l'ordre de 0.05cm pour EN et 0.1 cm pour J1.

La moyenne des différences entre les deux corrections de marée oscille avec une période de ~60 jours pour Jason-1 et ~180 jours pour Envisat. Cela est dû au problème de l'aliasing du signal de marée, ie. au repliement des hautes fréquences du spectre sur les plus basses fréquences à cause de la fréquence d'échantillonnage des satellites de 9.9 jours (Jason-1) et de 35 jours (Envisat) : pour J1, les principales ondes semi-diurnes sont ainsi aliasées à 62 jours (M2) et 58 jours (S2), ce qui explique le signal résiduel observé à ~60 jours.

3. Impact sur la SSH aux points de croisements

3.1. Cartographie du gain en variance

La Figure 3 présente le gain en variance entre les deux corrections de marée concernant la différence de SSH aux points de croisements pour la mission Jason-1. Le même paramètre est présenté sur la Figure 4 pour la mission Envisat.

Les valeurs négatives indiquent une amélioration de la correction de marée GOT4.7, et sont localisées essentiellement dans le domaine côtier. La mission Envisat montre en particulier que la correction GOT4.7 permet de réduire la variance aux points de croisement le long de l'Antarctique et de l'Arctique ; dans la baie d'Hudson (tel que montré avec Jason-1) et au nord du détroit de Béring, les valeurs positives indiquent que la nouvelle correction de marée GOT4.7 est détériorée localement dans ces régions.

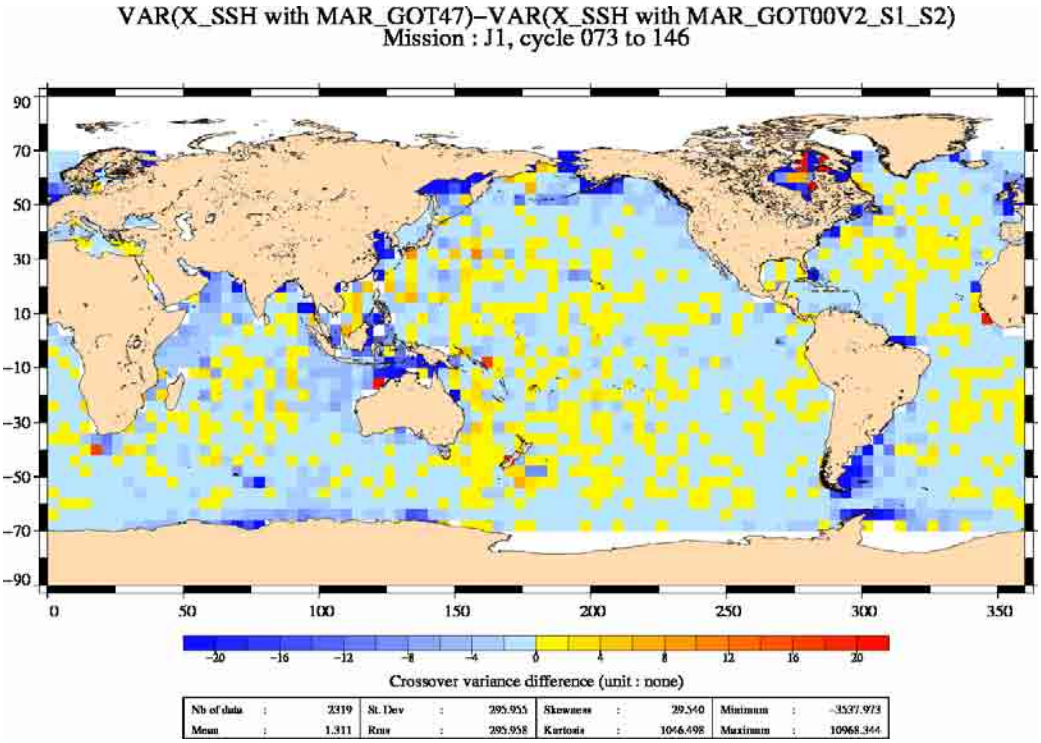

Figure 3 : Gain en variance entre les deux corrections de marée concernant la différence de SSH aux points de croisement pour la mission Jason-1 sur les années 2004-2005 (cm²)

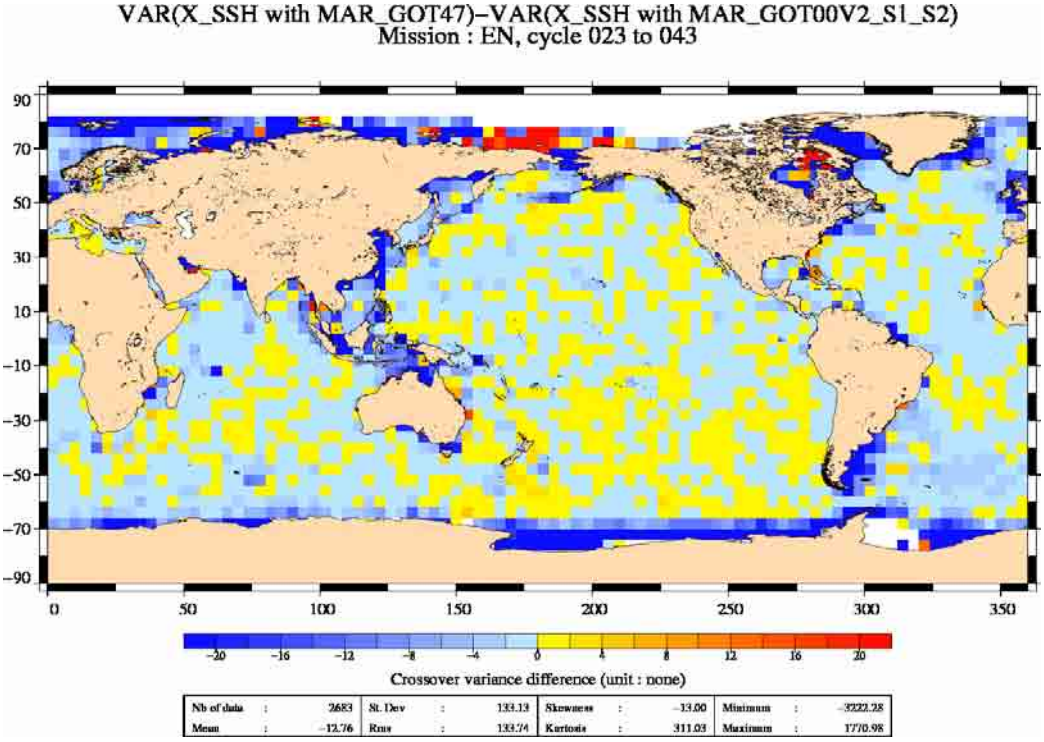

Figure 4 : Gain en variance entre les deux corrections de marée concernant la différence de SSH aux points de croisement pour la mission Envisat sur les années 2004-2005 (cm²)

3.2. Evolution temporelle du gain en variance

La Figure 5 présente l'évolution temporelle du gain en variance concernant la différence de SSH aux points de croisement pour la mission Jason-1. Les valeurs négatives indiquent que la nouvelle correction de marée (GOT4.7) permet de mieux réduire la variance de la différence de SSH aux points de croisement par rapport à la correction de référence (GOT00V2), i.e. que la correction est améliorée.

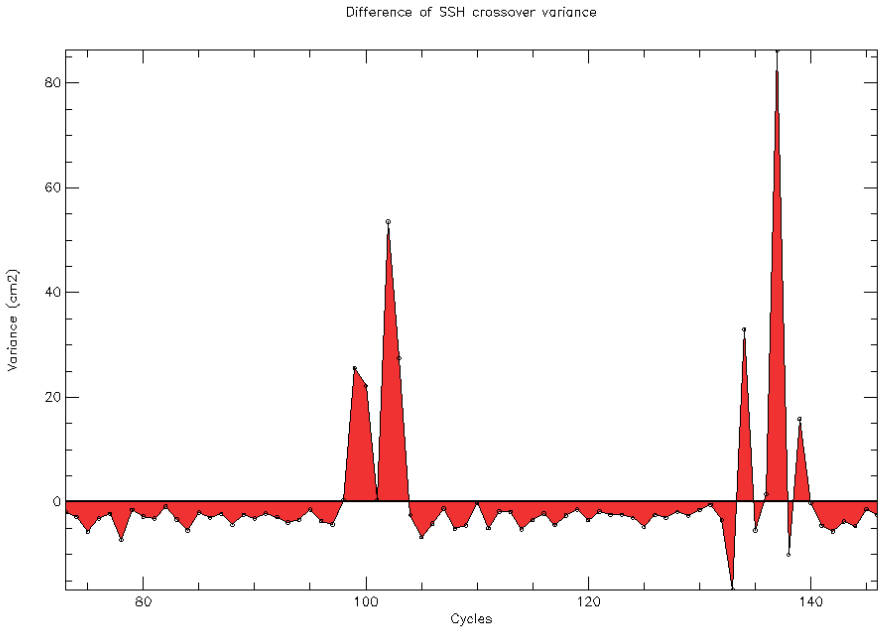

Figure 5 : Différence des variances des différences de SSH aux points de croisement avec les corrections GOT4.7 et GOT00V2 pour la mission Jason-1 sur les années 2004-2005. Variances moyennes par cycle J1.

On observe une détérioration ponctuelle de la nouvelle correction de marée GOT4.7 durant les mois de septembre/novembre des deux années étudiées (pics positifs sur la Figure 5). Cette détérioration est localisée dans la baie d'Hudson, comme montré sur les figures précédentes. Cette dégradation ponctuelle correspond à la période où l'eau est libérée des glaces dans ces régions arctiques.

La même analyse par cycle du gain en variance pour la mission Envisat ne montre pas une telle détérioration ponctuelle. En effet, l'analyse sur la mission Jason-1 montre que la détérioration est très localisée et la mission Envisat fournit des mesures à des latitudes plus élevées sur tout le pourtour de l'océan Arctique où la correction de marée est très améliorée. Cette forte amélioration masque donc les détériorations locales en baie d'Hudson et dans le détroit de Béring (Figure 4).

4. Impact sur la SLA le long de la trace

La Figure 6 présente le gain en variance pour la SLA le long de la trace lorsqu'on utilise la nouvelle correction de marée GOT4.7 au lieu de GOT00v2, sur les années 2004-2005 et pour la mission Envisat.

Cela confirme les résultats précédents selon lesquels la nouvelle correction de marée n'apporte pas de changement pour l'océan hauturier mais est de meilleure qualité dans le domaine côtier, sauf dans la baie d'Hudson et au nord du détroit de Béring où le signal est détérioré (uniquement pendant la période de fonte des glaces).

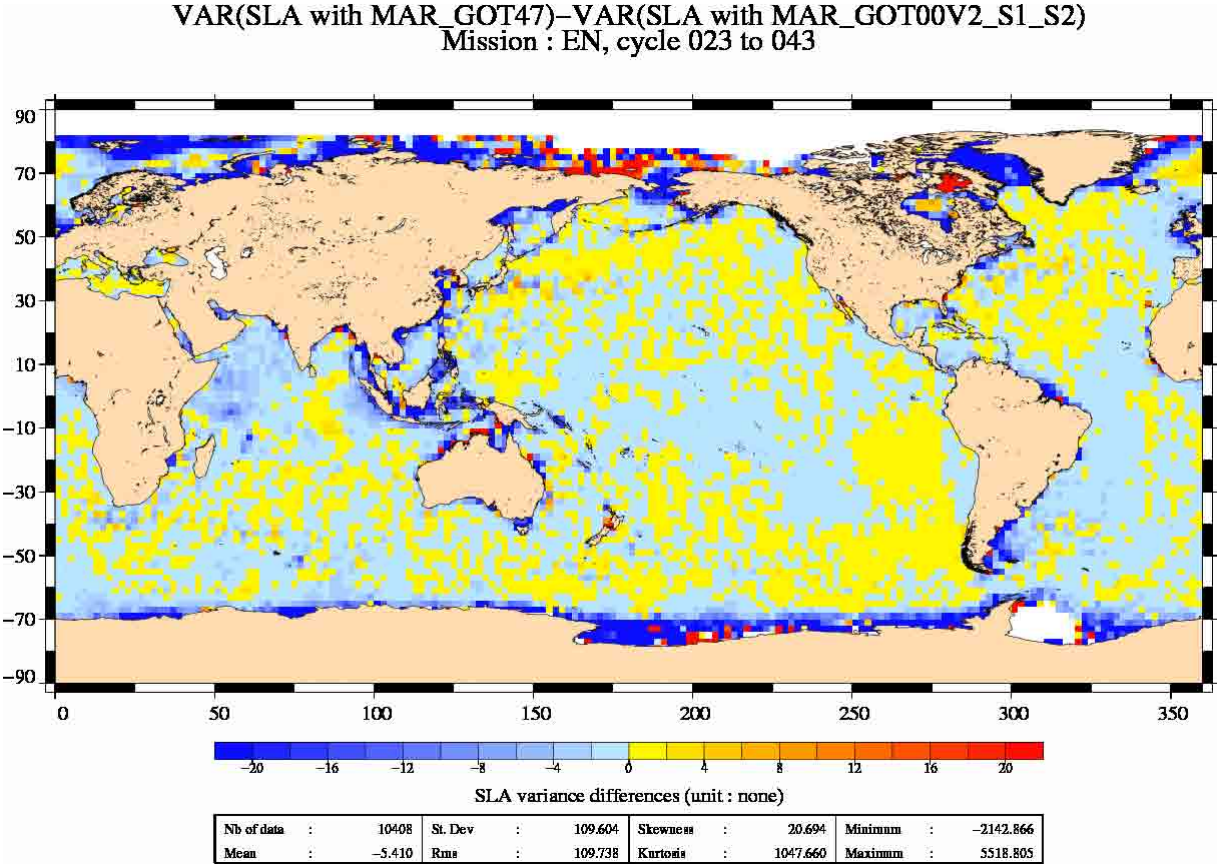

Figure 6 : Gain en variance de la SLA entre les corrections GOT4.7 et GOT00v2 sur les années 2004-2005 pour la mission Envisat (cm²)

5. Diagnostic côtier

L'analyse présentée dans les paragraphes précédents est une approche globale et nous cherchons ici à quantifier l'amélioration de la correction de marée en se restreignant au domaine côtier. Nous étudions pour cela l'évolution en fonction de la distance à la côte du gain apporté par la nouvelle correction de marée (GOT4.7 par rapport à GOT00v2) en terme de réduction de la variance des différences de SSH aux points de croisement.

La Figure 7 présente ce type de graphique pour la mission Jason-1 de manière globale sur les années 2004-2005 (à gauche) et pour les points de croisements situés à des latitudes inférieures à 50° (à droite). De manière globale (Figure 7, à gauche), la correction de marée est détériorée à moins de 100km de la côte et améliorée plus au large ; cette détérioration n'est pas observée si on se limite aux basses et moyennes latitudes (Figure 7, à droite). La même allure de courbe est obtenue en séparant la période janvier/juin de la période juillet/décembre. En accord avec les résultats précédents, la forte détérioration locale de la correction de marée dans la baie d'Hudson permet d'expliquer les valeurs négatives de différence d'écart type sur la Figure 7 (à gauche).

La Figure 8 présente la même approche pour la mission Envisat. La restriction en latitude n'apporte pas de changement significatif car comme mentionné précédemment, la correction de marée aux hautes latitudes est majoritairement améliorée et les détériorations locales ne sont pas assez marquées pour avoir une signature au niveau global (Figure 8, à gauche).

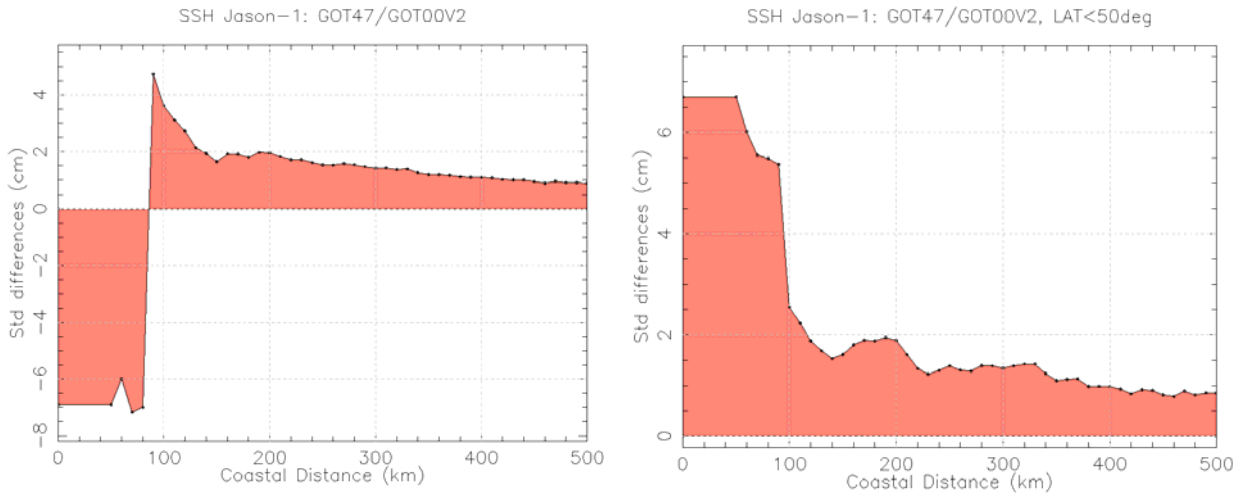

Figure 7 : Gain apporté par la correction GOT4.7 aux points de croisement Jason-1 en fonction de la distance à la côte sur les années 2004-2005 (différence d'écart-type en cm): sur le domaine global (à gauche) et aux latitudes <50° (à droite)

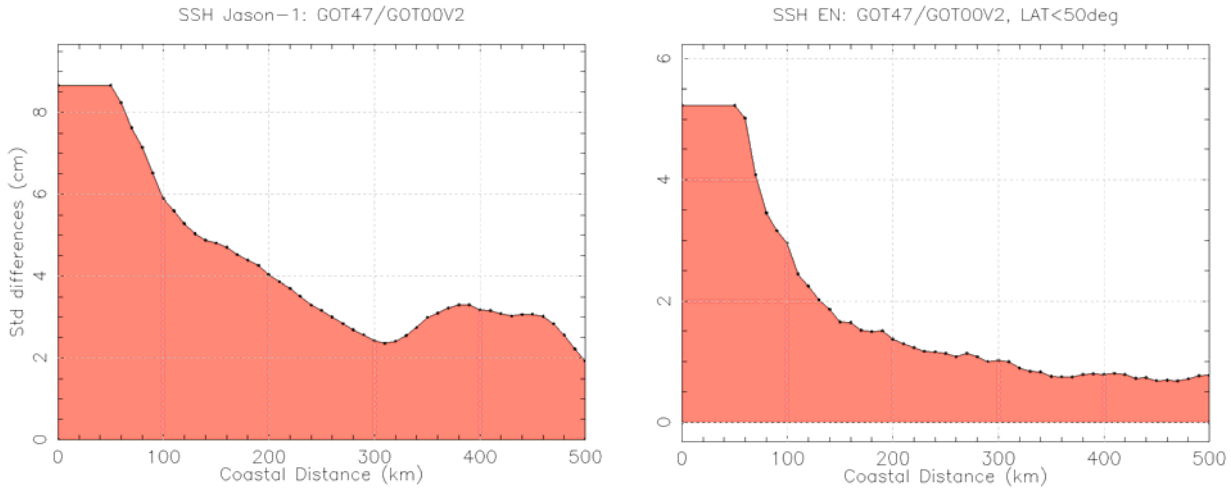

Figure 8 : Gain apporté par la correction GOT4.7 aux points de croisement Envisat en fonction de la distance à la côte sur les années 2004-2005 (différence d'écart-type en cm): sur le domaine global (à gauche) et aux latitudes <50° (à droite)

6. Comparaison aux mesures marégraphiques : gain en variance

Nous utilisons ici les données marégraphiques du réseau WOCE réparties sur l'océan global en domaine côtier (continent et îles), dont la répartition est visible sur la Figure 9. L'exclusion des mesures ne répondant pas à certains critères de qualité (pas de sauts dans les enregistrements, correction de la dérive crustale qui sont les mouvements verticaux de la croûte terrestre) conduit à un ensemble d'environ 120 séries de mesures pour chacune des trois missions utilisées : Jason-1, Envisat et Topex-Poséidon sur des périodes de 4ans.

La période d'étude choisie pour Topex-Poséidon est 2000-2004 permet de couvrir le changement d'orbite ayant eu lieu en août 2002 (cycles 365-369). Les périodes choisies pour Jason1 (2002-2006) et Envisat (2003-2007) ne sont pas identiques pour des raisons de disponibilité et de validité des données.

La Figure 10 présente le gain en variance des différences de SLA altimétrique et marégraphique avec les corrections de marée GOT4.7 et GOT00V2 pour chacune des trois missions. Le gain en variance est la différence entre :

- la variance de la différence entre la SLA altimétrique calculée avec GOT4.7 et marégraphique et

- la variance de la différence entre la SLA altimétrique calculée avec GOT00V2 et marégraphique.

Des valeurs négatives signifient que la SLA altimétrique utilisant la correction de marée GOT4.7 est plus cohérente avec la SLA marégraphique que la SLA altimétrique corrigée avec GOT00V2. C'est ce que montrent les résultats avec les trois missions utilisées sur la Figure 10 : le gain moyen sur la période d'étude atteint 4 cm² pour J1, 0.6 cm² pour EN et 2.5 cm² pour T/P.

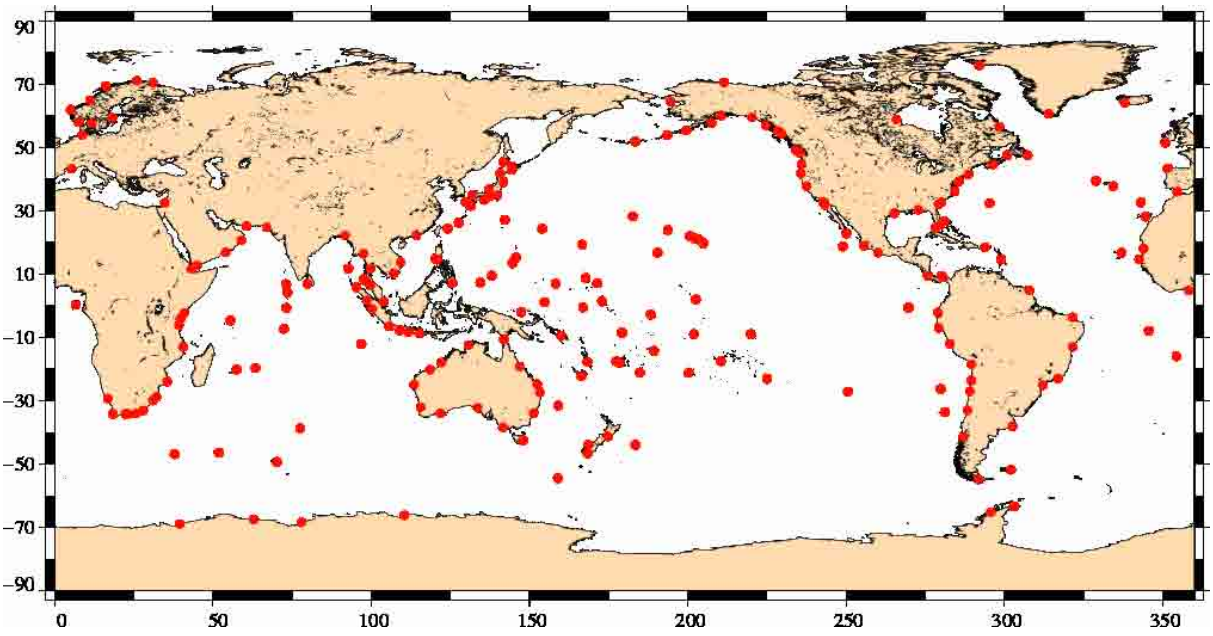

Figure 9 : Distribution des marégraphes utilisés pour l'étude

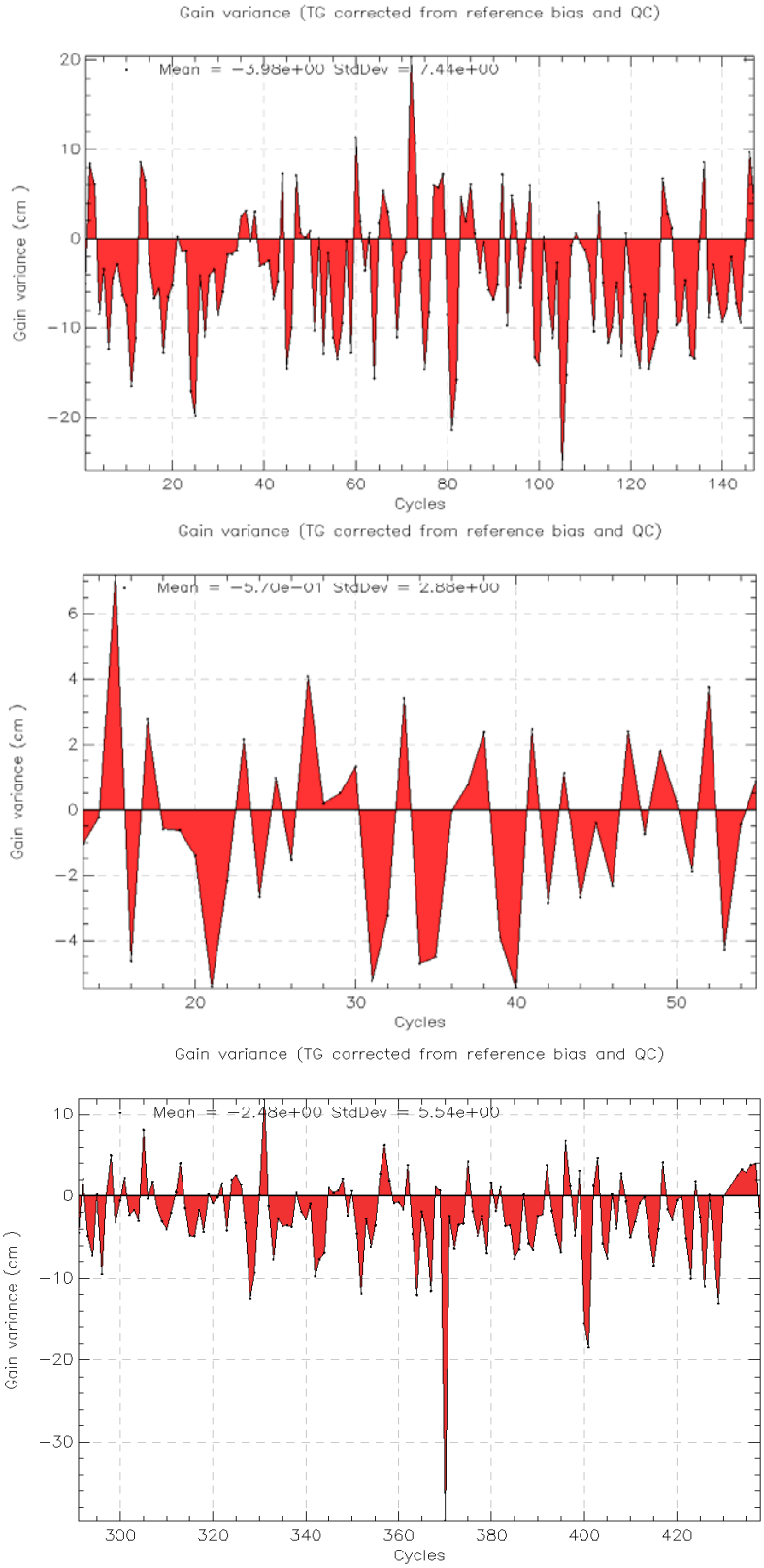

Figure 10 : Gains en variance de la différence de SLA altimétrique et marégraphique avec les corrections de marée GOT4.7 et GOT00V2 pour les missions Jason-1 2002/2006 (en haut), Envisat 2003/2007 (milieu) et Topex-Poseidon 2000/2004 (en bas). Gain en cm².

7. Conclusion

L'analyse statistique globale effectuée ainsi que la comparaison aux mesures marégraphiques ont permis de montrer que la nouvelle correction de marée GOT4.7 est de meilleure qualité que la correction précédente (GOT00V2) dans le domaine côtier sauf dans la baie d'Hudson et au nord du détroit de Béring. Aucun changement significatif n'est observé dans l'océan hauturier.

7.4. New SSB validation

7.4.1. New 2007 Sea State Bias model analysis on Envisat (in French)

The analysis performed on the new sea state bias correction shows better performances in terms of along track and cross over statistics, therefore validating the improvement of this new correction compared to the previous one currently used (2006 version).

1 Introduction

Le but de cette étude est d'étudier l'impact de l'évolution du biais électromagnétique sur les calculs de hauteur de mer. Pour cela, nous comparons ici les résultats obtenus en utilisant la nouvelle variable d'étude, BEM_NPARAM_2007, à ceux obtenus avec la variable de référence, BEM_NPARAM.
L'étude est menée sur la mission ENVISAT, des cycles 9 à 75, soit du 24 Septembre 2002 (1er cycle disponible) au 26 Janvier 2009.
Nous étudierons d'abord les statistiques le long de la trace, puis l'impact sur les calculs de SSH aux points de croisement, et enfin l'impact sur les anomalies de hauteur de mer le long de la trace.

2 Statistiques le long de la trace

2.1 Cartographie de la moyenne des différences

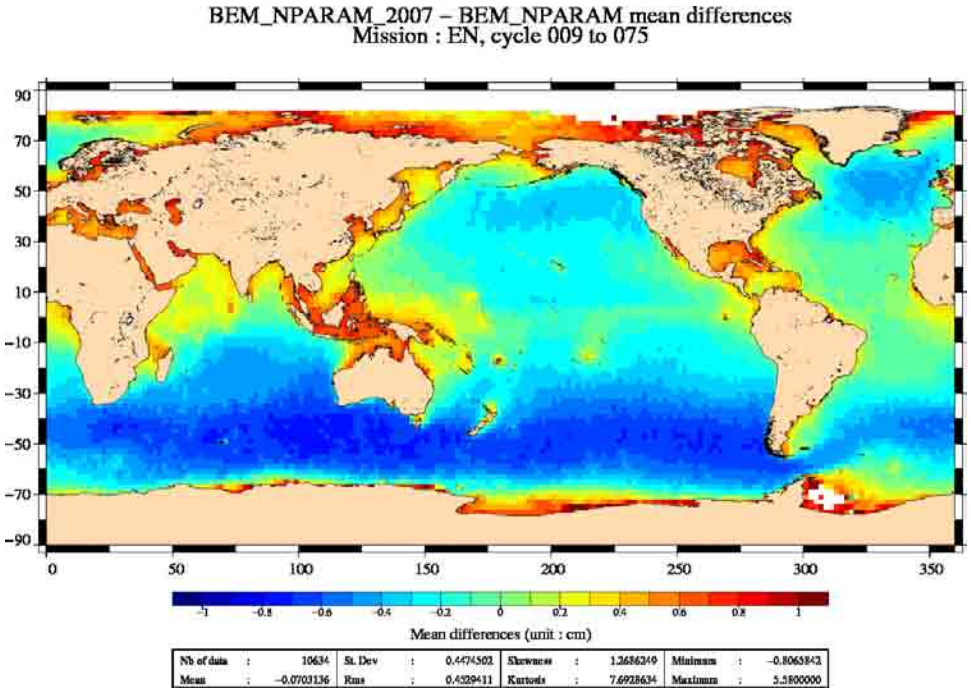

Figure 1: *VarEtu - VarRef mean differences.*

Cette carte montre la moyenne des différences entre le paramètre d'étude et celui de référence sur toute la période. Cette moyenne est faible : elle a elle-même une moyenne de l'ordre de 2mm.
On observe que les plus importantes différences se trouvent aux hautes latitudes, ainsi que dans les zones de forte variabilité océanique.
Néanmois, ces différences n'ont pas une amplitude conséquente.

La figure 2 montre la moyenne des différences pour les traces paires.

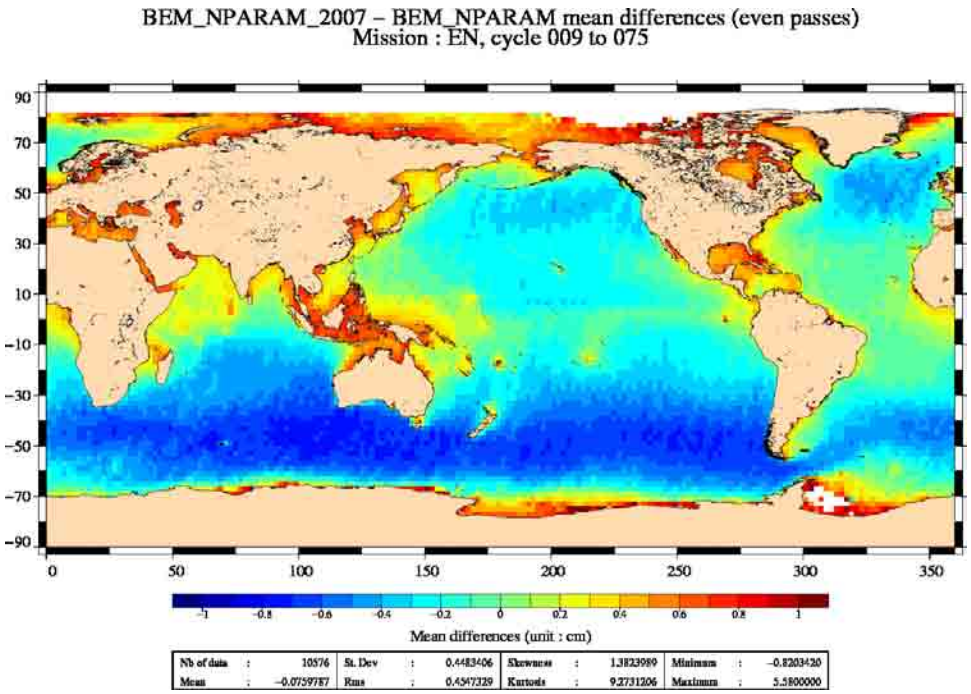

Figure 2: *VarEtu - VarRef mean differences.*

La figure 3 montre la moyenne des différences pour les traces impaires.

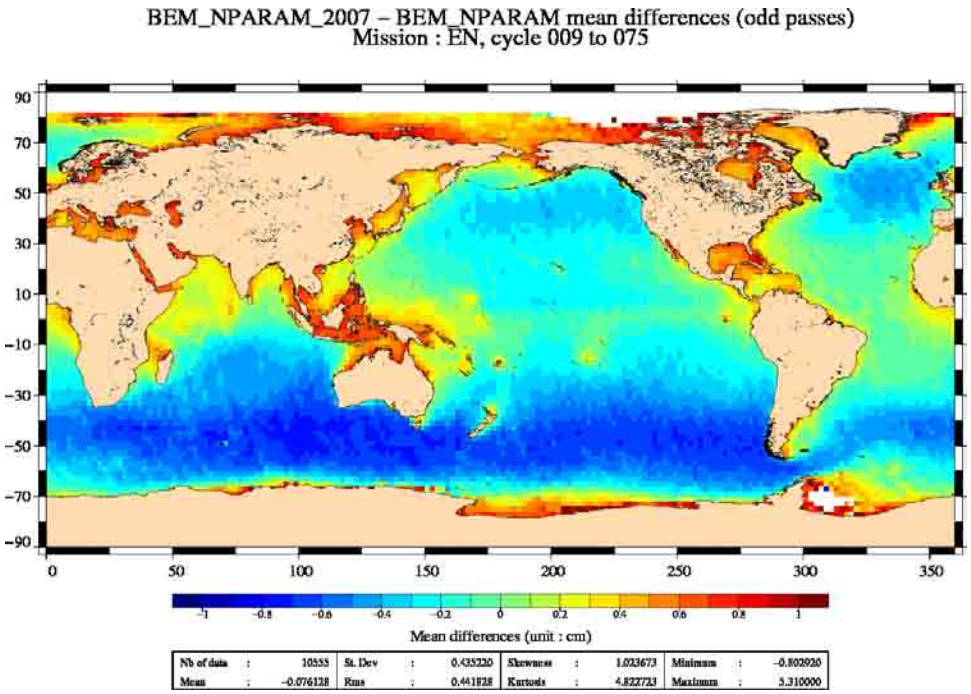

Figure 3: *VarEtu - VarRef mean differences.*

Nous observons ici la moyenne des différences pour les traces ascendantes (figure 2) et descen-

dantes (figure 3). Ces deux cartes sont très similaires entre elles, mais également à la précédente (toutes traces confondues).
Elles n'apportent donc pas d'information supplémentaire sur les conséquences du changement de la correction BEM_NPARAM.

2.2 Cartographie de la variance des différences

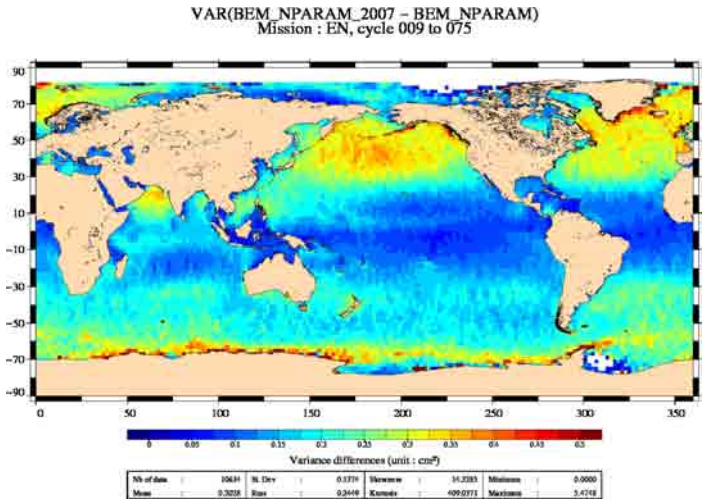

Figure 4: *VAR(VarEtu - VarRef).*

Nous avons cartographié ici la variance des différences des deux biais électromagnétiques.
Nous observons que les valeurs en question sont faibles (de l'ordre du centimetre carré).
Toutefois nous remarquons qu'autour des tropiques la variance de la nouvelle correction BEM_NPARAM_2007 est inférieure à l'ancienne correction BEM_NPARAM, alors que c'est l'inverse aux hautes latitudes.

2.3 Cartographie de la différence des variances

La Figure 5 montre la différence des variances de chaque paramètre.
Nous observons que le paramètre d'étude BEM_NPARAM_2007 a une variance plus élevée que le paramètre de référence BEM_NPARAM, et ce sur toute la surface du globe.
C'est encore plus vrai aux hautes latitudes, et notamment dans le Pacifique et l'Atlantique Nord.

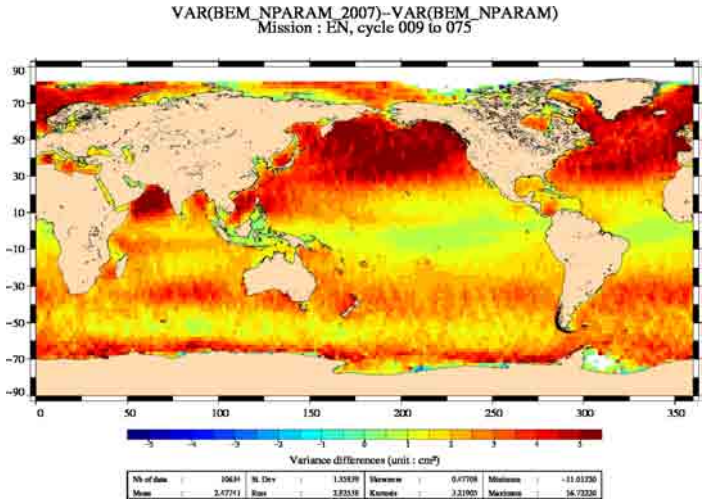

Figure 5: *VAR(VarEtu) - VAR(VarRef).*

2.4 Suivis des statistiques par cycle

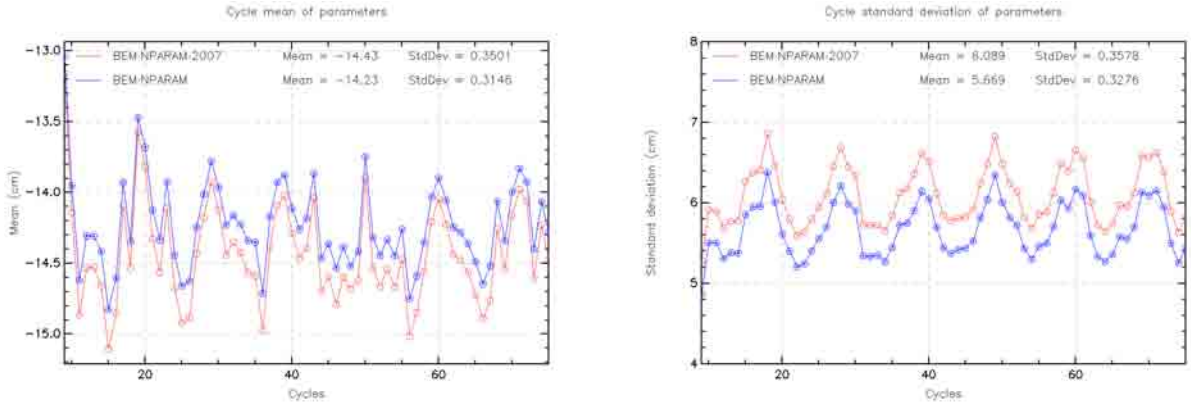

Figure 6: *Statistics per cycle of VarEtu and VarRef: mean (left) and std (right).*

Nous avons ici les suivis par cycle des variables d'étude et de référence (figure 8), ainsi que le suivi de leur différence (figure 9) : VarEtu - VarRef. Les graphes de gauche présentent la moyenne, ceux de droite la variance. Nous observons que ces suivis sont très proches : la moyenne de la différence est de l'ordre de 1.5mm, la variance de la différence de 3cm. Une fois encore nous voyons donc que le nouveau biais électromagnétique est très proche de celui qui est actuellement utilisé dans les chaînes de traitement.

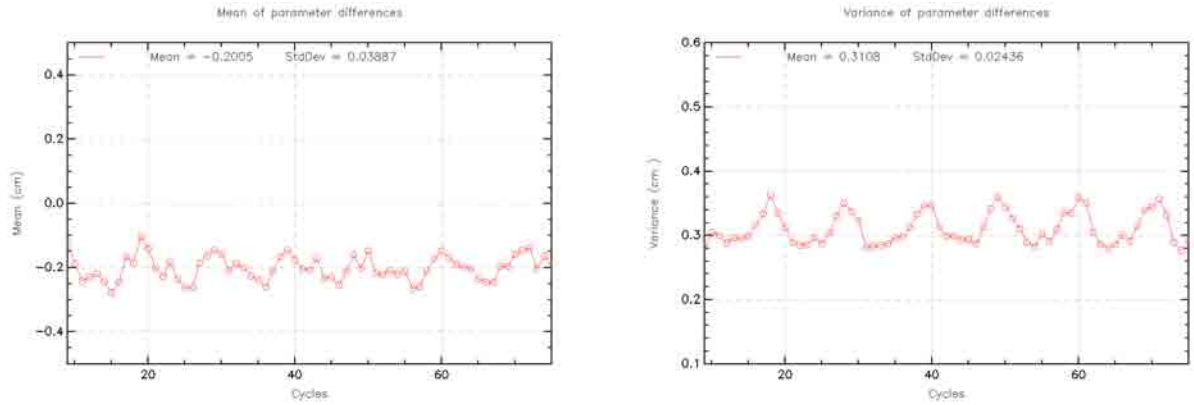

Figure 7: *Statistics per cycle of differences between VarEtu and VarRef: mean (left) and variance (right).*

2.5 Suivis des statistiques par jour

La Figure 8 montre la moyenne et la variance, par jour, de VarEtu et VarRef. La Figure 9 montre la moyenne et la variance, par jour, de la différence entre VarEtu et VarRef.

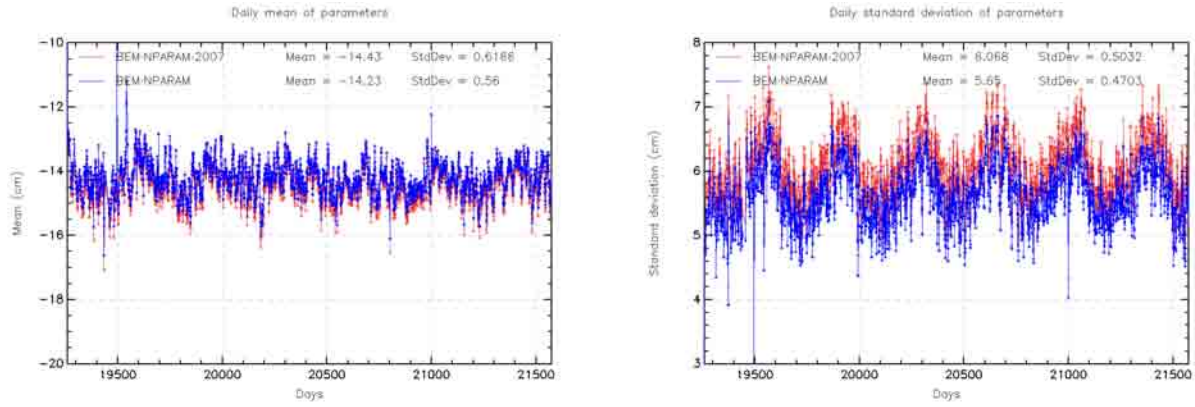

Figure 8: *Statistics per day of VarEtu and VarRef: mean (left) and std (right).*

Nous avons ici les mêmes suivis, mais cette fois présentés par jour. Nous en tirons les mêmes conclusions : la différence est faible entre les deux corrections étudiées.

3 Impact sur la SSH aux points de croisement

3.1 Cartographie de la moyenne des différences

Regardons maintenant l'impact sur la SSH aux points de croisement. Sur la carte de gauche, les différences de SSH aux points de croisement sont calculées avec la nouvelle correction BEM_NPARAM_2007. Sur la carte de droite, ces différences de SSH aux points de croisement sont calculées avec l'ancienne

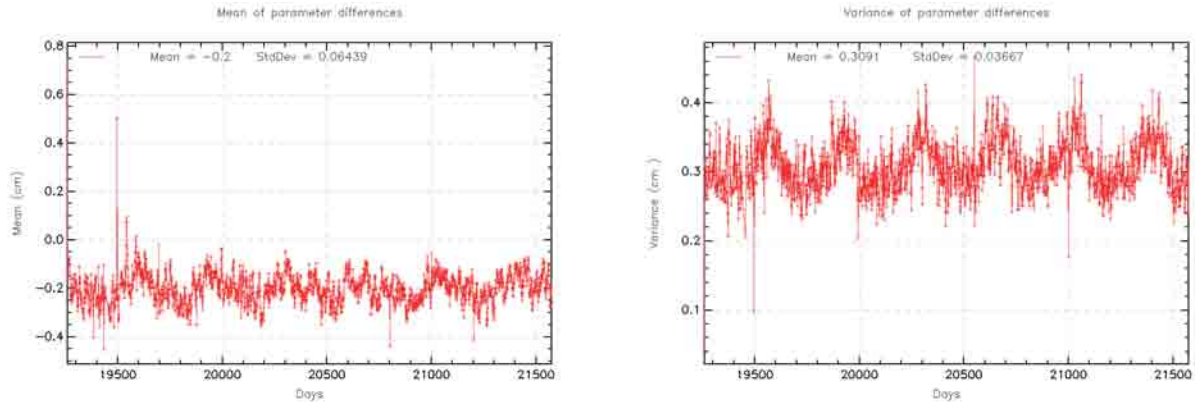

Figure 9: *Statistics per day of differences between VarEtu and VarRef: mean (left) and variance (right).*

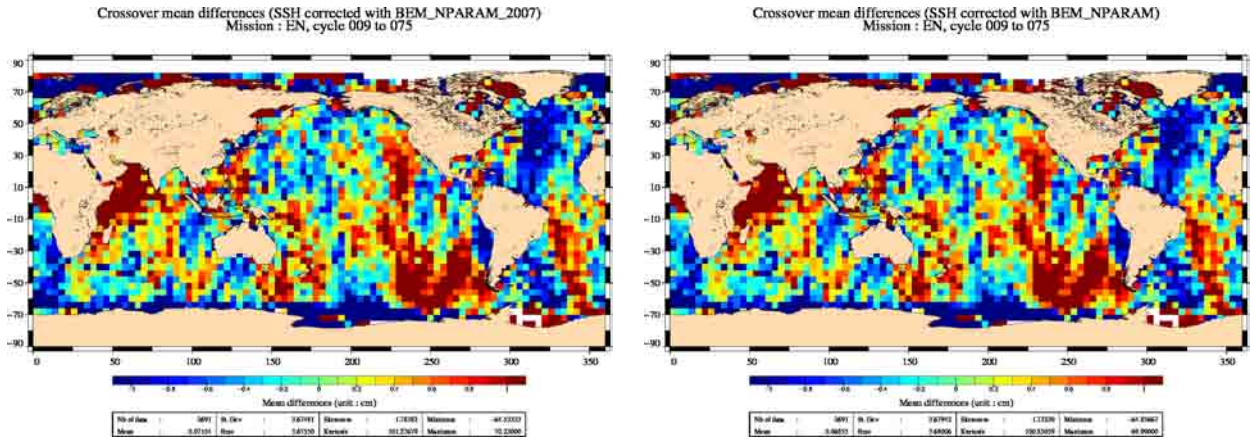

Figure 10: *Crossover mean differences. SSH corrected with VarEtu (left) and VarRef (right).*

correction BEM_NPARAM.
Les deux cartes sont très similaires, avec une amplitude de l'ordre du centimètre : comme prévu, l'impact du changement de correction sur les XSSH n'est pas conséquent.

3.2 Cartographie de la difference de variance

La figure 11 montre le gain en variance des différences de SSH aux points de croisement en utilisant VarEtu au lieu de VarRef. La figure 12 montre le gain en variance des différences de SSH aux points de croisement, normalisé par la variance de SSH aux points de croisement calculée avec VarEtu.
La couleur bleue signifie que VarEtu a une variance des différences de SSH aux points de croisement plus faible que VarRef.

L'amplitude de cette différence des variances est également faible : de l'ordre du centimetre carré. On n'observe pas de région qui présente une différence bien supérieure aux autres, si ce n'est une tendance à ce que cette difference soit plus importante dans l'Est des bassins océaniques.

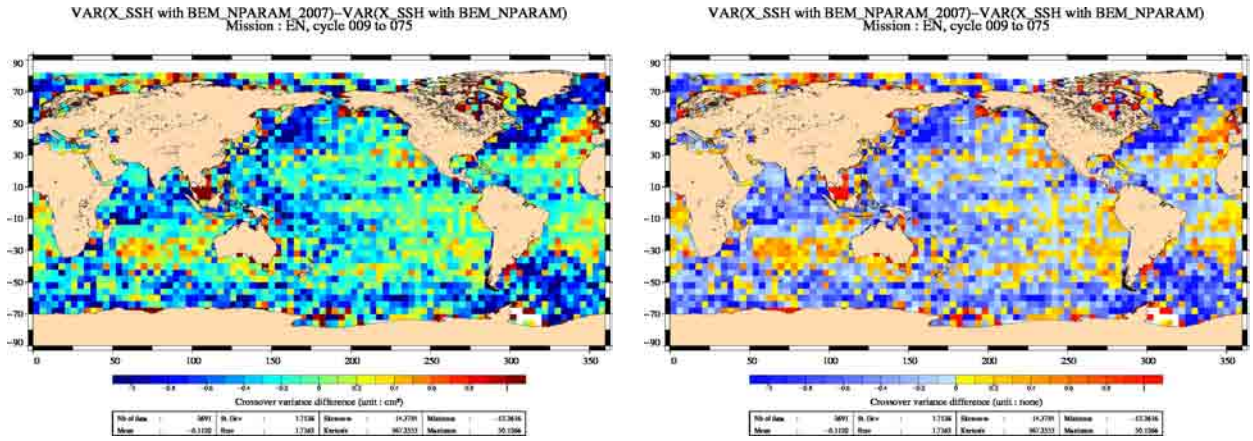

Figure 11: *VAR(X_SSH VarEtu) - VAR(X_SSH with VarRef).*

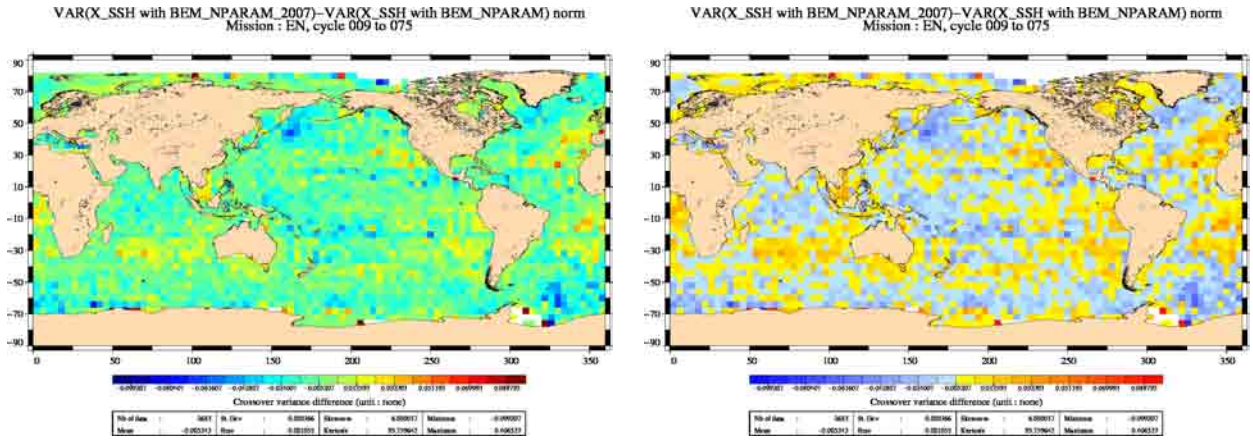

Figure 12: *[VAR(X_SSH VarEtu) - VAR(X_SSH with VarRef)]/VAR(X_SSH VarEtu).*

3.3 Suivis des statistiques par cycle

3.3.1 Comparaison des statistiques par cycle

La figure 13 montre la moyenne et l'écart-type cycle par cycle de la SSH aux points de croisement. Le gain en variance est tracé à la Figure 14.

Sur ces deux graphes nous observons que les courbes des SSH calculées aux points de croisement avec VarEtu ou VarRef sont confondues : les performances sont exactement les mêmes.

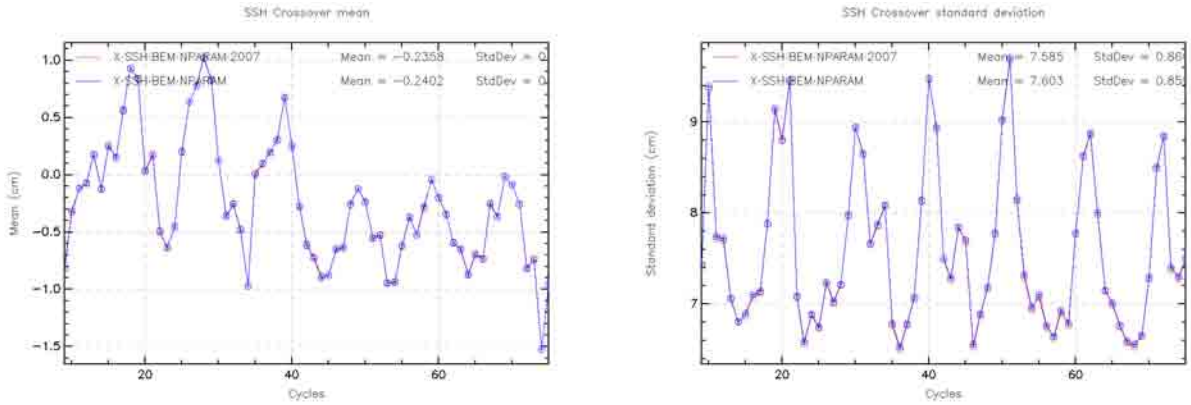

Figure 13: *Statistics per cycle of SSH: crossover mean (left) and crossover standard deviation (right).*

3.3.2 Differences de variance

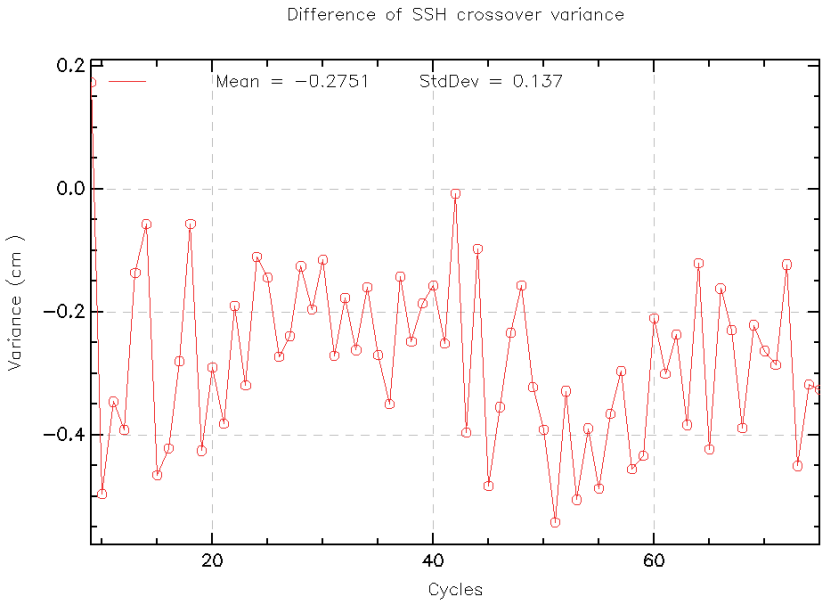

Figure 14: *Var(SSH differences at Xovers with VarEtu) - Var(SSH differences at Xovers with VarRef).*

Ce graphe nous montre le gain en variance dans la SSH aux points de croisement. Nous observons donc que la variance calculée avec la variable d'étude est inférieure à la variance calculée avec la variable de référence. Nous montrons donc bien que les performances sont améliorées grâce au nouveau SSB utilisé dans cette étude.

4 Impact sur la SLA le long de la trace

4.1 Cartographie de la différence de variance

La Figure 15 montre le gain en variance de la SLA moyennée par boîte, en utilisant VarEtu par rapport à VarRef.
La figure 16 montre également le gain en variance calculé de la même façon, mais normalisé par la variance de la SLA calculée avec VarEtu.

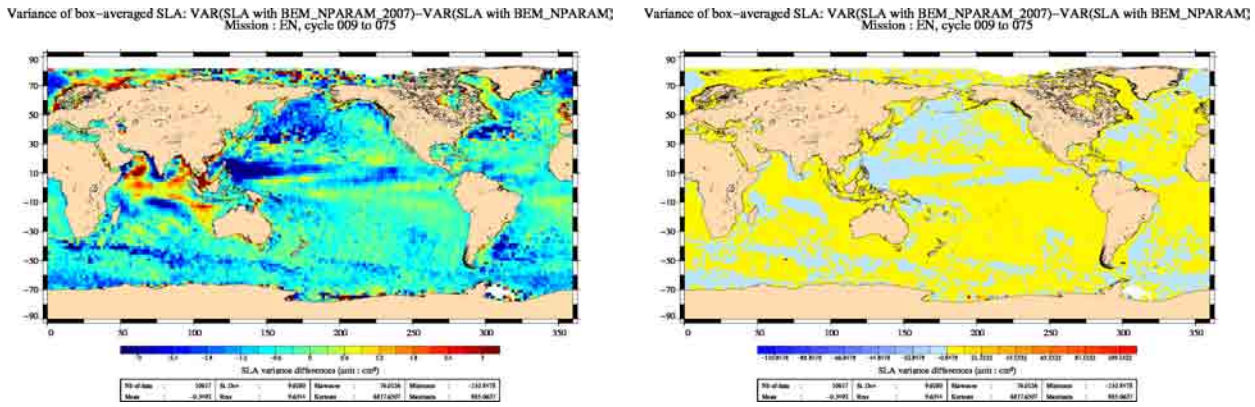

Figure 15: *Var(SLA with VarEtu) - Var(SLA with VarRef) by averaging the time series per box.*

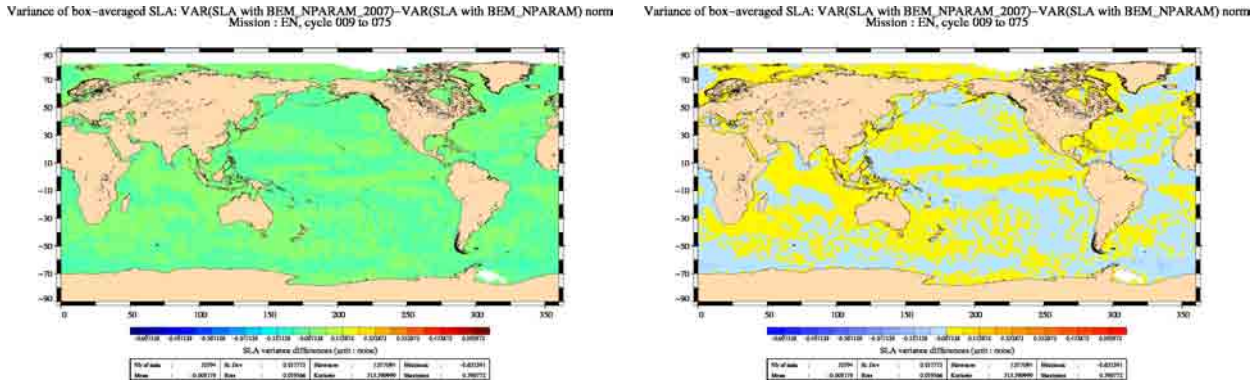

Figure 16: *[Var(SLA with VarEtu) - Var(SLA with VarRef)]/Var(SLA with VarEtu) by averaging the time series per box.*

4.2 Ecart-Type des différences par cycle et par jour

La Figure 17 montre l'écart-type de la SLA par cycle, et par jour, avec les variables.
Le gain en variance est tracé sur la Figure 18.

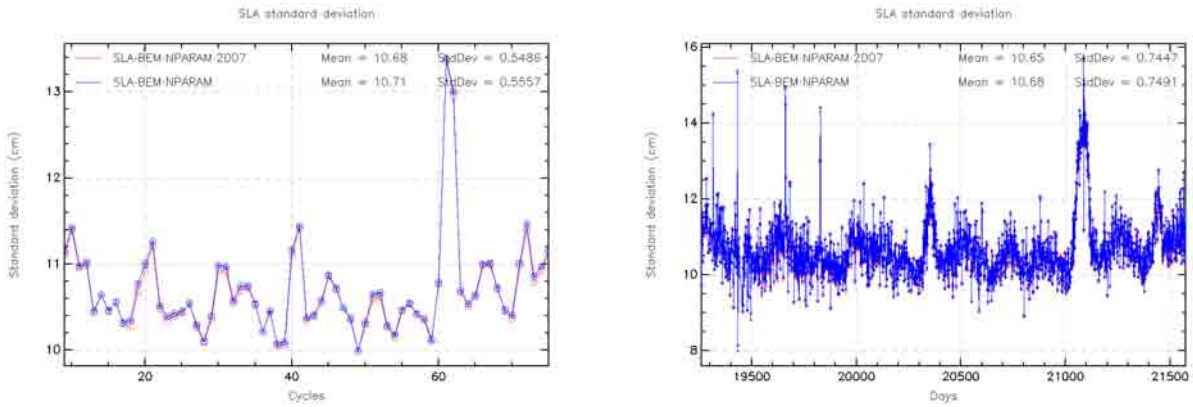

Figure 17: *SLA standard deviation per cycle (left) and per day (right).*

Nous observons que les écart-type le long de la trace sont confondus pour chacun des paramètres : le changement apporté à la correction n'a pas d'impact sur ses caractéristiques statistiques.
De plus, cet écart-type est stable, mis à part pour le cycle 61. Pour tous les autres cycles, il est compris entre 10 et 12cm, avec une moyenne de 10.68cm pour VarEtu, et 10.71 pour VarRef (respectivement 10.65cm et 10.68 pour le suivi par jour).

4.3 Différences de variance par cycle et par jour

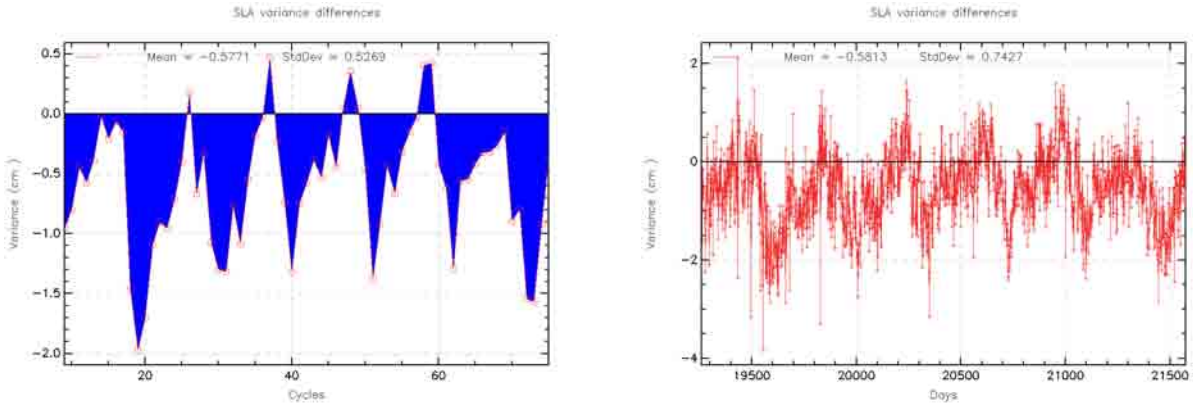

Figure 18: *Var(SLA with VarEtu) - Var(SLA with VarRef) per cycle (left) and per day (right).*

Cette figure nous montre les différences de variance le long de la trace, par cycle et par jour. Nous observons que les valeurs sont négatives pour la plupart du temps : la variance de la SLA est plus faible lorsqu'elle est calculée avec VarEtu.
Nous avons donc amélioré les calculs par le changement de correction BEM.

5 Conclusion

Nous montrons par cette étude que les résultats obtenus sont meilleurs lorsque l'on utilise la nouvelle correction du biais électromagnétique.
En effet, nous obtenons une variance réduite, que ce soit le long de la trace ou aux points de croisement.
Pour cela, nous validons donc l'utilisation du nouveau paramètre BEM_NPARAM_2007 en comparaison du paramètre actuellement utilisé dans les études CALVAL, à savoir BEM_NPARAM.

8. Conclusion

A statistical evaluation of Envisat altimetric measurements over ocean has been presented in this report. With more than seven years of data now available in Geophysical Data Record (GDR) products, Envisat altimetric measurements show good general results:

- A very good **availability** of Envisat data on the last 18 months was noticed thanks to an improvement of the data dissemination since May 2008.

- The **S-Band loss** is considered to be permanent and all the S-band parameters MUST NOT be used anymore. The dual ionospheric correction could efficiently be replaced by the JPL GIM Ionospheric correction with no visible impact on the data quality, presumably thanks to the low solar activity period when it occured. However, this could be problematic for MSL studies regarding the instabilities noticed on the GIM correction.

- The **USO anomaly** still did not affect Ra-2 this year and since January the 23th 2008. Auxiliary files correction allows Envisat Ra-2 data to recover their nominal quality during anomaly period. They are also recommended to be used in non anomaly periods as well in order to take into account the long term aging drift.

- The **SLA performance** is very good, at the same level as Jason-1 with geographical differences between Envisat and Jason-1 reaching the cm level using recent (September 2005's IPF/CMA update) orbit and geophysical correction. The current standards (orbit configuration, instrumental and geophysical correction) used since September 2005 in the IPF/CMA, allow Envisat products to have a high geophysical quality.

- The ocean-1 **altimeter and radiometer parameters** are consistent with expected values. However, differences between MWR and ECMWF wet troposphere correction are still periodically noticed due to version changes of the ECMWF Model with a strong impact on the MSL trend. Homogeneous model time series would be very useful.

- Very good consistency was found between Envisat and **Jason-2** data whith the longer and longer time series. This is encouraging for insuring a good continuity on the long term monitoring already initiated with Jason-1 since 2002.

- This year, a new SSB model (2007) as well as a new tidal model (GOT4.7) were validated. Both correction show a great improvement of the SLA restitution in terms of variance gain at cross overs and along track.

- Recent validation of the GDRC CNES orbit enabled to show a significant reduction of the SLA performnecs of the mission on the whole time series. It also solved the until then unexplained ascending/descending inconsistencies on the SSH. The difference is now around 0.7mm/year, at the same level as the inconsistency noticed on Jason-1's reference MSL. This is a very good result, allowing a greater confidence is the Envisat's time series.
- The Envisat **Mean Sea Level trend** is still an issue and was still studied this year. It is unfortunatly still unusable at the beginning of the mission (until cycle 22). However, this year, after the extensive studies perfomed on all the terms of SLA we could update (including the new official GDRC Orbit), a particular care was brought to instrumental calval monitoring. A

term of the instrumental correction is being suspected to be wrongly applied on the data which could introduce errors in Envisat's MSL time series. Investigations are carrying on to prove that the correction of such instrumental term could significantly reduce MSL discrepencies with Jason-1.

- A **reprocessing** of the whole Envisat altimetric mission is expected in 2010. The major evolutions will be a new precise orbit based on recent Grace data and new ITRF model (validated thisd year from cycle 15 onwards), better ECMWF meteo fields, new geophysical and instrumental (USO) corrections, new SSB correction, updated wet tropospheric correction. Besides it is planned to re-process ERS-2 data with similar algorithms (REAPER project). Then, performances and comparisons will be carried out again using these new data in order to assess the consistency between Envisat and ERS-2 parameters.
These new products will further improve the high quality level of the Envisat altimetric mission and will make easier the data merging for multi-mission altimetry, as it is essential for oceanography and applications.

9. Bibliography

References

[1] Abdalla, S., "A wind retrieval algorithm for satellite radar altimeters", ECMWF Technical Memorandum, in preparation, 2006.

[2] Ablain, M., G. Pontonnier, B. Soussi, P. Thibaut, M.H. de Launay, J. Dorandeu, and P. Vincent. 2004. Jason-1 GDR Quality Assessment Report. Cycle 079. SALP-RP-P2-EX-21072-CLS079, May.

[3] M. Ablain., S. Philipps, Dorandeu J., 2006: Jason-1 validation and cross calibration activities. Yearly report. Technical Note CLS.DOS/NT/06-302, Contract N° 03/CNES/1340/00-DSO310 - lot2.C http://www.jason.oceanobs.com/documents/calval/validation_report/annual_report_j1_2006.pdf

[4] M. Ablain., S. Philipps, 2007: Jason-1 validation and cross calibration activities. Yearly report. Technical Note CLS.DOS/NT/06-302, Contract N° 03/CNES/1340/00-DSO310 - lot2.C http://www.jason.oceanobs.com/documents/calval/validation_report/annual_report_j1_2007.pdf

[5] Ablain M., Cazenave A., Guinehut S., Valladeau G., (submitted for publication), A new assessment of global mean sea level from altimeters highlights a reduction of global slope from 2005 to 2008 in agreement with in-situ measurements, submitted to Ocean Sciences.

[6] Faugere Y., Granier N., Ollivier A., 2007: Envisat RA-2/MWR ocean data validation and cross-calibration activities. Yearly report. Technical Note CLS.DOS/NT/08.006, Contract N° SALP-RP-MA-EA-21516-CLS http://www.aviso.oceanobs.com/fileadmin/documents/calval/validation_report/EN/annual_report_en_2007.pdf

[7] Commien L., S. Philipps, M. Ablain., 2008: Jason-1 validation and cross calibration activities. Yearly report. Technical Note CLS.DOS/NT/09-006, Contract N° 60453 - lot2.C http://www.jason.oceanobs.com/documents/calval/validation_report/annual_report_j1_2008.pdf

[8] Beckley, B. D., F. G. Lemoine, S. B. Luthcke, R. D. Ray, and N. P. Zelensky A reassessment of global and regional mean sea level trends from TOPEX and Jason-1 altimetry based on revised reference frame and orbits, Geophys. Res. Lett., 34, L14608, 2007, doi:10.1029/2007GL030002.

[9] Carrère, L., and F. Lyard, Modeling the barotropic response of the global ocean to atmospheric wind and pressure forcing - comparisons with observations. 2003. Geophys. Res. Lett., 30(6), 1275, doi:10.1029/2002GL016473.

[10] Commien, L., 2009. Différences entre l'orbite des GDR-C et GDR-B Jason-1, NT08.338

[11] Commien, L., S. Philipps, M. Ablain, and N. Picot, 2008. SSALTO CALVAL Performance assessment Jason-1 GDR "C" / GDR "B". Poster presented at OSTST meeting, Nice, France, 09-12 November 2008. Available at: http://www.aviso.oceanobs.com/fileadmin/documents/OSTST/2008/commien.pdf

[12] Legeais JF. and Carrere L, July 2008, Complement de validation de la DAC_HR par rapport à la DAC , en zone cotiere, Technical Note CLS.DOS/08.189.

[13] Cazenave, A., et al.,1999: Sea Level Change from Topex/Poseidon altimetry and tide gauges, and vertical crustal motions from DORIS, G. Res. Let., 26, 2077-2080.

[14] Celani C., B. Greco, A. Martini, M. Roca, 2002: Instruments corrections applied on RA-2 Level-1B Product. 2002: Proceeding of the Envisat Calibration Workshop.

[15] Chambers, D., P., J. Ries, T. Urban, and S. Hayes. 2002. Results of global intercomparison between TOPEX and Jason measurements and models. Paper presented at the Jason-1 and TOPEX/Poseidon Science Working Team Meeting, Biarritz (France), 10-12 June.

[16] Dorandeu, J. and P.Y. Le Traon, 1999: Effects of Global Atmospheric Pressure Variations on Mean Sea Level Changes from TOPEX/Poseidon. J. Atmos. Technol., 16, 1279-1283.

[17] Dorandeu J., Y. Faugere, F. Mertz, F. Mercier, N. Tran, 2004a: Calibration / Validation Of Envisat GDRs Cross-calibration / ERS-2, Jason-1 Envisat and ERS Symposium, Salzburg, Austria.

[18] Dorandeu, J., M. Ablain, Y. faugere, F. Mertz, B. Soussi, 2004b, Jason-1 global statistical evaluation and performance assessment. Calibration and cross-calibration results Mar. Geod. 27(3-4): 345-372.

[19] Doornbos E., Scharroo R., 2005: Improved ERS and Envisat precise orbit determination, Proc. of the 2004 Envisat and ERS Symposium, Salzburg, Austria.

[20] ECMWF, The evolution of the ECMWF analysis and forecasting system Available at: http://www.ecmwf.int/products/data/operational_system/evolution/

[21] EOO/EOX, October 2005, Information to the Users regarding the Envisat RA2/MWR IPF version 5.02 and CMA 7.1 Available at http://earth.esa.int/pcs/envisat/ra2/articles/

[22] EOP-GOQ and PCF team, 2005: Envisat Cyclic Altimetric Report, Technical Note ENVI-GSOP-EOPG-03-0011 Available at: http://earth.esa.int/pcs/envisat/ra2/reports/pcs_cyclic/

[23] Eymard L., E. Obligis, N. Tran, February 2003, ERS2/MWR drift evaluation and correction, CLS.DOS/NT/03.688

[24] http://earth.esa.int/brat/html/alti/dataflow/processing/pod/orbit_choice_en.html

[25] Envisat RA-2 Range Instrumental correction: USO clock period variations and associated auxiliary file, ENVI-GSEG-EOPG-TN-03-0009

[26] Faugere Y., Mertz F., Dorandeu J., 2003: Envisat GDR quality assessement report (cyclic), Cycle 015. SALP-RP-P2-EX-21072-CLS015, May. Available at http://www.aviso.oceanobs.com/html/donnees/calval/validation_report/en/welcome_uk.html

[27] Faugere Y., Mertz F., Dorandeu J., 2003: Envisat validation and cross calibration activities during the verification phase. Synthesis report. Technical Note CLS.DOS/NT/03.733, ESTEC contract N°16243/02/NL/FF WP6, May 16 2003 Available at http://earth.esa.int/pcs/envisat/ra2/articles/Envisat_Verif_Phase_CLS.pdf

[28] Faugere Y., Mertz F., Dorandeu J., 2004: Envisat RA-2/MWR ocean data validation and cross-calibration activities. Yearly report. Technical Note CLS.DOS/NT/04.289, Contract N° 03/CNES/1340/00-DSO310 Available at http://earth.esa.int/pcs/envisat/ra2/articles/Envisat_Yearly_Report_2004.pdf

[29] Faugere Y., Estimation du bruit de mesure sur jason-1, December 2002, CLS.ED/NT.

[30] Y.Faugere, J.Dorandeu, F.Lefevre, N.Picot and P.Femenias, 2005: Envisat ocean altimetry performance assessment and cross-calibration. Submitted in the special issue of SENSOR 'Satellite Altimetry: New Sensors and New Applications'

[31] Faugere Y., Mertz F., Dorandeu J., 2005: Envisat RA-2/MWR ocean data validation and cross-calibration activities. Yearly report. Technical Note CLS.DOS/NT/04.289, Contract N° 03/CNES/1340/00-DSO310 http://www.jason.oceanobs.com/documents/calval/validation_report/en/annual_report_en_2005.pdf

[32] Faugere, Y., J. Dorandeu, N. Picot, P. Femenias. 2007. Jason-1 / Envisat Cross-calibration, presentation at the Hobart OSTST meeting

[33] Faugere, Y., Ollivier, A., 2007, Investigation on the differences between CLS and Altimetrics Envisat MSL trend, CLS.DOS/NT07-261

[34] Faugere, Y., Ollivier, A., 2008, Investigation on the High frequency content of Jason and Envisat, CLS.DOS/NT08-119

[35] Dibarbour, G., Bruit Jason et Analyse spectrale, March 2001, CLS.ED/NT

[36] Imel, D., Evaluation of the TOPEX/POSEIDON dual-frequency ionosphere correction, J. Geophys. Res., 99, 24,895-24,906, 1994

[37] Labroue, S. and P. Gaspar, 2002: Comparison of non parametric estimates of the TOPEX A, TOPEX B and JASON 1 sea state bias. Paper presented at the Jason 1 and TOPEX/Poseidon SWT meeting, New-Orleans, 21-12 October.

[38] Labroue S. and E. Obligis, January 2003, Neural network retrieval algorithms for the ENVISAT/MWR, Technical note CLS.DOS/NT/03.848

[39] Labroue S., 2003: Non parametric estimation of ENVISAT sea state bias, Technical note CLS.DOS/NT/03.741, ESTEC Contract n°16243/02/NL/FF - WP3 Task 2

[40] Labroue S., 2004: RA-2 ocean and MWR measurement long term monitoring, Final report for WP3, Task 2, SSB estimation for RA-2 altimeter, Technical Note CLS-DOS-NT-04-284

[41] Labroue S., 2005: RA2 ocean and MWR measurement long term monitoring 2005 report for WP3, Task 2 SSB estimation for RA2 altimeter, Technical Note CLS-DOS-NT-05-200

[42] Labroue S., 2006: Estimation du Biais d'Etat de Mer pour la mission Jason-1, Technical note CLS-DOS-NT-06-244

[43] Laxon and M. Roca, 2002: ENVISAT RA-2: S-BAND PERFORMANCE, S., Proceedings of the ENVISAT Calibration Workshop, Noordwijk

[44] Le Traon, P.-Y., J. Stum, J. Dorandeu, P. Gaspar, and P. Vincent, 1994: Global statistical analysis of TOPEX and POSEIDON data. J. Geophys. Res., 99, 24619-24631.

[45] Le Traon, P.-Y., , F. Ogor, 1998: ERS-1/2 orbit improvement using TOPEX/POSEIDON: the 2 cm challenge. J. G. Res., VOL 103, p 8045-8057, April 15, 1998.

[46] Lefèvre, F., and E. Sénant, 2005: ENVISAT relative calibration, Technical Note CLS-DOS-NT-05.074.

[47] Lillibridge J, R. Scharroo and G. Quartly, 2005: rain and ice flagging of Envisat altimeter and MWR data, Proc. of the 2004 Envisat and ERS Symposium, Salzburg, Austria

[48] Luthcke. S. B., N. P. Zelinsky, D. D. Rowlands, F. G. Lemoine, and T. A. Williams. 2003. The 1-Centimeter Orbit: jason-1 Precision Orbit Determination Using GPS, SLR, DORIS, and Altimeter Data. Mar. Geod. 26(3-4): 399-421.

[49] Martini A. and P. Féménias, 2000: The ERS SPTR2000 Altimetric Range Correction: Results and Validation. ERE-TN-ADQ-GSO-6001. 23 November 2000.

[50] Martini A., 2003: Envisat RA-2 Range instrumental correction : USO clock period variation and associated auxiliary file, Technical Note ENVI-GSEG-EOPG-TN-03-0009 Available at http://earth.esa.int/pcs/envisat/ra2/articles/USO_clock_corr_aux_file.pdf http://earth.esa.int/pcs/envisat/ra2/auxdata/

[51] A. Martini, P. Feminias, G. Alberti, M.P.Milagro-Perez, 2005: RA-2 S-Band Anomaly: Detection and waveform recontruction. Proc. of 2004 Envisat & ERS Symposium, Salzburg, Austria. 6-10 September 2004 (ESA SP-572, April 2005).

[52] Mertz, F., Y. Faugere and J. Dorandeu, 2003: Validation of ERS-2 OPR cycle 083-086. CLS.OC.NT/03.702 issue 083-086.

[53] Mercier, F., L.Cerri, S. Houry, A. Guitart, P. Broca, C. Ferrier, J-P. Berthias, 2006: DORIS 1b Product evolution, Symposium 15 Years of progress in radar altimetry, Venice.

[54] Mertz F., J. Dorandeu, N. Tran, S. Labroue, 2004, ERS-2 OPR data quality assessment. Long-term monitoring - particular investigations, Report of task 2 of IFREMER Contract n° 04/2.210.714. CLS.DOS/NT/04.277.

[55] Mitchum, G., 1994: Comparison of TOPEX sea surface heights and tide gauge sea levels, J. Geophys. Res., 99, 24541-24554.

[56] Mitchum, G., 1998: Monitoring the stability of satellite altimeters with tide gauges, J. Atm. Oceano. Tech., 15, 721-730.

[57] Obligis E., L. Eymard, N. Tran, S. Labroue, 2005: Three years of Microwave Radiometer aboard Envisat: In-flight Calibration, Processing and validation of the geophysical products, submitted

[58] Ollivier A.,Y. Faugere, P. Thibaut, G. Dibarboure, J. Poisson, 2008: Investigation on the high frequency content of Jason-1 and Jason-2, Technical note CLS-DOS-NT-09-027

[59] Ollivier A.,Y. Faugere, J.-P. Dumont, 2008: Envisat RA2-MWR ocean data validation and cross-calibration activities. Yearly report 2008, Technical note CLS-DOS-NT-09-040

[60] Ollivier, A., Y. Faugere and N. Picot, P. Femenias 2008. ENVISAT Jason-2 Cross calibration. Poster presented at OSTST meeting, Nice, France, 09-12 November 2008. Available at: http://www.aviso.oceanobs.com/fileadmin/documents/OSTST/2008/ollivier.pdf

[61] Picard B., M-L Frery, E. Obligis: ENVISAT Microwave Radiometer Assessment Report Cycle 039, Technical Note CLS.DOS/NT/05.147 Available at http://earth.esa.int/pcs/envisat/mwr/reports/

[62] Product disclaimer available on http://earth.esa.int/dataproducts/availability/

[63] R D Ray and R M Ponte, 2003: Barometric tides from ECMWF operational analyses, Annales Geophysicae, 21: 1897-1910.

[64] Roca M., A. Martini, 2003: Level 1b Verification updates, Ra2/MWR CCVT meeting, 25-26 March 2003, ESRIN, Rome

[65] Roca M., A. Martini, PTR Study, QWG meeting, November 2008, ESRIN, Rome

[66] Rudolph A., D.Kuijper, L.Ventimiglia, M.A. Garcia Matatoros, P.Bargellini, 2005: Envisat orbit control - philosophy experience and challenge, Proc. of the 2004 Envisat and ERS Symposium, Salzburg, Austria

[67] R. Scharroo and P. N. A. M. Visser, 1998: Precise orbit determination and gravity field improvement for the ERS satellites, J. Geophys. Res., 103, C4, 8113-8127

[68] Scharroo R., A decade of ERS Satellite Orbits and Altimetry, 2002: Phd Thesis, Delft University Press science

[69] Scharroo R., December 12, 2002, Routines for iono corrections, internet communication to the CCVT community

[70] Scharroo R., J. L. Lillibridge, and W. H. F. Smith, Cross-Calibration and Long-term Monitoring of the Microwave Radiometers of ERS, TOPEX, GFO, Jason-1, and Envisat, **Marine Geodesy, 27:279-297**, 2004.

[71] Scharroo, R., RA-2 USO Anomaly: predictive correction model, Tech. Rep. N1-06-002, Altimetrics LLC, Cornish, New Hampshire, May 2006.

[72] Stum J., F. Ogor, P.Y. Le Traon, J. Dorandeu, P. Gaspar and J.P. Dumont, 1998: "An intercalibration study of TOPEX/POSEIDON, ERS-1 and ERS-2 altimetric missions", Final report of IFREMER contract N_97/2 426 086/C CLS.DOS/NT/98.070.

[73] Tran, N., D. W. Hancock III, G.S. Hayne. 2002: "Assessment of the cycle-per-cycle noise level of the GEOSAT Follow-On, TOPEX and POSEIDON." J. of Atmos. and Oceanic Technol. 19(12): 2095-2117.

[74] Tran N. and E. Obligis, December 2003, Validation of the use of ENVISAT neural algorithm on ERS-2. CLS-DOS-NT-03.901.

[75] Tran N., E. Obligis and L. Eymard, 2006, Envisat MWR 36.5 GHz drift evaluation and correction. CLS-DOS-NT-05.218.

[76] Valladeau G., Ablain M., Validation of altimetric data by means of tide gauge measurements for TOPEX/Poseidon, Jason-1 and Envisat, Reference : CLS.DOS/NT/08-256, Nomenclature : SALP-NT-MA-EA-21589-CLS

[77] Vincent, P., S. D. Desai, J. Dorandeu, M. Ablain, B. Soussi, P. S. Callahan, and B. J. Haines 2003. Jason-1 Geophysical Performance Evaluation. Mar. Geod. 26(3-4): 167-186.

[78] Witter, D. L., D. B. Chelton, 1991: "A Geosat altimeter wind speed algorithm development", J. of. Geophys. Res. (oceans), 96, 8853-8860, 1991.

[79] Zanife, O. Z., P. Vincent, L. Amarouche, J. P. Dumont, P. Thibaut, and S. Labroue, 2003. Comparison of the Ku-band range noise level and the relative sea-state bias of the Jason-1, TOPEX and Poseidon-1 radar altimeters. Mar. Geod. 26(3-4): 201-238.

10. Appendix 1: Instrument and plateform status

10.1. ACRONYMS

The main acronyms used to described the events are explained below.
CMA: Centre Multimission Altimetrique
CTI tables: Configuration Table Interface. They Contain the setting of the instruments and are uploaded on board after a switch off, a reset
HTR Refuse: Heater Refuse
ICU: Instrument Control Unit, a part of the distributed command and control function implemented on ESA spacecraft. The unit receives, decodes and executes high-level commands for its instrument, and autonomously performs health-checking and parameter monitoring. In the event of anomalies it takes autonomous recovery actions.
IPF: Instrument Processing Facilities
MCMD: Macrocommand
OBDH: On Board Data Handling
OCM: Orbit Controle Mode/maneuvre
P/L SOL: Payload Switch Off Line
SEU: Single Event Upset
SM-SOL by PMC: SM Switch Off Line by Payload Main Computer
SW: Software
TM: Telemetry
USO: Ultra Stable Oscillator

10.2. Cycle 010

- RA-2 went to STBY/Refuse (2002/10/09 09 13:34:22 to 2002/10/10 08:56:53)

10.3. Cycle 011

- Ra2 switch-down - Planned SM-SOL by PMC1 (2002/11/18 04:38:00 to 2002/11/19 19:19:21,Pass 382-429)
- DORIS Navigator switch-down - Planned SM-SOL by PMC1 (2002/11/18 04:38:02 to 2002/11/22 12:40:00, Pass 382-505)
- MWR switch-down - Planned SM-SOL by PMC1 (2002/11/18 04:37:59 to 2002/11/20 12:20:06, Pass 382-448)
- Orbit Maintenance Maneuver (2002/11/07 18:15:51 to 2002/11/07 21:06:17,Pass 83-85)
- Orbit Maintenance Maneuver (2002/11/29 03:35:30 to 2002/11/29 06:25:57,Pass 696-698)

10.4. Cycle 012

- RA-2 went to HTR-0 Refuse (2002/12/21 04:31:26 to 2002/12/21 12:52:00, Pass 325-333)
- Orbit Inclination Maneuver (2002/12/18 04:28:18 to 2002/12/18 06:36:46, Pass 238-240)

- Orbit Maintenance Maneuver (2002/12/18 22:17:22 to 2002/12/19 00:17:34, Pass 259-261)

10.5. Cycle 013

- RA-2 went to HTR-0 Refuse (2003-01-16 01:52:36 to 2003-01-17 17:00:35)
- RA-2 went to suspend mode (2003-01-25 23:56:36 to 2003-01-27 19:54:02)
- Orbit Maintenance Maneuver (2003/01/14 00:55:17 to 2003/01/14 03:45:42 TAI)
- Orbit Maintenance Maneuver (2003/02/11 23:04:49 to 2003/02/12 01:04:57 TAI)

10.6. Cycle 014

- SEU's caused a Software Anomaly (2003/03/02 02:46:44 to 2003/03/03 16:46:35).
- Subsystems unavailable - Autonmous P/L switch-off (2003/03/15 04:21:08 to 2003/03/17 19:00:13)
- RA2 in HTR0/Refuse due to HPA primery bus undercurrent (2003/03/17 21:09:32 to 2003/03/18 18:50:40)
- Orbit Maintenance Maneuver (2003/02/21 03:42:57 to 2003/02/21 05:53:24)
- Orbit Maintenance Maneuver (2003/03/03 23:51:14 to 2003/03/04 01:51:22)

10.7. Cycle 015

- Wrong setting of Ra2 parameters (no CTI tables have been up-loaded on-board) from 18 Mar 2003 18:50:40 to 9 Apr 2003 17:12:24, Pass 1 to 452
- RA-2 unavailability (Format Header Error forcing ICU to RS/WT/INI) from 8 Apr 2003 15:08:57.000 to 9 Apr 2003 17:12:24.000, Pass 437 to 452
- RA-2 unavailability (Format Header Error forcing ICU to RS/WT/INI) from 8 Apr 2003 15:08:57.000 to 9 Apr 2003 17:12:24.000, Pass 613 to 624
- RA-2 unavailability: Multiple SEU caused ICU switchdown (2003/04/24 13:20:09 to 2003/04/25 09:15:36,879 to 901)
- Orbit Maintenance Maneuver (2003/04/04 00:40:48 to 2003/04/04 02:40:56 TAI)

10.8. Cycle 016

- RA2 unavailability (known SEU failure) (from 5 May 2003 12:30:17.000 to 6 May 2003 10:01:10.000, Pass 191 to 215)
- RA-2 unavailability (ICU in SUSPEND due to TM FMT Error when a Reduced FMT was requested) (from 11 May 2003 11:06:33.000 to 12 May 2003 10:14:35.726, Pass 361 to 387)
- Orbit Maintenance Maneuver (from 2003/05/14 22:40:13 to 2003/05/15 00:40:19 TAI, Pass 460 to 462)

- RA-2 unavailability (Switch-down for PMC SW upgrade and OCM) from 18 May 2003 06:25:17.000 to 19 May 2003 15:59:28.000, Pass 548 to 602)
- MWR unavailability (Switch-down for PMC SW upgrade and OCM) from 18 May 2003 06:25:24.000 to 19 May 2003 14:45:40.000, Pass 548 to 602)
- DORIS unavailability (Switch-down for PMC SW upgrade and OCM) from 18 May 2003 06:25:25.000 to 19 May 2003 13:21:28.000, Pass 548 to 602)
- Orbit Inclination Maneuver (from 2003/05/20 04:11:53 to 2003/05/20 06:23:31 TAI, Pass 610 to 612)
- RA-2 unavailability (ICU went to RS/WT/INI) from 1 Jun 2003 14:36:40.000 to 2 Jun 2003 09:20:35.000, Pass967 to 987

10.9. Cycle 017

- Orbit Maintenance Maneuver (from 2003/06/07 01:08:16 to 2003/06/07 03:08:23 TAI, Pass 119 to 122)

10.10. Cycle 018

- Orbit Maintenance Maneuver (from 2003/07/11 0:58:45 to 2003/07/11 03:49:08 TAI, Pass 90 to 94)
- RA2 unavailability (RA-2 in STBY/REF due to MCMD timeout) (from 26 Jul 2003 15:28:11 to 26 Jul 2003 17:25:35, Pass 538)
- RA2 unavailability (RA-2 picked up Mission Planning schedule) (from 31 Jul 2003 16:11:02 to 31 Jul 2003 18:06:30, Pass 682)
- Orbit Maintenance Maneuver (from 2003/07/11 0:58:45 to 2003/07/11 03:49:08 TAI), Pass 91 to 94)

10.11. Cycle 019

- Orbit Maintenance Maneuver (from 2003/08/15 1:31:29 to 2003/08/15 03:31:35 TAI, Pass 91 to 93)
- RA-2 went to STBY/Refuse due to Individual Echoes MCMD Timeout (from 2003-08-15 16:40:21 to 2003-08-15 18:35:35, Pass 110)
- RA-2 went to STBY/Refuse due to Individual Echoes MCMD Timeout (from 2003-08-30 15:28:00 to 2003-08-30 20:47:35, Pass 538 to 543)
- PLSOL . Instrument Switch OFF/ON (from 2003-09-04 22:52:52 to 2003-09-06 16:41:09, Pass 689 to 738)

10.12. Cycle 020

- RA-2 in STANDBY / REFUSE MODE (from 2003-09-21 15:36:40 to 2003-09-21 17:33:30, Pass 166 to 167)

- RA-2 is in RS/WT/INT mode (from 2003-09-27 00:28:08 to 2003-09-27 12:52:00, Pass 320 to 333)
- Wrong setting of Ra2 parameters (no CTI tables have been up-loaded on-board) (from 2003-09-27 12:52:00 to 2003-09-30 12:45:00, Pass 334 to 407)
- Orbit Maintenance Maneuver (2003/09/30 00:40:53 to 2003/09/30 02:41:00 TAI, Pass 405 to 407)

10.13. Cycle 021

- Orbit Inclination Maneuver (2003/10/28 04:56:18 to 2003/10/28 07:09:44 TAI, Pass 210 to 212)
- RA-2 is in RS/WT/INT mode. 29 Oct 2003 06 :47 :04 to 29 Oct 2003 12 :58 :35, Pass 242 to 247)
- Orbit Maintenance Maneuver (2003/10/31 01:13:10 to 2003/10/31 03:13:25 TAI, Pass 291 to 293)
- RA-2 is in RS/WT/INT mode. TM format header error (02 Nov 2003 15 :16 :56 to 03 Nov 2003 12 :08 :35, Pass 366 to 389)
- Orbit Maintenance Maneuver (2003/11/18 23:02:30 to 2003/11/19 01:52:55 TAI, Pass 833 to 835)

10.14. Cycle 022

- RA-2 is in RS/WT/INT mode (2003-11-26 13:31:20 to 2003-11-26 19:39:35, Pass 49 to 54)
- RA-2 PLSOL . Instrument Switch OFF/ON (2003-12-03 07:18:43 to 2003-12-05 16:35:05, Pass 241 to 308)
- MWR PLSOL . Instrument Switch OFF/ON (2003-12-03 07:18:43 to 2003-12-04 18:45:41)
- RA-2 is in RS/WT/INT mode. (2003-12-06 15:55:52 to 2003-12-10 19:16:36, Pass 338 to 455)
- Orbit Maintenance Maneuver (2003/12/15 21:02:28 to 2003/12/15 23:02:36, Pass 601 to 603)
- Orbit Maintenance Maneuver (2003/12/26 21:03:30 to 2003/12/26 23:03:34, Pass 916 to 918)

10.15. Cycle 023

- Orbit Maintenance Maneuver (2004/01/21 23:54:27 to 2004/01/22 01:54:37))
- Orbit Maintenance Maneuver (2004/01/26 22:26:07 to 2004/01/27 00:26:11))

10.16. Cycle 024

- Orbit Inclination Maneuver (2004/02/04 04:46:39 to 2004/02/04 06:58:05)

- Orbit Maintenance Maneuver (2004/02/05 11:17:21 to 2004/02/05 13:17:23)
- Orbit Maintenance Maneuver (2004/02/24 11:48:39 to 2004/02/24 13:48:45)

10.17. Cycle 025

- Orbit Maintenance Maneuver (2004/04/07 20:05:30 to 2004/04/07 22:05:34)

10.18. Cycle 026

- RA-2 in STANDBY/REF DUE TO MCMD H202 FAILURE (2004-22-04 15:15:36 2004-22-04 17:07:05)
- RA-2 Switch down to RESET/WAIT due to too many SEU's reported. (2004-05-10 02:06:31 2004-05-10 11:27:30)
- Orbit Inclination Maneuver (2004/04/14 04:43:02 2004/04/14 06:55:00)
- Orbit Maintenance Maneuver (2004/05/07 01:08:56 2004/05/07 03:09:04)

10.19. Cycle 027

- RA2 went to suspend owing to repeated type 10 entries in report format (2004/05/31 02:45:27 to 2004/05/31 12:01:50)
- No DORIS data from 2004/06/06 13:00:00 to 2004/06/14 14:52:00. Following an onboard incident, Doris instrument has been switched to the redundant chain. Doris data are unavailable from June, 6th to June, 14th. To allow GDR production, POE with laser only data have been produced during this period.
- RA2 in SUSPEND Mode (2004/06/21 14:47:51 to 2004/06/21 19:24:30, Pass 995 to 999)

10.20. Cycle 028

- RA2 in ICU rs/wt/ini (2004/07/18 13:47:03 to 2004/07/18 19:59:00, Pass 765 to 771)
- Orbit Maintenance Maneuver (2004/06/30 08:08:29 to 2004/06/30 10:08:35, Pass 242 to 244)

10.21. Cycle 029

- RA2 in ICU RS/WT/INI. (SDU problem in RAM) (2004/08/10 15:00:39 to 2004/08/11 10:59:30, Pass 423 to 445)
- Orbit Maintenance Maneuver (2004/08/17 02:04:20 to 2004/08/17 04:04:26 , Pass 607 to 609)

10.22. Cycle 030

- RA2 in ICU RS/WT/INI. (SDU problem in RAM) (2004/09/26 13:39:50 to 2004/09/27 16:23:30, Pass 765-795)

- Abnormal behaviour of the RA-2 sensor (2004/09/27 16:23:30 to 2004-09-29 10:21:07, Pass 796-846)
- Collision avoidance Maneuver (2004/09/01 22:52:27 to 2004/09/02 00:52:37, Pass 60-62)
- Collision avoidance Maneuver (2004/09/02 23:44:27 to 2004/09/03 01:44:37, Pass 89-91)
- Orbit Inclination Maneuver (2004/09/21 04:14:37 to 2004/09/21 06:29:19, Pass 610-612)
- Orbit Maintenance Maneuver (2004/09/24 03:53:38 to 2004/09/24 05:53:46, Pass 695-697)

10.23. Cycle 031

- Collision avoidance Maneuver (2004/10/22 03:20:22 to 2004/10/22 07:00:41, Pass 495-498)
- High solar activity (Pass 974-1002)

10.24. Cycle 032

- RA2 in RS/WT/INI. 2004/11/23 13:25:58 to 2004/11/24 14:10:10, Pass 421-449
- RA2 Format header error. 2004/12/01 10:22:30 to 2004/12/01 15:34:29, Pass 647-651
- Orbit Maintenance Maneuver (2004/11/12 01:07:57 to 2004/11/12 03:08:06,Pass 91-93)

10.25. Cycle 033

- RA-2 went to RS/WT/INI due RBI (2004/12/27 02:49:10 to 2004/12/27 13:49:30, 380 to 391)
- Orbit Maintenance Maneuver (2004/12/17 01:03:48 to 2004/12/17 03:03:52, 91 to 93)
- Orbit Maintenance Maneuver (2005/01/05 23:10:28 ro 2005/01/06 01:10:36, 661 to 663)
- Orbit Inclination Maneuver (2005/01/07 04:25:17 to 2005/01/07 06:38:53, 696 to 698)

10.26. Cycle 034

- RA-2 went to RS/WT/INI Mode (2005/01/26 15:50:30 to 2005/01/26 21:07:30, 252 to 257)
- Orbit Maintenance Maneuver (2005/02/18 01:23:24 to 2005/02/18 03:23:28, 893 to 894)

10.27. Cycle 035

- RA-2 went to RS/WT/INI Mode (2005/03/18 04:35:34 to 2005/03/18 12:58:00, 697 to 705)
- Orbit Maintenance Maneuver (2005/03/17 04:51:26 to 2005/03/17 07:06:31, 668 to 669)

10.28. Cycle 036

- RA-2 went to RS/WT/INI mode (2005/04/18 05:01:10 to 2005/04/18 13:22:32, 583 to 591)

- RA-2 went to RS/WT/INI mode (2005/04/18 37:58:10 to 2005/04/24 11:42:30, 742 to 761)

10.29. Cycle 037

- RA-2 went to ICU in RS/WT/INI (RBI ERR 71) (2005/05/14 23:56:37 to 2005/05/15 10:53:45, 348 to 359)
- RA-2 went to ICU in RS/WT/INI (2005/05/21 00:10:45 to 2005/05/21 10:55:35, 520 to 531)

10.30. Cycle 038

- RA-2 went to ICU in RS/WT/INI (2005/07/04 04:41:10 to 2005/07/04 11:19:39, 783 t0 789)

10.31. Cycle 039

- RA-2 went to ICU in RS/WT/INI (2005/07/16 13:32:21 to 2005/07/16 19:58:52,135 to 141)
- RA-2 went to ICU in RS/WT/INI (2005/07/17 14:43:49 to 2005/07/17 19:20:30,165 to 169)
- RA-2 went to ICU in RS/WT/INI (2005/07/29 00:41:41 to 2005/07/29 09:58:30,492 to 501)
- Orbit Maintenance Maneuver (2005/08/09 22:45:44 to 2005/08/10 00:45:50 TAI)

10.32. Cycle 040

- RA-2 went to ICU in RS/WT/INI (2005/08/16 16:41:57 to 2005/08/16 20:22:30,24 to 27)
- RA-2 went to ICU in RS/WT/INI (2005/08/30 16:01:25 to 2005/08/30 19:43:00,424 to 427)
- RA-2 went to ICU in RS/WT/INI (2005/09/12 15:53:09 to 2005/09/12 19:47:00,796 to 799)
- Orbit Maintenance Maneuver (2005/09/07 05:19:53 to 2005/09/07 07:36:31 TAI)

10.33. Cycle 041

- RA-2 went to ICU in RS/WT/INI (2005/09/20 12:19:17 to 2005/09/20 18:56:00,19 to 25)
- RA-2 went in RS/WT/INI (2005/10/04 12:47:33 to 2005/10/04 16:35:30,420 to 423)
- Orbit Maintenance Maneuver (2005/10/06 02:19:10 to 2005/10/06 02:19:14 TAI)

10.34. Cycle 042

- RA-2 went in RS/WT/INI following Uncontrolled S/W Action (2005/10/28 05:34:13 to 2005/10/28 10:39:00,97 to 101)

10.35. Cycle 043

- RA-2 went in RS/WT/INI following Uncontrolled S/W Action (2006/01/02 12:56:35 2006/01/02 18:09:30,993 to 997)

10.36. Cycle 044

- RA-2 went in RS/WT/INI following Multiple SEU Anomaly (ref AR-614) (2006/01/12 14:20:35 to 2006/01/12 19:12:30,279 to 283)
- RA-2 went in RS/WT/INI(2006/01/30 02:07:15 to 2006/01/30 11:29:00,780 to 789)
- RA-2 went in RS/WT/INI following Uncontrolled S/W Action (2006/02/01 05:17:56 to 2006/02/01 12:04:30,841 to 847)
- RA-2 went in RS/WT/INI following Uncontrolled S/W Action (2006/02/01 16:30:28 to 2006/02/01 18:36:30,854 to 855)
- Orbit Inclination Maneuver (2006/01/10 05:54:24 to 2006/01/10 06:11:24)

10.37. Cycle 045

- RA-2 went in RA2 back to operations following TM format anomaly (2006/03/13 09:36:51 to 2006/03/13 17:40:00,989 to 997))

10.38. Cycle 046

- RA-2 switch to STBY and back to measurement to get useful telemetry related to USO (2006/03/17 12:04:00 to 2006/03/17 13:26:00,104 to 107)
- Orbit Inclination Manoeuvre (2006/03/28 05:33:20 to 2006/03/28 05:52:11 TAI)
- Payload anomaly DORIS MVR switch off (no data from) (2006/04/06 02:09:00 to 2006/04/08 12:40:00 TAI)
- RA2 back to operations following TM format anomaly (2006/04/06 12:31:00 to 2006/04/08 12:31:00,664 to 735)
- Doris Doppler Instrument nominal mode with median frequency bandwith pre-positionning (required for DORIS incident recovery) (2004/04/08 12:40:00 to 2006/04/14 09:00:00 TAI)
- Payload anomaly DORIS Reset (2006/04/14 09:00:09)

10.39. Cycle 047

- On 12th-13th May, a special operation was executed to limit RA-2 Chirp Bandwidth to 80MHz (starting from 12/05/2006 at 15:51:37, pass 710) and then 20 MHz (starting from 13/05/2006 at 03:57:57, Pass 724). The instrument was returned to 320MHz on 13/05/2006 at 15:10:17, Pass 738. Users are strongly advised not to use passes 710-738

- The instrument sub-system Radio Frequency Module (RFM) was switched to its B-side on 15 May 2006 at 14:21:50, Pass 790
- RA-2 BACK TO OPERATIONS AFTER 2 CONSECUTIVE SEU ANOMALIES (19 May 2006 09:24:32 and 19 May 2006 19:13:00)

10.40. Cycle 048

- RFM switched to its nominal configuration side (A-side) on the 2006/06/21 at 13:20:15, Pass 850
- RA-2 Back to Measurement following Uncontrolled S/W Action (2006/06/25 15:01:36 to 2006/06/25 19:46:00, passes 967-971)

10.41. Cycle 049

- none

10.42. Cycle 050

- RA-2 Back to Measurement following Multiple SEU Anomaly (2006/08/01 01:14:40 to 2006/08/01 08:54:30,6 to 13)
- Foccserver have been re-booted and is up and running. The problem was probably due to a HW failure at ESRIN (IECF) which caused all the user slots to be occupied(2006/08/17 00:00:41 to 2006/08/17 11:10:00,TAI)

10.43. Cycle 051

- RA-2 Back to Measurement following a Service Module Anomaly (2006/09/7 16:40:30 to 2006/09/10 15:47:30,80 to 166)
- Orbit Inclination Maneuver (2006/09/13 05:22:17 to 2006/09/13 05:40:29)
- Interruption of the Envisat data transmission via the ESA Data Relay Satellite Artemis (anomaly with Envisat Ka-band antenna) from 2006/09/26 until 2006/10/1,630 to 641, 658 to 669, 686 to 697, 716 to 725, 744 to 755)

10.44. Cycle 052

- RA-2 Back to Measurement following a Service Module Anomaly (2006/10/26 04:02:43 to 2006/10/26 10:32:00,467 to 473)
- RA-2 Back to Measurement following a Service Module Anomaly (2006/11/02 15:20:19 to 2006/11/02 20:07:00,681 to 685)

10.45. Cycle 053

- RA-2 Back to Measurement following Multiple SEU Anomaly (2006/11/26 08:01:06 to 2006/11/26 17:32:00, 358-367)
- Available again in Measurement after SM Memory Maintenance (2006/11/28 07:40:00 to 2006/11/29 17:23:00,413-469)
- The entire payload switched off (Due to a LVL 3 PROTOCOL ERROR AND INTERRUPT) (2006/12/12 18:02:17 to 2006/12/15 15:54:00,826-909)

10.46. Cycle 054

- HSM input reset (2006/12/27 14:18:50 to 2006/12/28 10:51:48)

10.47. Cycle 055

- Orbit Inclination Maneuver (2007/01/23 04:33:06 to 2007/01/23 04:51:50; 9)
- RA-2 recovered from STANDBY / REFUSE MODE and back to MEASUREMENT (2007/02/01 15:15:30 to 2007/02/01 17:11:30, 280-281)
- RA-2 return to operation from RESET/WAIT due to MCMD Transfer Acknowledge Error (2007/02/16 00:47:49 to 2007/02/16 11:07:00, 692-703)
- RA-2 return to operation from HT0/REF due to low HPA PBC current (2007/02/17 00:45:47 to 2007/02/19 11:11:00, 721-789)

10.48. Cycle 056

- No event

10.49. Cycle 057

- Orbit Inclination Maneuver (2007/04/03 04:34:42 to 2007/04/03 04:50:14)
- RA-2 Return to Mesurement from HEATER 0 / REFUSE MODE due to HPA bus current OOL (2007/04/03 12:37:27 3 to 2007/04/03 13:48:00)
- RA-2 Return to Measurement after HEATER 0 / REFUSE MODE due to HPA bus current OOL (2007/04/04 09:49:12 to 2007/04/04 11:30:00)
- RA-2 back to measurement from STBY/REFUSE following HTR0/REFUSE MODE (2007/04/09 05:08:51 to 2007/04/09 10:36:30)

10.50. Cycle 058

- The MWR instrument switched into Stand-by/Refuse mode following an on-board anomaly (2007/05/26 13:20:29 to 2007/05/30 13:41:06, 535-649)

10.51. Cycle 059

- RA-2 recovered back to measurement from HTR1/REF0 (2007/06/30 00:37:55 to 2007/06/02 09:51:00,520-587)

10.52. Cycle 060

- RA-2 returned to Measurement from HTR1/REF due to a Telemetry error.(2007/07/19 01:08:026 to 2007/07/19 07:38:00,63-69)
- Orbit Inclination Maneuver (2007/07/17 04:41:26 to 2007/07/17 04:43:42,9)

10.53. Cycle 061

- Payload switch-off due to Service Module Anomaly (Global AOCS Surveillance triggered) (24 Sep 2007 12:27:00 to 27 Sep 2007 11:13:30,993-1002)

10.54. Cycle 062

- Payload switch-off due to Service Module Anomaly (Global AOCS Surveillance ered).(24 Sep 2007 12:27:00 to 27 Sep 2007 11:13:30,1-7)
- Orbit Inclination Maneuver (27 Sep 2007 05:16:25 to 27 Sep 2007 05:31:15)
- MCMD Transfer Acknowledge Error caused the ICU to be put into Reset/Wait Mode. This is one of the expected anomalies and RA-2 was back to measurement on the same day. (2 Oct 2007 16:15:55 to 2 Oct 2007 20:09:30,224-227)

10.55. Cycle 063

- The instrument was switched to Suspend by the PMC following consecutive TM format errors, the mode was commanded back to Measurement on the same day.(8 Nov 2007 13:31:47 to 8 Nov 2007 17:24:30)

10.56. Cycle 064

- Planned payload unavailability for OCM and Maintenance (3 Dec 2007 22:00:00 to 4 Dec 2007 13:50:00, passes 2 to 21)
- Orbit Inclination Maneuver (4 Dec 2007 04:34:54 to 4 Dec 2007 04:49:55)
- RA-2 Back to Measurement following TM Format Anomaly (9 Dec 2007 20:45:11 to 10 Dec 2007 09:14:30, passes 172 to 187)
- RA-2 was switched down into Standby for the System Memory Test (13 Dec 2007 06:44:00 to 13 Dec 2007 12:39:30, passes 270 to 277)

10.57. Cycle 065

- On 16th January an anomaly occurred in the HSM from 16 Jan 2008 16:11:00 to 17 Jan 2008 10:35:21, passes 253 to 276
- Envisat RA-2 (A-Side) S-band transmission power suddenly dropped on 17 January 2008, 23:23:40, UTC. Consequently, all S-band parameters as well as the dual ionospheric correction are not relevant anymore and must not be used from this date onwards.

10.58. Cycle 066

- Orbit Inclination Maneuver (2008/02/12 03:35:23 to 2008/02/12 05:49:28, 9)

10.59. Cycle 067

- None

10.60. Cycle 068

- Orbit Inclination Maneuver (2008/04/22 start : 04:37:04 TAI, end : 04:47:48 TAI).

10.61. Cycle 069

- None

10.62. Cycle 070

- Orbit Inclination Maneuver (2008/07/01 from 04:41:17 to 04:43:49 TAI).

10.63. Cycle 071

- None

10.64. Cycle 072

- Orbit Inclination Maneuver (2008/09/09 from 04:34:21 to 2008/09/09 04:50:26 TAI).
- From 2008/09/11 18:59:00 TAI to 2008/09/12 01:13:00 TAI, ARTEMIS (ENVISAT relay satellite) was unavailable due to ATV operation. This impacted the data availability from pass 86 to 90.

10.65. Cycle 073

- During the period covered by cycle 073 one SFCM maneuvre was executed as planned on the 7th of September at 01:36:05.

10.66. Cycle 074

- 2008/11/18 04:35:33 Orbit Inclination Maneuver (end : 2008/11/18 04:49:13 TAI)
- 2008/11/30 20:25:00 Artemis acquisition antenna was damaged by a strong hail. No data from 2008/11/30 20:25:00 TAI to 2008/12/01 07:14:00 TAI
- 2008/12/19 03:12:32 Orbit Maintenance Maneuver (end : 2008/12/19 03:12:34 TAI)

10.67. Cycle 075

- None

10.68. Cycle 076

- 2009/01/27 03:35:18 Orbit Inclination Maneuver (end : 2009/01/27 05:49:30 TAI)
- 2009/01/28 01:26:31 Orbit Maintenance Maneuver (end : 2009/01/28 03:26:37 TAI)
- 2009/02/17 03:27:51 Orbit Maintenance Maneuver (end : 2009/02/17 03:27:54 TAI)

10.69. Cycle 077

- 2009/03/13 03:06:29 Orbit Maintenance Maneuver (end : 2009/03/13 03:06:31 TAI)

10.70. Cycle 078

- 2009/04/07 04:34:26 Orbit Inclination Maneuver (end : 2009/04/07 04:50:21 TAI)
- 2009/04/15 22:16:36 Orbit Maintenance Maneuver (end : 2009/04/15 23:56:44 TAI)
- 2009/04/21 02:50:33 Orbit Maintenance Maneuver (end : 2009/04/21 02:50:35 TAI)
- 2009/04/28 13:04:50 Failure of the HSM (High Speed Mutliplexer), no data from 2009/04/28 13:04:50 TAI to 2009/04/29 14:57:28 TAI

10.71. Cycle 079

- 2009/05/20 01:32:33 Orbit Maintenance Maneuver (end : 2009/05/20 03:13:11 TAI)

10.72. Cycle 080

- 2009/07/09 03:01:12 Orbit Maintenance Maneuver (end : 2009/07/09 03:01:16 TAI)

10.73. Cycle 081

- 2009/07/21 04:40:21 Orbit Inclination Maneuver (end : 2009/07/21 04:44:35 TAI)

- 2009/07/23 02:00:32 Orbit Maintenance Maneuver (end : 2009/07/23 02:50:50 TAI)

10.74. Cycle 082

- None

10.75. Cycle 083

- 2009/09/29 04:33:42 Orbit Inclination Maneuver (end : 2009/09/29 04:51:00 TAI)
- 2009/10/15 01:56:42 Orbit Maintenance Maneuver (end : 2009/10/15 01:56:44 TAI)

10.76. Cycle 084

- 2009/11/04 07:51:36 Orbit Maintenance Maneuver (end : 2009/11/04 09:32:30 TAI)
- 2009/11/06 02:35:08 Orbit Maintenance Maneuver (end : 2009/11/06 02:35:10 TAI)
- 2009/12/03 03:04:03 Orbit Maintenance Maneuver (end : 2009/12/03 03:04:06 TAI)

10.77. Cycle 085

- 2009/12/08 04:34:40 Orbit Inclination Maneuver (end : 2009/12/08 04:59:57 TAI)
- 2009/12/09 22:18:47 Orbit Maintenance Maneuver (end : 2009/12/09 22:18:53 TAI)
- 2009/12/18 02:24:03 Orbit Maintenance Maneuver (end : 2009/12/18 02:24:05 TAI)